How bioturbating lugworms and stabilizing seagrasses shape the morphology of a Wadden Sea tidal basin

Sanne Vaassen

February 28, 2022

Supervisors: Muriel Brückner & Maarten Kleinhans
Student Number: 5318696
Version: Version 2
Utrecht University MSc Thesis

Abstract

Ecosystem engineering species are mostly known for their ability to affect abiotic conditions and change the morphology of their habitat. Most often to improve habitat suitability for the species itself. Within the Wadden Sea a bioturbating lugworm digs burrows into the tidal flat bed where it feeds on the nutrients which these soils contain. The bioturbating activities of the lugworm facilitate the erosion of mud and fine sediments from the mudflat. Biostabilisers, like seagrasses, facilitate the deposition of mud in their canopy, since these species locally reduce flow velocities. The lugworm and seagrasses compete over space as they both find their suitable habitat in the intertidal range of the tidal flat, where low-energy conditions are prominent and mud concentrations are above 5%.

Extensive research has already been conducted into how these species interact with the abiotic environment and in what ways they affect sediment dynamics and morphology. Most of these studies are carried out on the scale of single mudflats or within flume experiments. However, studies have shown that these species also affect the environment on a larger scale (estuaries and tidal basins). To be able to understand the mechanisms behind these large-scale effects further research is required. Furthermore, there is still a lack of understanding on how the interactions between ecosystem engineers affect morphology on such scales. The objective of this research is to identify what the combined effect of the stabilising seagrasses and the bioturbating lugworm is on the morphology of tidal basins in the Dutch Wadden Sea.

To tackle this objective and answer the main research question, the hydrodynamic FLOW module of Delft 3D is coupled to a species model (MATLAB). The study is carried out in a model domain inspired by one of the smaller tidal basins near the outlet of the Ems river in the Northeastern part of the Dutch Wadden Sea. The species model establishes the suitable areas in the model domain for lugworm and seagrass settlement, and accounts for competition between the two species. The species are parameterised to change certain physical conditions on the locations of settlement. The lugworm lowers the critical bed shear stress for the erosion of mud and increases the erosion parameter, whereas the seagrasses locally increases the drag coefficient. These changes are fed into the Delft 3D environment which computes sediment dynamics and basin morphology. A coupling between the Delft 3D environment and the species model is repeated every morphological month, which represents one tidal cycle. The scenarios with only lugworms, only seagrasses or both species with competition accounted for are compared to each other and to the control scenario without ecosystem engineers.

The results of the model scenarios show how the lugworm erodes the higher elevations of the tidal flats. Generally, the bioturbating activities result in a decrease of mean mud fraction in the tidal basin. Seagrasses, on the other hand, locally increase bed elevations and mud fraction. However, scale-dependant feedbacks result in an increase in flow velocity around the seagrass fields. This results in the fixation and incision of tidal channels. The stabilising activities of the seagrass show a positive feedback on habitat suitability for this species, whereas eco-engineering activities of lugworms have a negative impact on their habitat. When competition is considered, the lugworm colonises a significantly larger area of the tidal basin than the seagrasses. Where the latter are restricted to the lower intertidal zones. The sediment eroded from the higher elevations where bioturbation occurs, are captured in the canopy of the seagrasses which settle on the lower elevations. Promoting incision and erosion of the tidal channels.

Contents

1 Introduction

1.1 Problem definition and relevance of study

Past studies have identified how ecosystem engineers interact with the morphology of coastal landscapes. They have shown that we cannot be ignorant of these species when trying to understand the mechanisms determining sediment transport and the morphology of coastlines. Most of this research is however done on a smaller scale or has been done in experimental set-ups. So, we lack knowledge on what the effects of these species are on morphology and sediment dynamics on larger scales, like tidal basins or estuaries. Furthermore, the effects of several ecosystem engineering species in combination has been addressed sparsely. This study will focus on the interactions between the bioturbating lugworm (*Arenicola Marina*) and a stabilising seagrass species (*Zostera Noltii*) which both thrive in the intertidal zone on the mudflats of the Wadden Sea. By studying the interactions between these species and the effects of both species on sediment dynamics and the morphology of a tidal basin in the Wadden Sea, we will gain a better understanding in these processes shaping coastal landscapes.

1.2 Document outline

2 Background will provide the reader with background knowledge about the subject of the thesis.

3 Literature review will touch upon already existing literature on the subject. Also, knowledge gaps, the research questions and the hypothesis are outlined in this section.

4 Materials and methods describes the methods used in this research. This section explains the way the results are obtained and the mechanisms behind the modelling process. The different model scenarios and choices made during the modelling process are described. Additional model runs are elaborated on in the **Appendices**.

5 Results the model output is explained in this section. Furthermore, answers to the research questions are formulated.

6 Discussion The results are linked to findings in relevant studies. Also, the methodology used for this study is discussed.

7 Conclusions the results and discussion are combined into a final conclusion of this work.

2 Background

2.1 The Wadden Sea - an overview

The Wadden Sea is best known for having the largest area of tidal flats in the world, next to a remarkably high ecological value (Reise et al., 2010).

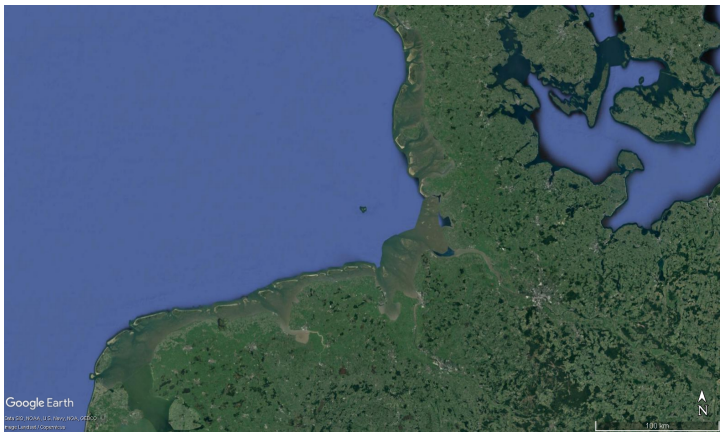

Figure 1: Overview of the Wadden Sea area stretching from the West coast of Denmark towards the Northern coastline of the Netherlands (Google Earth Pro).

The intertidal area of the Wadden Sea is closed off from the North Sea by numerous barrier islands. About 8000 years ago sea level rise began to slow down as a result of a post-glacial period. This lays at the base of the formation of this UNESCO World Heritage Site (Zagwijn, 1986; Flemming, Davis, & Jr, 1994). On the seaward side, dune islands started to form and on the landward side tidal flats and salt marshes emerged as sediments were piled up along the shore. This process stretched all the way from the northern parts of the Netherlands up to Germany and Denmark (Fig. 1). Due to changing rates of sea level rise and changes in sediment supply, the coastal system became an extremely dynamic area. These dynamics resulted in deep channels and tidal inlets at the locations where the tides are relatively strong. Dunes, sandbanks and tidal flats were formed where sediments are deposited, and areas are more dominated by waves rather than tides (Reise et al., 2010).

Overall, the Wadden Sea consists of a series of separate tidal basins which are closely dependant on the position and shape of the barrier islands (E. P. L. Elias, Spek, Wang, & Ronde, 2012). Between two barrier islands the tides are pushed in and out of the tidal basins, which results in strong currents, deep inlet channels formed between the heads of the two barrier islands and a significant amount of sediment transport in and out of the basin (Davis & Hayes, 1984). Often the comparison is made between a tidal inlet system and an estuary system where a river would flow in two directions. A typical feature of these tidal inlets is the ebb- and flood tidal delta, where sediment is deposited at the seaward and the landward side of the inlet. The shapes and sizes of these tidal deltas depend on the availability of sediments, current strength and current direction at the mouth of the inlet system (Davis & Hayes, 1984). Furthermore, the inlet is often very dynamic dependant on changes in tidal currents, waves and alongshore currents (Davidson-Arnott, 2011).

Nowadays, the Wadden Sea is still a very dynamic landscape with a total area of 4700 km2 of tidal flats which are inundated by the incoming tides through the tidal inlets in between the barrier islands twice a day (Reise et al., 2010). During low water it is even possible to walk from the mainland to some of the barrier islands over the mudflats.

When focussing on how tides have shaped the landscape of the Wadden Sea, three main areas can be distinguished (Reise et al., 2010). In the northern and the southern part of the area, tides vary between 0-1.5 metres. At these locations barrier islands have developed and are protecting the inner area against strong tidal currents and waves. In the middle region, where the tidal range goes up till about 3 metres, barrier islands are absent.

Although the Wadden Sea is specified as an UNESCO World Heritage Site in 2009, it is not free of human interference (Reise et al., 2010). One of the main examples is the closure of the Lauwerszee and the Zuiderzee by the placement of closure dikes. These changes severely impacted the dynamics of the area and the morphology of these parts of the system (Wang et al., 2012). Furthermore, mining activities, extraction of gas and salt and dredging and dumping activities have resulted in land subsidence. Because of the expected sea level rise as a result of climate change which is threatening flood safety, more human impact in the area can be expected in the coming decades (Wang et al., 2012).

2.2 Tidal basins within the Wadden Sea

As has been noted before, the western part of the Dutch Wadden Sea comprises of inlet systems between the barrier islands. In general, six tidal inlet systems are distinguished. All systems are classified as mixed-energy systems as both waves and tides shape morphology here (Davis & Hayes, 1984).

Figure 2: Satellite image of the eastern Dutch Wadden Sea obtained from satelliedataportaal.nl showing two tidal inlet systems (Satelliedataportaal.nl).

The tides approaching the shores of this part of the Wadden Sea are travelling from the Atlantic Ocean and through the Strait of Dover (E. P. L. Elias et al., 2012). These two tidal waves will meet each other and combine into a complex tidal wave with the impacts of the Coriolis effects and bottom friction where the water gets shallower as the waves approach the shoreline. Due to the amphidromic point somewhat offshore where the tidal amplitude is consistently 0, the tide propagates from the south up to the north along the Dutch Wadden Sea coastline. Near the head of the island of Texel it meets another eastward moving tidal wave, which causes the tidal amplitude to increase in the more eastern parts of the sea. Tidal ranges in the eastern Wadden Sea, are for this reason larger than the tidal amplitudes in the western parts (1.5 m and 2.5 m respectively) (E. P. L. Elias et al., 2012).

These complex tidal currents form the basis of the shapes of the tidal inlet systems and the channel systems which are formed in the back-barrier basins (Figure 2). Since different tides are penetrating through each tidal inlet, watersheds will appear as these tides bump into one another, and sediment is deposited. In this way the six somewhat separate tidal inlet systems can be distinguished (E. P. L. Elias et al., 2012).

2.3 Sediment dynamics within the Wadden Sea

Since tidal currents are penetrating through the inlet systems into the Wadden Sea twice each day, these currents can be considered important for the transport of sediments (Oost et al., 2021). Furthermore, waves generated within the basin and waves coming in from the North Sea will impact sediment transport over the watersheds between two tidal inlet systems (E. Elias, 2006). Although, tides are considered being the dominant drivers of sediment transport (Buijsman & Ridderinkhof, 2007). Within the Wadden Sea basin, tides are easily deformed, and residual currents and higher harmonics come into existence. These will result in a rather asymmetric tide, which is able to cause a net sediment transport (Dronkers, 1986; Ridderinkhof, 1988; Friedrichs & Aubrey, 1988; Oost et al., 2021).

Next to sand transport, also mud transport is significant in the area. Since sand is rather coarse, it will often be transported as bedload, where the finer mud particles will be transported as suspended load (Postma, 1961; Oost et al., 2021). Sand transport mainly depends on the tidal asymmetry described above. It depends on the current speed and differences herein during ebb and flood. When the currents during flood for example would be fiercer or longer than the currents during ebb, sand will be transported in the flood direction. Suspended load, mud, will also move with the currents in the water column. Only during a period of slack water on the brink of low and high water, will the particles settle to the bottom before they are picked up again and transported in the other direction with the new tidal current. Net transport of fine-grained sediments will for this reason only occur when there is a difference in time of slack water between high and low tide and low and high tide (Postma, 1961).

Another mechanism able to induce net sediment transport is tidal mixing caused by density gradient as a result of the running tides. During flood, water from the North Sea enters the basin which has a different density from the water already present in the basin. This will cause a density gradient within the water column as a result of which currents and thus mixing will occur. During ebb the whole density spectrum of the water column will be reversed as the water from the basin is flowing out into the North Sea. The density gradients will cause an asymmetry in the velocity profile of the tides which again causes net sediment transport. Although, it is yet defined that tidal mixing plays a role in the Wadden Sea basin, not enough research has yet been conducted on sediment transport as a result of this mechanism (Flöser, Burchard, & Riethmüller, 2011; Burchard & Hetland, 2010; Burchard, Flöser, Staneva, Badewien, & Riethmüller, 2008).

Furthermore, there are biological processes which have to be considered when trying to predict sediment transport in the Wadden Sea. Biological creatures are found to have a significant impact on the way landscapes (e.g., mudflats) are formed. Species affect sediment transport, which may modify mudflat morphology. Also, they have an impact on the growth and abundance of one another (Wang et al., 2012). Biogeomorphology is the study that links biological activities and morphology.

Overall, research is still required to be able to make up the sediment budget for the Wadden Sea. Next to the processes and mechanisms described above, human impacts on the sediment dynamics should be considered. Within the Dutch part of the sea, dredging, dumping and sand nourishments to account for sea level rise are carried out, which have a large impact on the sediment dynamics in the system (Schultze & Nehls, 2018).

2.4 Ecology of the Wadden Sea

As can be derived from the sections above, the Wadden Sea system is overall dynamic and knows many different conditions which vary widely over time and space. These varying conditions lay at the base of the large biodiversity of the area (Reise et al., 2010). Overall, the abundance of a certain species within the Wadden Sea mainly depends on the sediment composition and the inundation period (Reise et al., 2010). In the tidal areas on the brink of the intertidal and subtidal area, filter feeders like mussels and oysters thrive. These species filter their food out of the water column and also stabilize the sediment as suspended particles are captured inbetween the structures of the mussel bed. Furthermore, the sea has known one of the world's largest intertidal seagrass areas. Also, these plants may stabilize the sediments between their roots and leaves (Reise & Kohlus, 2008). In the sandier areas, lugworms are reworking the sediments and keeping the soil oxidated. This again enables many bacterial species to grow in these areas as well (Volkenborn, Hedtkamp, van Beusekom, & Reise, 2007).

Since the biological activity and productivity within the sea is rather high, there is a possibility for a complex food web to come into existence. Fish, shrimps and crabs feed on the smaller bacteria and use the seagrass and saltmarsh areas as a nursery location (Strasser, 2002). Larger mammals like seals are again feeding on these smaller species. Next to these species, the Wadden Sea is able to feed over 10-million birds over the course of a single year. Many of these birds are travelling south from Arctic regions and think of the Wadden Sea as a perfect stop to build up some strength before travelling further south towards warmer places like Africa (Blew et al., 2005).

2.5 Ecosystem engineers in tidal systems

Biogeomorphology and ecosystem engineering are two terms which are closely interwoven. Already since the 1970s, research has been done into biogeomorphology and ecosystem engineering (Viles, 2020). Biogeomorphology is a term used to describe the interactions between biotic and abiotic factors shaping the morphology of a natural area. Morphology is not only determined through physical conditions and sediment characteristics. Also, vegetation and other biotic species like algae, bivalves or worms interact with the environment and determine the shape of a natural landscape. These plant and animal species overall, are so-called ecosystem engineering species. These species are known to create and modify their habitat to make them more suitable for their own desired conditions. These activities may have positive or negative effects on other species living in the same environment (Jones, Lawton, & Shachak, 1997). Jones, 2010 (Jones et al., 2010), distinguishes four main cause-and-effect relationships within ecosystem engineering. This starts off with a certain species causing structural change to the environment. Think of lugworms digging channels in the soft and sandy sediments of a tidal flat. Or seagrass rooting down in the soil of a shallow channel. This structural change causes changes in abiotic conditions. The roots of the seagrass will cause less sediments to be able to suspend in the water column, whereas the bioturbating movements of the lugworms will cause an opposite effect. This biotic change will cause a structural change; the turbidity of the water column will be high on the locations where the lugworm has settled when compared to a low suspended particle matter on the locations of seagrass establishment. The fourth relationship entails these changes to feed back to the ecosystem engineers. When there is less erosion in the case of the seagrass bed, it makes it easier for more seagrass seeds to stabilise and grow, since they are then less easily eroded.

3 Literature review

3.1 Ecosystem engineers within the Wadden Sea

Within the Wadden Sea already some research has been carried out concerning ecosystem engineering and biogeomorphology (Austen, Andersen, & Edelvang, 1999; Andersen, Lanuru, van Bernem, Pejrup, & Riethmueller, 2010; Borsje, 2006; Borsje, Hulscher, de Vries, & de Boer, 2007; Bos, Bouma, de Kort, & van Katwijk, 2007; van Leeuwen, Augustijn, van Wesenbeeck, Hulscher, & de Vries, 2010). Most of these research projects have been done on a small scale, where ecosystem engineering is expected to happen on large scales as well, like estuaries and tidal basins (M. Z. M. Brückner et al., 2019).

3.1.1 Seagrasses as ecosystem engineers

Seagrasses are only one of the many ecosystem engineering species which thrive within the Wadden Sea. These species are mostly known for their capability of protecting shorelines an impact on sedimentation and erosion processes. The leaves of the grasses growing on the seabed are able to attenuate the incoming waves and are capable of trapping sediments in their vegetation and rooting system. Wave attenuation in combination with an increase in sedimentation protects the coast from eroding (Christianen et al., 2013; Ondiviela et al., 2014; Dolch et al., 2018). Within the Wadden Sea seagrasses have reduced extensively over the past decades. One of the reasons for its decline being eutrophication and grazing (James et al., 2020; Dolch et al., 2018). Today, there are still some areas where two species of seagrasses dominate: *Zostera Marina* and *Zostera Noltii*.

Both species occurring within the Wadden Sea, are able to survive in both subtidal and intertidal zones, although intertidal zones are often more suitable. Within their leaves they are able to reduce the loss of water and continue photosynthesis during low water periods. However, in the upper intertidal zone, not many of the species survive due to long exposure periods and severe loss of water (Folmer et al., 2016). In the subtidal zone, the hydrodynamics and light are limiting the growth of *Zostera Marina* and *Zostera Noltii*. In these areas,tidal currents moving in and out of the channels are causing damage to the rooting plants or preventing the settling of seedlings at all. However, since seagrasses are ecosystem engineering species, they are able to stabilize sediments in their environment and reduce current strengths through wave attenuation as the waves propagate through the vegetation. This results in calmer conditions and positive feedback back to the settlement and growth of the species. Since sediment characteristics and slope mainly depend on the hydrodynamic conditions which again determine the abundance of the seagrasses, the species are predominantly found on locations where slopes are fairly shallow, and sediments are relatively fine and muddy. As seagrass species settle on the bare soil, overall the mud fraction will increase and the sand fraction will decrease (Bos et al., 2007). Seagrass meadows with a shoot density of about 80 shoots per m^2, have shown to accrete 4.7 mm of sediment during the period of one growing season. Denser seagrass meadows (about 200 shoots per m^2) have shown an annual accretion of 7.1 mm of sediments. Seagrass meadows are most dense during the late summer months (August). As fall comes, seagrass meadows are fed upon by grazing birds.

During winter periods the leaves of both seagrass species disappear, and the soil becomes bare. Muddy sediments are picked up and transported in the water column. During this time of the year, erosion of the sediments deposited during the warmer months of the year takes place on the bed (Bos et al., 2007). After winter *Zostera Noltii* often revives from rhizomes, where *Zostera Marina* revives from newly settling seedlings.

Next to changes in sediment dynamics, seagrasses have an effect on currents and waves.

Research has shown that seagrass meadows are very effecting in wave attenuation (25-49 %, (Reidenbach & Thomas, 2018)). Furthermore, the shoots are able to reduce shear stress below the critical bed shear stress for mud (0.034 Pa on a vegetated site compared to 0.07 Pa on bare control plots (Reidenbach & Thomas, 2018)). In the study of Reidenbach and Thomas (2018), blade lengths of 40 cm, widths of 20 cm and shoot densities of 200 shoots per m2 were documented.

Seagrasses are not only interacting with abiotic conditions, but also interact with other species. Between the roots and vegetation of the plants, organic matter settles. Lucinid bivalves feed on these accretions and reduce sulphide levels in the meadows with their gill bacteria, which again benefits the seagrasses (Heide et al., 2012). Phytoplankton and micro-and macroalgae floating in the water column compete with the seagrasses over light resources. However, between the stems of the plants there is a suitable habitat for species that graze on algae and phytoplankton. These grazing activities have a positive effect on the turbidity of the water and again on the growth of seagrass species (Baden, Emanuelsson, Pihl, Svensson, & Åberg, 2012).

Another species living on the tidal flats of the Wadden Sea and impacting the growth of seagrasses is the lugworm, (*Arenicola Marina* L.). This worm digs a tunnel into the soil where it feeds on nutrients in the sediments. Faeces of this species pile up on the tidal flat and form a small bump on the soil. Lugworms are bioturbating species which rework the soil and affect the possibility for seagrass seedlings to settle and grow. Only when the rhizomes of the seagrasses are dense enough, the seagrasses may dominate the lugworms. Though, during periods or at locations where the seagrass species are less dominant (e.g. winter and in deeper channels) the lugworm easily dominates over the *Zostera* species. For this reason, lugworms and seagrasses are barely ever found on the same locations (Philippart, 1994).

3.1.2 Lugworms as ecosystem engineers

The lugworm is the most abundant worm living on the tidal flats within the Wadden Sea as it accounts for about 20% of the total macrozoobenthic biomass (Beukema & De Vlas, 1979). The small animal digs a J-shaped burrow in the soil where it will stay for most of its life (Fig. 3). The burrow has two connections to the surface, where the worm is positioned in the lowest part of the funnel. Through the head shaft sediment will spill into the funnel upon which the lugworm will feed. Once sediments are digested and valuable nutrients are extracted, the worm will move back and upwards to the other end of the shaft (tail shaft). Once every 15 to 40 minutes the worm will deposit its faeces on the surface of the seabed where the typical humps of sediment are formed (Riisgård & Banta, 1998). The movement of the lugworm up and down the shaft can be seen as a pumping effect where water is transported into the funnel and out again through the other end. The pumping mechanism causes nutrients and oxygen to travel through the funnel and percolate trough the walls. This results in the enrichment of the soil with nutrients and oxygen, where otherwise the soil would be anoxic (Riisgård & Banta, 1998).

Besides the effects of the lugworm on the chemical characteristics of the soil, the worm affects physical characteristics as well. Since lugworms are often occurring in rather large densities up to a hundred individuals per square meter (average of 17 individuals per square meter in the Wadden Sea), bioturbating activities by the species are able to turn over the uppermost layer of the seabed a few times over the timespan of a year (Riisgård & Banta, 1998). As the lugworm prefers rather small grain sizes, the finest sediments are always deposited back on the surface again, whereas the larger sediments are able to sink downwards to the deeper layers (Cadée, 1976). The pumping and the digging of the

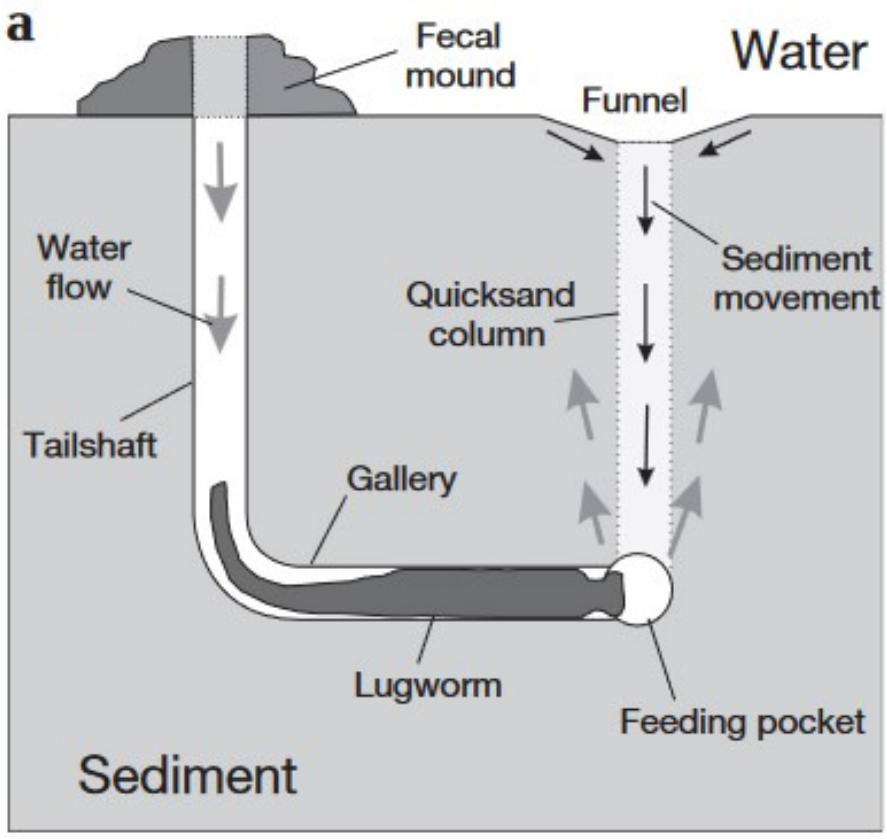

Figure 3: Lugworm in its burrow. the worm will feed on the nutrients in the sediment which comes into the burrow on one side, the other end of the burrow will be used for the deposition of faeces at the surface. (Meysman et al., 2005)

lugworms in the soil also make sure the sediments are very permeable, which facilitates the positive feedback onto the lugworm itself, since burrows are created more easily in permeable soils (Volkenborn et al., 2007).

Adult lugworms will settle on one location for most of their lives. However, juvenile lugworms are not able to settle and grow close to the larger individuals due to the strong reworking activities which make the settlement of larvae almost impossible. For this reason, juvenile lugworms are mainly found on the upper areas of the tidal flats where inundation periods are short and mud contents are higher (Beukema & De Vlas, 1979; Farke, de Wilde, & Berghuis, 1979). Although, once temperatures drop during winter, these juvenile lugworms migrate towards the deeper sections of the tidal flat where inundation periods are longer and temperatures are more constant (Beukema & De Vlas, 1979; Reise, Simon, & Herre, 2001). Adult lugworms are settled in between the summer and winter grounds of the juvenile individuals. These are the locations where the juveniles will also settle once they have reached the postlarval migration state (Farke & Berghuis, 1979).

Overall the adult lugworms prefer to live in burrows of 10-40 centimetres deep in the intertidal zone of the tidal flat where mud concentrations are not lower than 1%, but also not higher than 30-40% (Beukema & De Vlas, 1979).

3.1.3 Interactions between ecosystem engineers: seagrass and lugworms

Where the lugworm is a bioturbating ecosystem engineer, seagrasses stabilise the sediment. Since both species have such a different effect on the environmental conditions, it is expected that the species will also have an effect on the growth and prosperity of the

other. Moreover, since both species do not differ much in habitat requirements concerning sediment composition or inundation period. Both species are mainly intertidal and occur on locations where mud contents are higher than 1% (Philippart, 1994). Multiple studies confirm that seagrasses and lugworms almost never occur on the same location (Philippart, 1994; Valdemarsen, Wendelboe, Egelund, Kristensen, & Flindt, 2011). Lugworm faeces are almost never found in between the leaves of seagrass beds. The sandworm seems to be the dominant species prevailing over seagrasses. This can be clarified through the effect of reworking activities by lugworms on the juvenile shoots of seagrasses. Seedlings of the seagrasses are easily sucked into the head shafts of the lugworms burrows which are numerous on locations with an average lugworm density. Furthermore, the faeces of lugworms will cover the seedlings. Both events will result in the seagrass seeds being too deeply buried by sediments to germinate successfully (Philippart, 1994; Valdemarsen et al., 2011; Govers et al., 2014). Furthermore, seagrasses experiences resistance during the period of rhizome growth, as a result of the turbating activities of the lugworm. Seedlings which settle within a lugworm area are found to have completely disappeared within six weeks, most often due to burying (Philippart, 1994). It is for these reasons, not strange that seagrasses have overall retreated to areas where the subsoil contains a fixed clay or natural shell layer, impossible for the lugworms to penetrate (Rijken, 1979; Philippart, 1994; Reise, 2002).

On the other hand, the lugworm is known to increase nutrient availability and permeability of the soil. This could result in more suitable conditions for seagrasses to grow, though only in locations where lugworm densities are rather low (Philippart, 1994; Govers et al., 2014). Once the seagrass has settled and the rhizomes are evolved to a dense layer in the subsoil, it becomes rather hard for the lugworm to dig a burrow through this dense rooting system. Furthermore, the blocking of light by seagrasses leaves hampers the growth of microphytobenthos on the soil, which serve as a nutrient source for lugworms (Rijken, 1979).

3.2 Knowledge gap

The effects of ecosystem engineers on the morphology of a landscape have been intensively studied over the last decades (Flach, 1992; Govers et al., 2014; Saaltink, 2018). However, much of the work on ecosystem engineers has yet been done on a small scale (singular tidal flats, flume experiments). Predictions have been made that these species also affect sediment dynamics and shape the landscape on a larger scale. A recent investigation done on the effects of these species on the morphology of an estuary indeed confirms these predictions (M. Z. Brückner et al., 2021; M. Z. M. Brückner et al., 2019). To be able to understand the ways in which coastal landscapes are formed, it is of importance to consider the effects of ecosystem engineers on a larger scale. Scale-dependant feedbacks affect morphology beyond the location where the ecosystem engineer is settled (Temmerman et al., 2007). Furthermore, the competition and interactions between stabilising and bioturbating species is likely to affect large scale sediment dynamics. As such, a better understanding of these interactions and scale-dependant feedbacks is required to understand sediment dynamics and morphology of coastal systems. This study will focus on two different classes of ecosystem engineers in a tidal basin. The interactions and competition mechanisms between a stabilising seagrass species and the bioturbating lugworm will be modelled, together with the ecosystem engineering effects already established in former literature. The results of this research will contribute to both an understanding of the interactions between two ecosystem engineers, as well as the way in which bioturbators and biostabilisers affect morphology on a larger scale.

3.3 Research questions

The objective of this MSc thesis research is to identify how the stabilising seagrasses and the bioturbating lugworm shape, or modify, the morphology of tidal basins in the Dutch Wadden Sea. The subject is divided into three specific research questions:

1. Which abiotic factors (mud content, flow velocity or inundation period) are most limiting settlement and growth of lugworms and seagrasses in a Wadden Sea tidal basin?
2. How do the stabilising activities of the seagrasses and the bioturbating activities of the lugworm individually affect the morphology of a Wadden Sea tidal basin?
3. What is the combined effect, including competition mechanisms, of stabilising seagrasses and bioturbating lugworms on the morphology of a Wadden Sea tidal basin?

3.4 Hypotheses

Since the lugworm shows a strong preference for the intertidal zones where mud content are intermediate, mud content and inundation period are expected to be the most limiting factors in determining lugworm establishment. On these locations, the species will actively turbate the soil and cause local erosion of the tidal flats. The sediments brought into suspension by these activities are expected to be transported towards low energy environments within the tidal basin. These locations comprise of deep channels or very shallow areas where flow velocities are low. As the lugworm promotes permeability of the soil it is expected that the species will have a positive effect on its habitat suitability. However, the bioturbating activities will likely lead to a local decrease in mud content, which affects the settlement of lugworms negatively.

Seagrasses are restricted to the intertidal zones and certain inundation periods. Since, the vegetative species is sensible for desiccation in the upper intertidal and flow velocities

combined with a lack of light limits growth in the lower intertidal. For this reason, inundation period and flow velocity are expected to be the main limiting factors in seagrass habitat suitability. Seagrasses are known to attenuate waves effectively and promote the sedimentation of fine particles (mud) in their canopy. This will create calmer local conditions which promotes the settlement of seagrasses. However, scale-dependant feedbacks cause an increase of flow velocities next to the seagrass fields which will lead to either channel stabilisation or channel formation.

A combination of two species in a tidal basin is expected to result in the lugworm being dominant over the seagrass. Since lugworms prevent successful germination of seedlings. The area colonised by lugworms is expected to be significantly larger than the area colonised by seagrasses. The lugworm will erode the intertidal areas. But, on the locations where seagrasses are present, sedimentation will elevate the beds. At these locations the dense rhizome mats in the soil will prevent the colonisation by lugworms. Since seagrasses have a positive feedback on their own habitat, the area colonised by these species may slowly grow over time.

4 Materials and Methods

4.1 General approach

For answering the research questions of this study, a numerical modelling approach is used. The model domain established for the research is inspired on a small tidal basin in the eastern Wadden Sea. The Delft 3D FLOW environment accounts for hydrodynamic and geomorphological computations in this model domain. To be able to add ecosystem engineers, which interact with the abiotic environment, the Delft 3D environment will be coupled to a benthos and vegetation model desinged by Brückner (M. Z. M. Brückner et al., 2019; M. Z. Brückner et al., 2021). These MATLAB models account for the geomorphological changes as a result of species presence which are fed back into the computations of Delft 3D.

4.2 The research area

The model domain is inspired by a relatively small tidal basin in the eastern part of the Dutch Wadden Sea, near the outlet of the Ems river (coordinates: 53.48968753173607, 6.686005446658971) (Fig. 4). Seawater is penetrating into the system through one single inlet where it forms multiple branches which bring the salty water deeper into the system during high tide. The upper tidal flats lie about 0.3 m above NAP (Dutch chart datum). Channels have an average depth of a few centimetres further into the basin, but near the inlet they are about 2 metres deep. The Ems-Dollard estuary knows a depth of about 8 metres close to the inlet of the tidal basin (*Dataregister Rijkswaterstaat*, n.d.). The whole of the basin covers an area of about 28 km^2 where mud contents vary between 2% and 20% where the highest concentrations can be found further onto the tidal flat where conditions are calmer, and elevations are higher (*Dataregister Rijkswaterstaat*, n.d.). The tidal amplitude of the semidiurnal tide near the inlet system is about 1.5 metres (*Dataregister Rijkswaterstaat*, n.d.). Mud concentrations, bed elevations and tidal hydrodynamics in the area allow for suitable habitat conditions for both lugworms and seagrasses (Beukema & De Vlas, 1979; Philippart, 1994).

4.2.1 The model domain - a rectangular basin

The tidal basin in the eastern Wadden Sea is translated into a rectangular model domain using MATLAB version R2020a and Delft3D version 2.33. Within MATLAB, a grid file and a basic bathymetry are designed. The grid has a resolution of 50x50 metres per grid cell and the whole area of the model domain is 28 km^2, 4 kilometres wide and 7 kilometres long. The bathymetry is set up by comparing the elevation profile within Google Earth and DEM's (digital elevation maps) in ArcGis. The bathymetry of the model domain is divided into three main components, as shown in Figure 5. The ocean basin on the right side of the domain, which is set as a rectangular basin with a uniform depth of 18.5 metres, which about 10 metres deeper than the average depth of the Wadden Sea near the outlet of the tidal basin. This extra depth is created to account for the eroded sediment which will end up in the ocean basin, but is not transported out of the model domain as compared to a natural tidal system. The ocean basin slopes up onto the tidal flat over a distance of 800 metres. On the location where the tidal flat starts, the bed elevation is put to zero. From here, the flat is set up with a slope of $0.4\text{E}^{-5} m/m$ to the other boundary of the bathymetry domain (elevation = 0.3 m). In the centre of the domain, on the boundary between the ocean basin and the tidal flat, in indent with a depth of 2.5 metres is added. The indent has a rectangular shape with a width of 200 metres and a length of 1 kilometre. The indent will be used to concentrate the flow in the centre of the

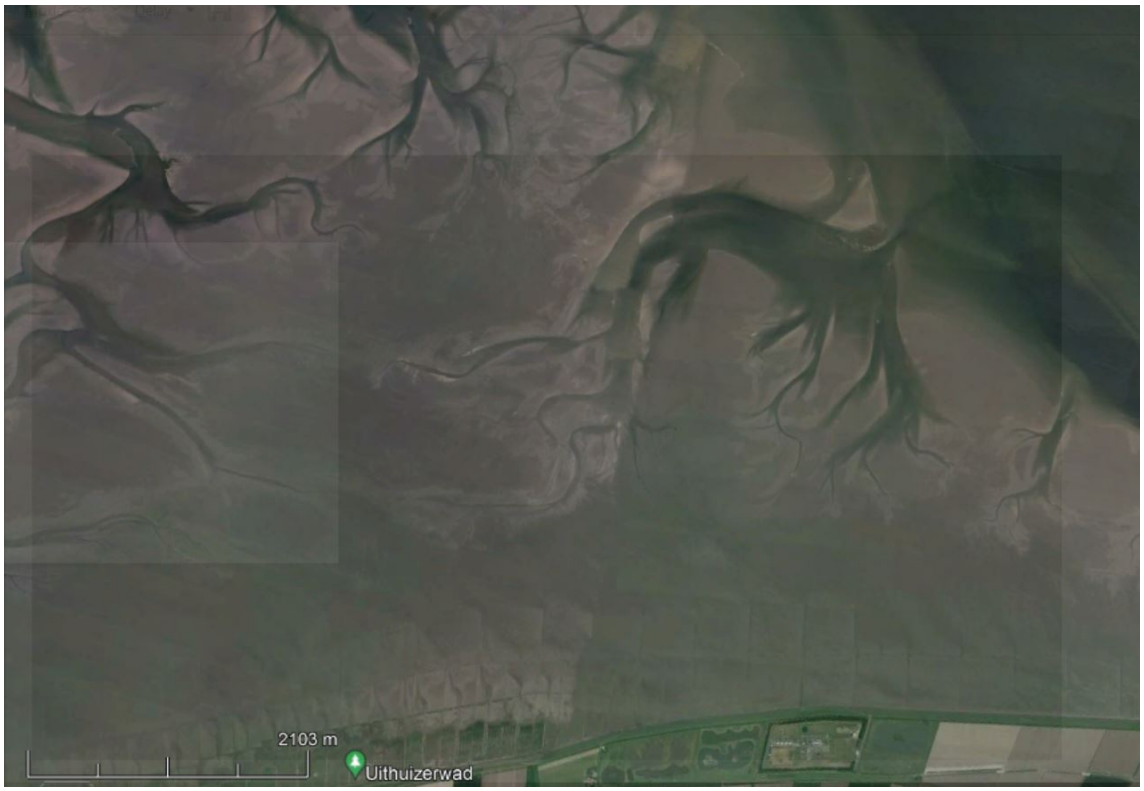

Figure 4: The small tidal basin visualised represents the research area near the outlet of the Ems river in the eastern Dutch Wadden Sea, coordinates: 53.48968753173607, 6.686005446658971 (Google Earth Pro, 2021)

domain and to initialise the development of a branching system here during the run of the Delft 3D Flow module.

4.2.2 The model domain - boundary conditions

To the model domain, a semi-diurnal tide and a mud inflow discharge are added as boundary conditions. On the seaward side of the domain, tides are induced over the whole width of the ocean basin. A harmonic boundary within Delft 3D is able to initiate a change in water level over time. To determine the changes in water level over a tidal cylce, literature is consulted concerning the tides near the tidal basin in the Wadden Sea. Tidal gauge data for the location of the Eemshaven over the year of 2021 is obtained from the website of Rijkswaterstaat (*Dataregister Rijkswaterstaat*, n.d.). Using MATLAB, a tidal analysis is done to identify the dominant tidal constituents. Different tidal constituents are plotted, and the calculated signal is then compared to the original signal from the gauge data (Fig. 6). The RMSE (root mean square error) was calculated and minimised. The most optimal tidal signal uses three tidal constituents: M2 (principal lunar semidiurnal), S2 (principle solar semidiurnal) and M4 (shallow water overtides of principal lunar) with each their own periods of respectively 12.42, 12 and 6.21 hours. A conversion of the tides makes sure that the M2 matches the S2 constituent of 12 hours, to guarantee a constant forcing for the coupling with the MATLAB model (coupling time-step of 12 hours).

On the landward side of the domain, up onto the tidal flat, the mud inflow boundary is located which regulates the mud inflow into the model domain. The inflow of mud into the system is a requirement for the macrobenthic species to settle in the domain. Studying Google Earth images, no fluvial form of mud inflow into the system can be found, like a river bringing in mud from upstream to the mouth of an estuary. Instead, the mud supply represents the gradual overflow coming in from the southwestern part of the basin (Fig 4). On this location in the model domain, a discharge boundary regulates the inflow

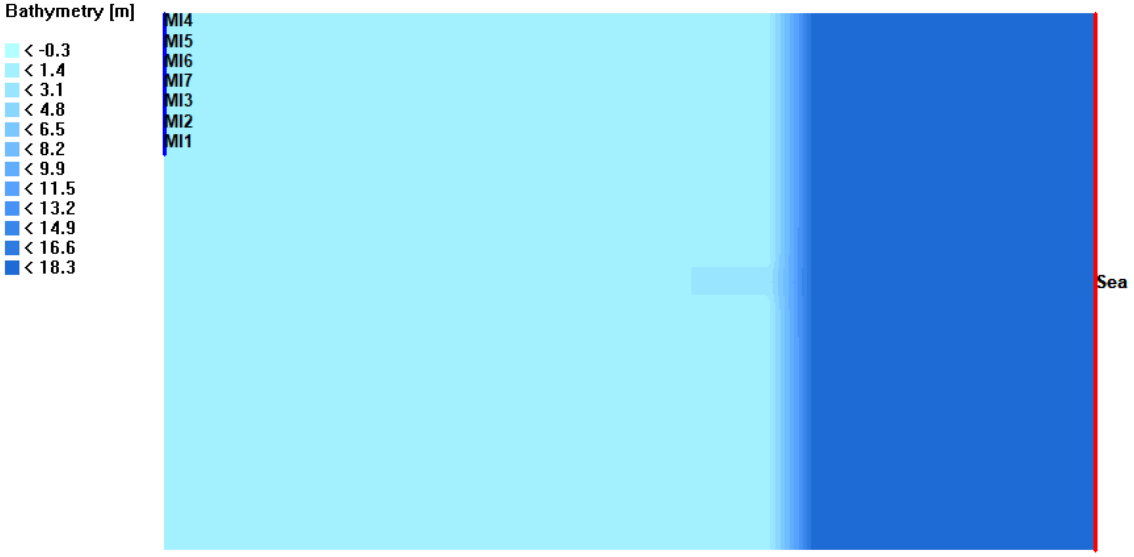

Figure 5: Bathymetry of the basin as computed from a MATLAB code. The deepest, dark blue side of the domain visualises the ocean basin which is 18.5 m deep. Where the tidal flat meets the ocean basin the elevation is set to 0 m (transition from dark blue to lightl blue). From this brink, the landscape slopes up to an elevation of 0.3 m near the end of the tidal flat. A small indent is situated on the brink of ocean and tidal flat to encourage the concentration of flow in this area which will start the process of channel formation (shaded rectangle on the brink of ocean and tidal flat). There are two open boundaries: the sea boundary where the tides are set using a harmonic boundary (based on tidal gauge data near the Eemshaven) and a mud inflow boundary up onto the tidal flat where the mud is flowing into the domain. The mud inflow boundary was divided into 7 sub-boundaries with each an inflow of 0.5 m^3/sec and a mud concentration of 0.1 kg/m^3.

and concentration of mud into the system. The mud inflow only starts after the first spring/neap cycle of the model run, after the morphodynamics in the model are properly activated. For each cell a discharge of 0.5 m^3/sec is specified over the whole width of 1 kilometre. The incoming flow had a mud concentration of 0.1 kg/m^3. From the inflow, the mud is picked up by the incoming tides during flood, when the whole of the tidal flat is inundated, and transported into the system. This open boundary (total length = $1km$) consists of seven sub-boundaries with even mud inflow rates. The use of one singular boundary causes the incoming mud to concentrate on one location. Whereas, the use of the sub-boundaries ensures an even distribution of mud inflow over the open boundary of one kilometre.

The model domain and its boundary conditions are fed into the FLOW module of Delft 3D. The computations for calculating changes in morphodynamics are run for 500 morphological years (where one morphological year represents 12 tidal cycles) with a morphological scale factor of 120. This morfac specifies the rate at which morphodynamical change is happening within the domain.A value of 120 means that one tidal cycle of 720 minutes (12 hours), represents about 120 tidal cycles in morphological time (two months). This parameter is used to speed up the model process ("Delft3D-FLOW User Manual", n.d.), and has been investigated for applicability in a similar longterm morphological study (M. Z. Brückner et al., 2021). Other important parameters and model specifications can be found in Table 1. Paragraph 8.2, 8.3, 8.4 and 8.5 (Appendices) elaborates on other considerations and decisions made in the process of setting up the model domain.

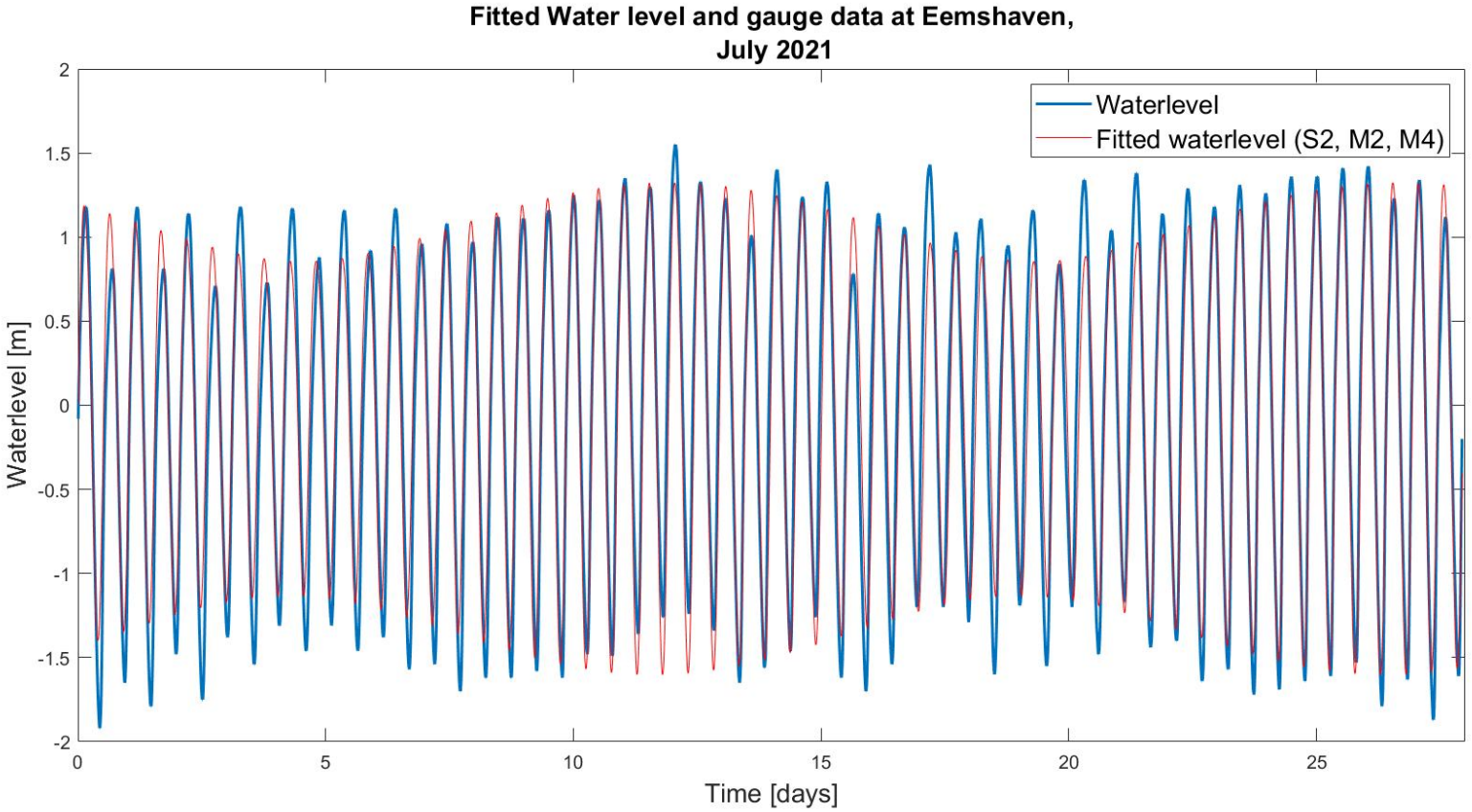

Figure 6: Fitted water level when choosing M2, M4 and S2 constituents, Root mean square error (RMSE): 0.088. Calculations are done using a MATLAB code which calculates a theoretical tidal signal using different tidal constituents and compares this tidal signal to a tidal signal measured at a gauge station. The theoretical tidal constituents are compared to tidal gauge data at the Eemshaven over July 2021.

Physical parameters	Values	Units
Specific gravity	9.81	m/sec^2
Water density	1000	kg/m^3
Chezy value	50	$sqrt(m)/sec$
Eddy viscosity	1	m^2/sec
Eddy diffusivity	10	m^2/se
Sand		
Specific density	2650	kg/m^3
Dry bed density	1600	kg/m^3
Median sediment diameter	200	μ m
Mud		
Specific density	2650	kg/m^3
Dry bed density	500	kg/m^3
Settling velocity	0.25	mm/sec
Critical bed shear stress for sedimentation	1000	N/m^2
Critical bed shear stress for erosion	0.2	N/m^2

Table 1: Physical parameters which can be defined in the Delft 3D FLOW module. Sediment properties for mud (cohesive) and sand (non-cohesive) sediments. The dry bed density for mud is significantly lower than the value for sand as this will promote the erosion for the mud in the low-energy model domain.

4.2.3 The Delft 3D model environment

For hydrodynamic and morphological computations in this research, the FLOW module within Delft 3D is used. The module, based on the shallow water computations, accounts for processes both in the horizontal and the vertical direction (Lesser, Roelvink, van Kester, & Stelling, 2004). Where the computations in the vertical direction are simplified for shallow water cases and are calculated over the different vertical layers which the domain consists of.

Along the horizontal plane, equations are computed along these layers using the Boussinesq approximation for pressure and the horizontal Reynold's stress based on the eddy viscosity (Rodi, 1980).

Other important shallow water equations used in the model are the depth-averaged continuity equation, the advection-diffusion equation for the transport of the water particles and multiple turbulence closure models based on eddy viscosity (Prandtl, 1945).

The module in itself does not account for water movement as a result of waves, but only takes currents into account. When one would want to add the effects of waves to the model computations, a connection should be made to the WAVE module of the Delft3D environment (Lesser et al., 2004). Since this research focuses on processes in a tidal basin, currents are considered being the dominant force and wave forces are neglected.

The FLOW module accounts for sediment transport. The user can add different sand constituents to the model as cohesive (mud) or non-cohesive (sand) sediment types ("Delft3D-FLOW User Manual", n.d.). For the calculation of total sediment transport, the Engelund-Hansen equation is used which sums the suspended load and bed load sediment transport rate as a result of currents (Eq. 1) (Engelund & Hansen, 1967):

$$S = S_b + S_{s,eq} = \frac{0.05\alpha q^5}{\sqrt{g}C^3\Delta^2 D_{50}}, \tag{1}$$

where S is the sediment transport rate ($m^3 m^{-1} s^{-1}$), q is the magnitude of flow velocity

(m/sec), Δ, the relative density $(\rho_s - \rho_w)/\rho_w$, C, the Chézy friction coefficient and α, the calibration coefficient. Waves are not taken into account when establishing the sediment transport rate. Although, the transverse bedslope effect is considered for in the establishment of the direction and magnitude of the bedload sediment transport (Bagnold, 1966; Ikeda, 1982).

For the calculation of the transport of cohesive sediments (mud) the Partheniades-Krone approach is used (Eq. 2) (Partheniades, 1965):

$$E = Mmax(0, \frac{\tau_{cw}}{\tau_{cr,e}} - 1)^n, \quad D = w_s c_b T, \tag{2}$$

where E is the erosion flux from the bed (kgm^{-2}), M is the erosion parameter ($kgm^{-2}s^{-1}$), n is the power of erosion, default = 1, D is the deposition flux ($kgm^{-2}s^{-1}$), w_s is the fall velocity (ms^{-1}), c_b is the average sediment concentration in the bottommost computational layer of thickness, T is the dimensionless reduction factor for deposition flux, τ_{cw} is the maximum bed shear stress ($Nm^{-}2$), $\tau_{cr,e}$ is the critical erosion shear stress (Nm^{-2}) and $\tau_{cr,d}$ is the ritical deposition shear stress (nm^{-2}). The equations determine the fluxes of cohesive sediments between the water column and the bed.

4.2.4 The benthos and vegetation model

Next to the hydrodynamical computations done within the Delft 3d environment, a MATLAB model is coupled to the environment to account for the ecosystem engineering activities affecting geomorphology, as a result of lugworm and seagrass settlement in the domain. This considers two MATLAB models, constructed by Muriel Brückner (M. Z. M. Brückner et al., 2019; M. Z. Brückner et al., 2021). The benthos model was used in a former study to model the interactions between macro- and microphytobenthos in the estuary of the Western Scheldt. The saltmarsh model (from here on called vegetation model) accounts for vegetative species, and is in this study used to represent seagrasses.

The lugworm is one of the most abundant ecosystem engineers thriving on the tidal flats of the Wadden Sea. Former studies have focused on the interactions between this bioturbating species and the coastal environment (Riisgård & Banta, 1998; Volkenborn et al., 2007; De Cubber, Lefebvre, Lancelot, Duong, & Gaudron, 2020), which makes this species relatively well studied and suitable for research. Seagrasses and lugworms compete over space as they have overlapping preferences regarding habitat suitability. The presence of one species excludes the ability of the other species to settle and grow (Philippart, 1994; Valdemarsen et al., 2011; Govers et al., 2014). Also, for seagrasses previous studies have been conducted on the effects of these stabilising species on sediment transport mechanisms and small-scale morphology (Philippart, 1995b; Heide et al., 2010, 2012; Folmer et al., 2016). The competition between the two species and the contradicting ways in which they affect morphology make these species suitable and interesting for this study. Furthermore, both species have been used in previous numerical modelling studies (Folmer et al., 2012; Heide et al., 2012; M. Z. Brückner et al., 2021).

Both benthos and vegetation models have a similar construction in MATLAB and can be coupled to the Delft 3D environment where physical conditions like mud content, flow velocity, water depth depth, bed elevation and inundation period are determined by the hydrodynamic and sediment transport equations (Fig. 7). These conditions are used as an input for the MATLAB models. Furthermore, textfiles with information on the habitat conditions of the engineering species are added to the input files of the benthos and vegetation model. The conditions for each of the two species saved in these textfiles are

documented in Table 2. The MATLAB model fits the habitat conditions with the physical conditions obtained from the Delft 3D model domain to determine species abundance and densities within the domain. It calculates how species will affect the physical parameters before it feeds the changes back into the Delft 3D model. The turbating activities of the lugworm are modelled in terms of a lowering in the critical bed shear stress (Table 2). This stress defines the force needed for a sediment particle to be eroded from the bed. As the critical value lowers, less force will be needed for erosion of the sediment. Furthermore, the erosion parameter is adjusted on the locations in the basin suitable for the lugworm to settle. The erosion parameter defines how much sediment will be eroded from the bed once the critical bed shear stress is reached. For the locations where the lugworm settles, the erosion parameter will increase as more sediment will be eroded once the critical bed shear stress, which is lower at these locations, is reached. The stabilising abilities of the seagrasses are translated into an increase of the drag coefficient on the locations where the species settle. The changes in environmental conditions as a result of species presence, will cause sediments to erode more or less easily on the locations where the different type of ecosystem engineering species is present. The Delft 3D model will compute the changes in bathymetry as a result of the normal hydrodynamic conditions and the changes herein due to the impact of lugworms and seagrasses. For each month, the model domain updated in the Delft 3D model, will be coupled to the benthos or vegetation model for the determination of species abundances.

Data from the Delft 3D model containing the bathymetry and physical parameters is saved for each timestep (every 36 minutes) in the *.trim-files*. The benthos and vegetation model save species distributions for each coupling with the Delft 3D model which is for each morphological month (one tidal cycle). All analyses are carried out using MATLAB.

Table 2 summarizes the parameterisation of seagrasses and lugworms used for the model computations based on literature. Seagrass is a species which knows seasonality throughout the year, where maximum biomass is observed during midsummer in July. From this month onwards, the plants will start to decay, until only the rhizomes in the soil are left by the beginning of December. From these rhizomes, the plant will grow again once temperatures increase from the beginning of March (Philippart, 1995b; Paul & Amos, 2011). During summer, shoot densities are up to 4500 shoots per square metre and stem heights of are considered to be around 25 centimetres, where the stem diameter is only 9 millimetres (Peralta, Brun, Pérez-Lloréns, & Bouma, 2006; Paul & Amos, 2011). The minimum root length is set to 1 millimetre, which is the root length of the seedlings. The intertidal plants require a habitat where the inundation periods are longer than 30% of one tidal cycle, to prevent desiccation of their leaves. Once desiccation periods are above 8 hours (60% of the tidal cycle) decay will start (Leuschner, Landwehr, & Mehlig, 1998; de Jong, van Katwijk, & Brinkman, 2005). Furthermore, the species will not be able to grow on the bed of the tidal channels where flow velocities exceed a value of 0.35 m/sec. Then seagrasses are no longer able to dig their roots into the soil successfully and are more likely to be picked up by the flow. It becomes harder for seedlings to settle and germinate on these locations (de Jong et al., 2005; Peralta et al., 2006). Concerning mud content, all habitats are suitable for seagrasses. Overall, they do prefer some percentage of mud, although they also are able to settle in sandy environments (Folmer et al., 2016). Within this modelling study, the age of seagrass is set to 50 years, which is equal to the duration of the modelled scenario runs. As a result, the species will only die when physical conditions are no longer suitable.Throughout their growth period, the continuous changes in blade length and species fractions affect the flow through a change in drag coefficient (Paul & Amos, 2011).

The lugworm settles within the model domain in February where it will bioturbate the

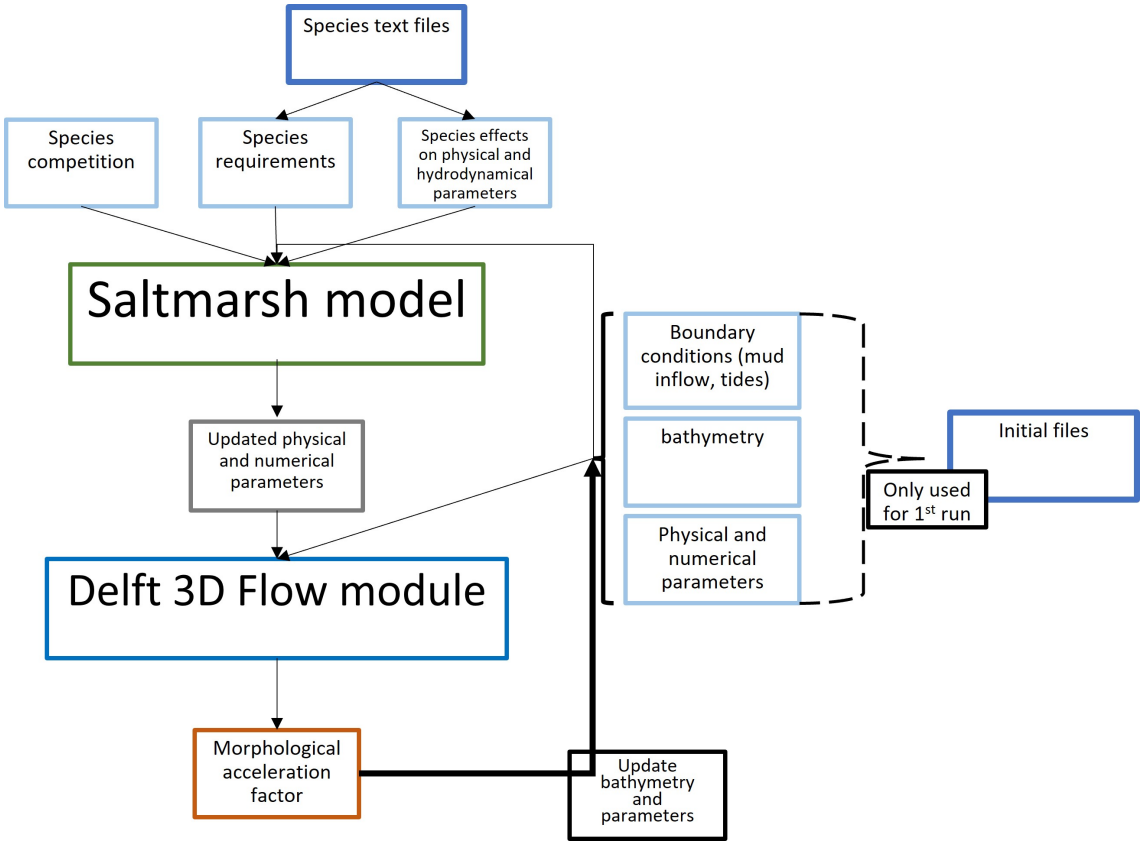

Figure 7: Schematic overview of the Benthos model, the Delft 3D FLOW module and their interactions. Initial files of which the contents can be specified by the user are visualised in the light blue boxes. The morphological scale factor will determine the speed of morphological change as a result of suspended sediment transport. Bathymetry and physical and numerical parameters are updated after each run in the FLOW module and fed back into the Benthos model.

soil until the end of December. The lugworm requires the sediments to have a certain mud content (at least 5%) (Beukema & De Vlas, 1979). It will survive merely in intertidal conditions. Flow velocities ought not to be higher than 0.85 m/sec for the worm to be able to settle successfully. Through turbation of the seabed and the loosening of sediments, the critical bed shear stress of the mud will lower and will be more easily eroded. Furthermore, the erosion parameter is modelled to increase on the locations of lugworm settlement. This increase will result in more mud being eroded from the bed once the critical bed shear stress is reached.

The critical values for mud content, inundation period and flow velocity will determine the window of opportunity where the species will be able to settle in the domain (Fig. 8).

Specification	**Values**	**Units**
Seagrasses		
Maximum age	50	years
months of seed dispersal	5	months, March til July
Initial root length	0.001	m
Initial shoot length	0.1	m
Initial stem diameter	0.0001	m
Month of start growth	March	
Month of end growth	July	
Month start winter	November	
Month start colonisation	March	
Month last colonisation	November	
Max plant height	0.25	m
Max stem diameter	0.009	m
Max root length	0.04	m
Shoot density	4500	shoots/m^2
Growth rate	0.07	
Drag coefficient	1.2	N/m^2
Mud percentage	0.00	% of sediment composition
Desiccation threshold start decay	65	% of tidal period
Desiccation threshold max mortality	70	% of tidal period
Flooding threshold start decay	60	% of tidal period
Flooding threshold max mortality	70	% of tidal period
Flow velocity threshold for start decay	0.35	m/sec
Flow velocity threshold max mortality	0.90	m/sec
Lugworms		
Critical bed shear stress for max biomass	0.11	N/m^2
Erosion parameter for max biomass	0.0005	
Critical bed shear stress sediment	0.20	N/m^2
Erosion parameter sediment	0.0001	
Month of settlement	February	
Month of max mortality	December	
mud threshold	5 - 95	% of sediment composition
Inundation threshold	0 - 100	% of tidal period
Flow velocity threshold	0 - 0.85	m/sec^2

Table 2: Specifications for modelling ecosystem engineering species. The parameters in this table are the input for the species computations done in the vegetation and benthos models. References are mentioned in the text.

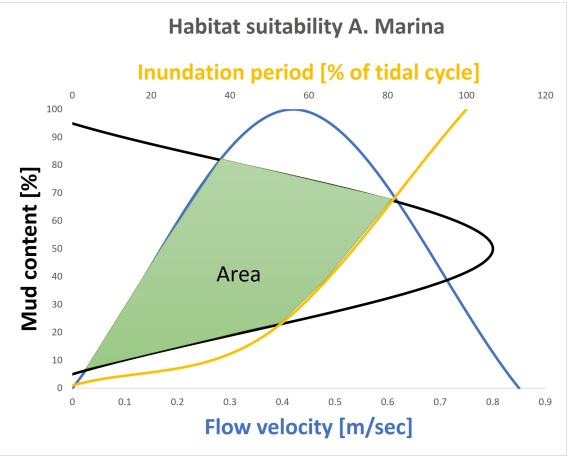

(a) Habitat suitability of the lugworm determined by mud fraction of the top layer of the bed, mean flow velocity over a tidal cycle and inundation period. The green area shows the habitat suitable for the lugworm.

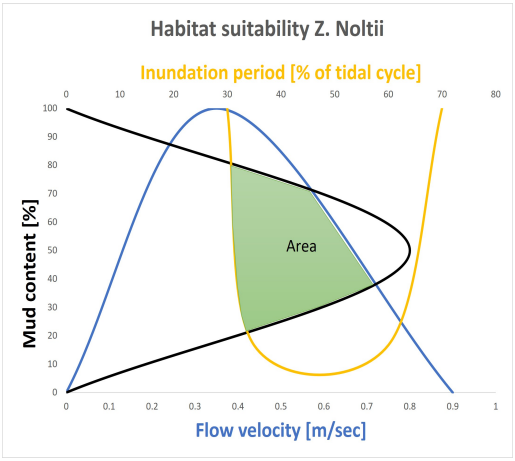

(b) Habitat suitability of seagrasses determined by mud fraction of the top layer of the bed, mean flow velocity over a tidal cycle and inundation period. The green area shows the habitat suitable for the seagrass species.

Figure 8: Graphs showing the habitat suitability for the lugworm and seagrasses dependant on mean flow velocity, mud content and inundation period. All values are based on findings in literature. References in text.

4.2.5 Model scenarios

To answer the research questions, five different model scenarios are run which are documented in Table 3. In all scenarios the initial bathymetry is used, computed in the Delft 3D environment over a timespan of 500 years from the initial ocean basin (paragraph 4.2.1 and paragraph 4.2.2). This domain is set as the starting bathymetry for all model scenarios, allowing for direct comparison between scenarios. For all combinations of species abundances in the model (seagrasses (3ab), lugworms (2ab), both (no competition 4ab, competition 5ab) and none (1ab)), the model is run once with a continuing mud inflow of 0.01 kg/m^3, which is the same concentration as during the computation of the initial bathymetry. In a different scenario, the mud inflow is cut-off. This distinction is made to be able to see the effect of the mud availability on species distribution and morphology of the domain. Once the mud inflow is cut-off at the beginning of the model runs, the predicted mud fractions as found in the eastern part of the Dutch Wadden sea can be observed in the modelled tidal basin (*Dataregister Rijkswaterstaat*, n.d.). Mud concentrations are higher in scenarios where the mud inflow is sustained. All different scenarios are run for 50 years with a morphological acceleration factor of 60 (1 calendar minute = morphological change of 60 minutes). For the scenarios where only lugworms or seagrasses are considered, the benthos and the vegetation models respectively are used in combination with Delft 3D. In the scenario where both lugworms and seagrasses are considered, both models are linked with Delft3D.

In the multi-species scenario where both seagrasses and lugworms are added to the model computations, competition between the two species is accounted for. As noted in the literature review (paragraph 3.1.3), seagrasses are not able to settle on the locations where the lugworm is reworking the sediments and most often the border between the habitat of the two species is quite abrupt (Philippart, 1994). For this reason, it is decided that on the locations where the lugworm settles, no seagrasses will be able to settle, regardless the lugworm concentration within that cell. However, once seagrass is settled, it will be impossible for the lugworm to settle in these same locations since the rhizomes of the seagrasses will prevent the lugworms from digging into the soil (Philippart, 1994). Once seagrasses or lugworms die because of changes in physical conditions, the model allows for

the other species to take over. Within the model environment, the species will only die as a result of changes in the abiotic environment which make the habitat unsuitable for the species. Other factors like age are not considered in the computations.

	Control run	**Lugworm**	**Seagrass**	**Multi-species, no competition**	**Multi-species, competition**
No mud inflow	1a	2a	3a	4a	5a
Mud inflow ($0.1kg/m^3$, $0.5m^3/sec$)	1b	2b	3b	4b	5b

Table 3: All model scenarios with two different mud inflow conditions (with or without active mud inflow). For the lugworm run, textfiles with species specifications are added to the Benthos model. For the runs with seagrass the vegetation model was used. For the multi-species scenarios, both matlab models are coupled to the Delft 3d environment.

4.2.6 Analysis of the model results

For each morphological month (which represents one tidal cycle) data is saved in the output files of the benthos and vegetation models. These files are organised in a folder for each of the 50 years. For each month, the fractions of the species is saved for each cell in the model domain. A different file contains the physical parameters in the domain saved for each 36 minutes. The contents of these files can be loaded into MATLAB where the data can be analysed. For data analysis, the data collected for the 7^{th} month of the year is used. Since, seagrass biomass is maximum in during this month. Lugworm concentrations are overall constant over the year. The species are removed from the model domain during the last month and new calculations for the lugworm distribution are made and updated from the second month of the new morphological year onwards. Seagrasses start to grow in the third month and reach maximum concentrations in the 7^{th} month after which it stays constant for 4 months before they die off in winter. By the start of the 12^{th} month, the stem height of the vegetation in the model domain will have decreased to 0 m. Their rooting system remains to calculate the habitat suitability of the lugworms. Overall, analysis of the results is done for the last year of the run, so the results of 50 years of hydro-morphodynamic and ecological interactions are analysed. Inundation periods, bed shear stresses and flow velocities are determined as the average value for the 7^{th} month of the last year. The data saved for each cell is used to compute maps, cross-sections and graphs to visualise model results over space and over time on different scales.

5 Results

5.1 Abiotic factors and the abundance of ecosystem engineers

Physical factors within the marine environment significantly determine the habitat suitability for lugworms and seagrass species (Fig. 8). Mud content, bed shear stress, flow velocity, and inundation period are considered to be the most important abiotic factors determining the presence of the two species on a certain location within a tidal embayment. In general, other factors like water temperature and salinity also have an impact on species distribution. Here I assume that water temperature and salinity do not differ significantly over the domain. Furthermore, wave forces are neglected and only tidal currents are accounted for in the model computations.

5.1.1 Lugworm distribution over the tidal basin

To study the effects of mud on species abundance, I compare species pattern for two mud inflow conditions, which result in different average mud content of the bed (Table 3 scenarios 2a and b). In scenario b (sustained mud inflow), the floors of the mud inflow channels are still covered with mud. Whereas in scenario a (no active mud inflow), tidal flow has eroded the mud from the bed in these inactive inflow channels over time. The tides will take up the mud from these channels and distribute it over the domain. Most of the mud will end up high on the tidal flats and near the inlet and the deep the ocean basin, where bed shear stresses are low because of very shallow and very deep water depths respectively. In scenario b, tidal currents transporting the mud out of the channels are not able to keep up with the mud inflow. Mud is still settling in the channels of the model domain, hence the relatively large bed shear stresses and flow velocities here.

In general, the lugworm mainly settles on the upper parts of the tidal flat where mud content in the bed is below 100% (Fig. 10 1A&1B). When comparing the scenario with a high mud content (b) with the scenario where the mud inflow is lower (a), it becomes clear that lugworm densities and the total area colonised by the species is significantly larger in scenario b (Fig. 9 A&D). Apparently, the amount of mud in the system does affect the lugworm positively. The areas with intermediate mud concentrations, the areas suitable for the lugworm, are larger in scenario b. On the other hand, the area unsuitable for the species, where mud contents are too high, also increases in this scenario. As a result, the species move more offshore as more mud concentrates on the upper ends of the tidal flat. In both scenarios, the lugworm settles on the banks along the channels where the mud comes into the system from upstream (Fig. 10 1A&1B). Generally, lugworm abundance is limited by mud content in most areas of the basin.

The lugworm is settles upon the banks of the tidal channels and some distance up onto the tidal flat where bed shear stresses, and thus flow velocities, are considerably low (Fig. 10 2A&B). In scenario b, where the mud content in the domain is high, shear stresses in the active feeding channels are higher compared to scenario a where the inflow channels are no longer active. Lugworm settlement does respond to these differences. Species concentrations near the active channels are low whereas, when the mud inflow is stopped (scenario a), the species seem to colonise the mud inflow boundary and the upper parts of the feeding channels.

The model outcomes show a distribution of lugworms along the intertidal, whereas no species are settling in the subtidal or supratidal zones (Fig. 10 3A&B). The species avoids the larger depths of the tidal channels and is not settling on the highest parts of the tidal flats where inundation periods are rather short. Figure 9C, shows a difference in distribution of the species over inundation period for the two scenarios. In scenario b,

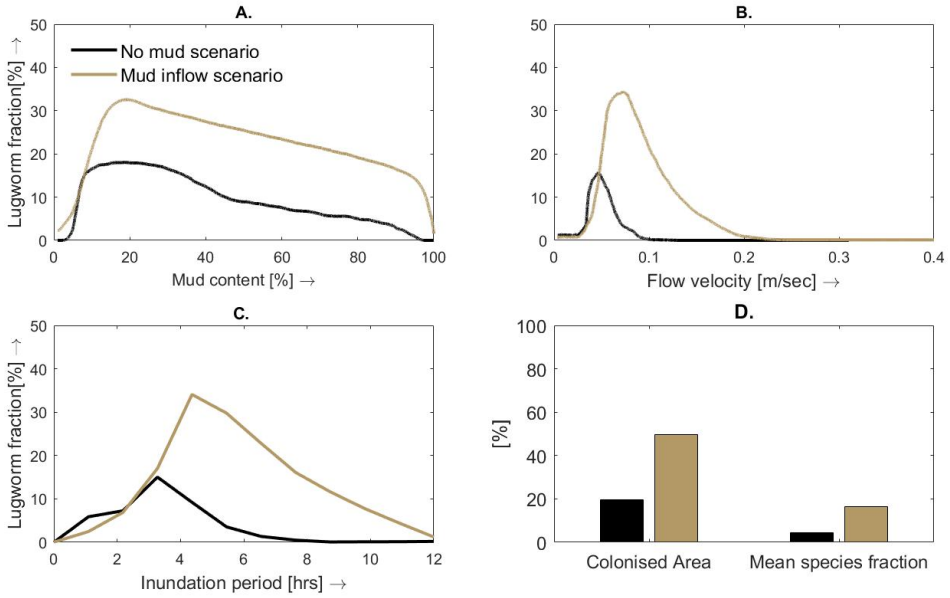

Figure 9: visualisation of lugworm fractions over mud content, flow velocity and inundation period for a scenario with and without an active mud inflow boundary (scenario 2a&b). Panel A. shows the distribution of lugworm fractions over mud content. For both scenarios the species show an even distribution over mud content. Panel B. shows the distribution of lugworm fractions over flow velocities. The highest lugworm fractions are concentrated below a flow velocity of $0.2m/sec$ for both scenarios. Panel C. visualises the distribution of lugworm densities over inundation period in the tidal basin. For scenario 2b, a higher lugworm densities are found for locations with longer inundation periods. Panel D. shows the colonised area by lugworms in the tidal basin for the two scenarios and the mean species fraction. Both values are larger for scenario 2b, where a mud inflow into the model domain was sustained

the species show a wider distribution over inundation period, when compared to scenario a. Since lugworm settlement is mainly limited by mud concentrations, the mud inflow in scenario by overall increases the mud contents in areas with a large inundation period. As such, these areas become suitable habitat for the species.

Mud content shows to be the most limiting factor as it comes to successful settlement of the lugworm in a tidal basin. Since the range over which the species settle over flow velocities and inundation period are much wider for scenario b (Fig. 9B&C). Furthermore, species concentrations and colonised area are significantly larger in scenario b. Lugworms seem to settle regardless of the inundation period, although they avoid subtidal and supratidal zones. Mud content and bed shear stresses are however limiting species settlement significantly. Lugworms settle in locations where mud contents are average and bed shear stresses are low. When comparing two scenarios, one with and one without an active mud inflow into the system, it becomes clear that more mud in the domain (scenario b) will not limit but rather enhance lugworm settlement. A larger area of the domain will know an intermediate mud content and will for this reason be more suitable for the lugworm species. However, shear stresses in the feeding channels are lower once the mud inflow is stopped (scenario a), which allows for species to settle at these locations.

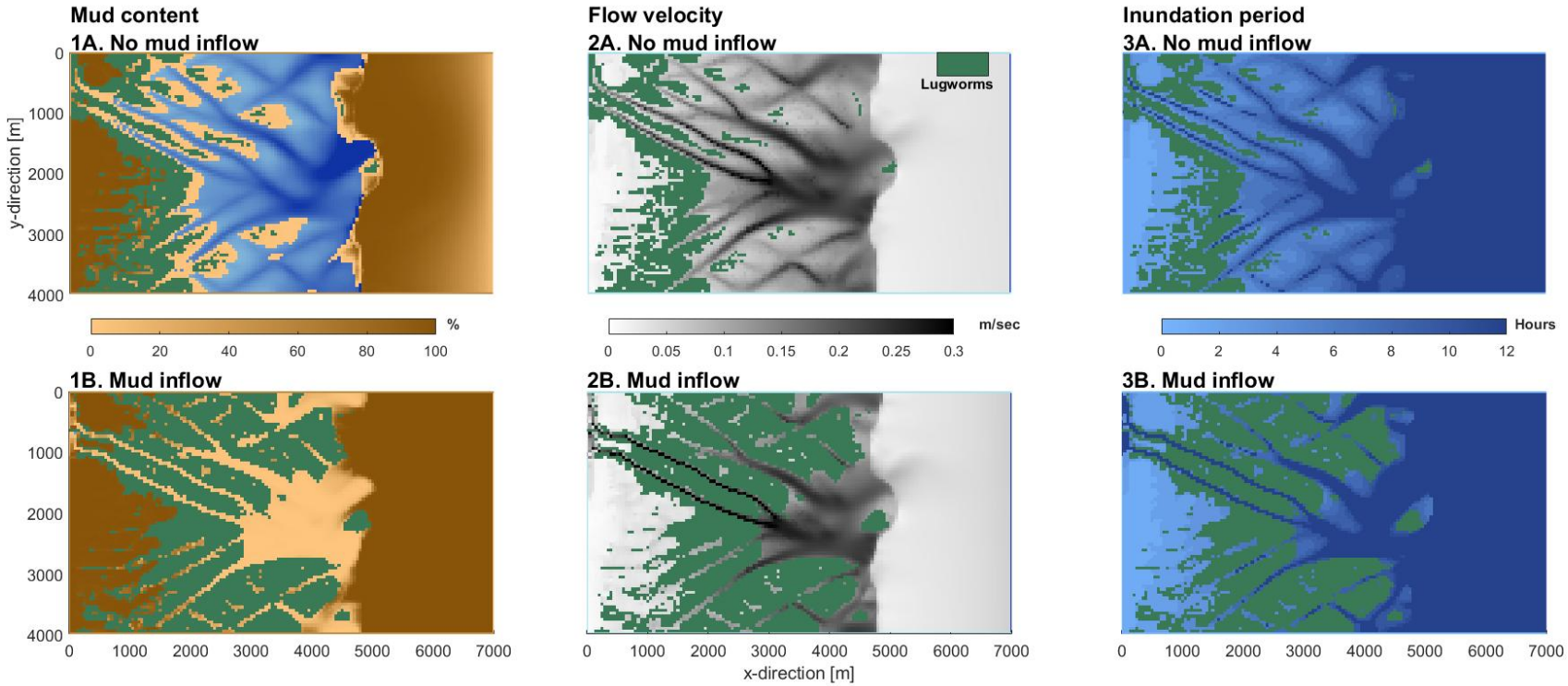

Figure 10: Lugworm distribution (green) over the model domain overlain on base layers showing different physical parameters: mud content, flow velocity (as an average over a tidal cycle) and inundation period. The upper row shows the model results for the scenario where the mud inflow was cut-off (scenario 2a). The lower row of panels shows the scenario where mud is still flowing into the basin (0.1 kg/m^3 with an inflow velocity of 0.5 m^3/sec) (scenario 2b). The area colonised by the species is significantly larger for scenario 2b. Furthermore, the species is settling in the locations where conditions are relatively calm (low flow velocities) at the upper elevations of the intertidal zone.

5.1.2 Seagrass distribution over the tidal basin

To identify what environmental parameters determine the distribution of seagrass over the tidal basin, species densities are analysed for different values of mud content (scenario 3a vs 3b, Table 3), bed shear stress and inundation periods (Fig. 12). When comparing model scenario 3a and 3b, it is observed that mud fraction in the domain barely affects the density and area colonised by seagrasses (Fig. 12 bar charts 2A&2B). The area colonised by the species only differs slightly over the two scenarios (Fig. 11D). In general the species are found on the locations where conditions are calm and the bed contains some mud in the intertidal zone. However, there are also locations of seagrass presence where the bed is sandy (Fig. 11A). When looking at Figure 11A, the differences in seagrass settlement over mud content between the both scenarios become clear. For scenario a, the species settles on much lower mud conditions than for scenarios b. When comparing this graph to the distribution map, is becomes clear that the species settle on the same locations in scenarios a and b. However, the mud content in these locations change as the mud inflow is sustained or stopped. It becomes clear that the seagrass easily adapts to different mud concentrations.

The distribution of seagrass over the tidal embayment shows a dependency on flow velocities in the tidal channels (Fig. 12 2A&B and fig. 11B). Overall the vegetative species is settling on the banks of the channels and does not grow on the channel floors where flow velocities are simply too high for the seedlings to settle and germinate. Seeds will not be able to settle in the channels and growth rates will be significantly lower in places where shear stresses and flow velocities are high (Peralta et al., 2006). In the centre of the domain, some seagrass fields of are found in areas where flow velocities are higher. However, species fractions quickly decrease with increasing flow velocities Fig. 11B). In scenario a, where the mud inflow into the tidal embayment has been stopped, the seagrass finds its way into the old channels of the inlet system. This is the only location and scenario where the species is found far up the tidal flat.

The inundation period is an important factor determining the seagrass distribution over the tidal basin domain. When looking at the inundation map, the distribution of seagrasses perfectly follows the inundation lines within the domain (Fig. 12, 3A&B). In general, no species are found on locations where the inundation period is shorter than 4 hours or longer than 8 hours per tidal cycle. Figure 11C, also shows species presence outside of the window of opportunity for seagrasses. This will be elaborated on more in the discussion section of this report. The mud inflow entering the system from the open boundary in the scenario b, has the possibility to affect the bed elevation in such a way that inundation periods differ between the two scenarios. When looking at the seagrass distribution differences between scenario a and b, some small differences are observed in the centre of the domain where inundation periods differ. The clearest differences between the two scenarios are however found near the mud inlet, where inundation periods are higher for scenario b where the inflow channels are active. The seagrass species is not able to settle in and around the inlet system due to high inundation periods and higher bed shear stresses.

Generally, seagrass distribution is mainly limited by inundation period and flow velocity rather than mud content. Not much differences in species concentrations and colonised area in the model domain are observed between the two scenarios with and without an active mud inflow (Fig. 11D). However, species settlement and distribution is significantly affected by flow velocity and inundation period. Species densities on locations with higher bed flow velocities are low compared to calmer conditions. Furthermore, seagrasses do not settle further up on the tidal flat where inundation periods are short.

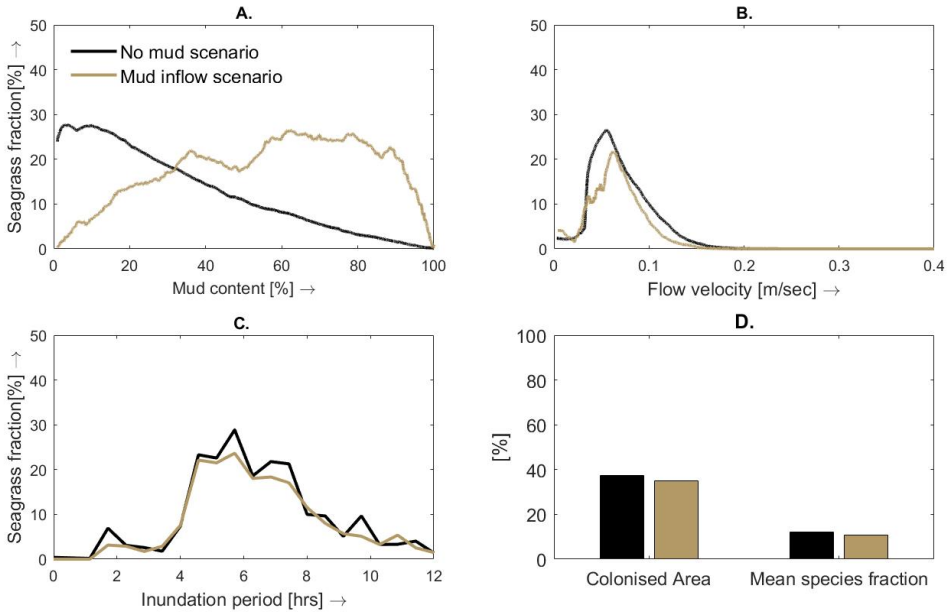

Figure 11: visualisation of seagrass fractions over mud content, flow velocity and inundation period for a scenario with and without an active mud inflow boundary (scenario 3a&b). Panel A. shows the distribution of seagrass fractions over mud content. For scenario 3b, species fractions are higher for higher mud concentrations. Explained by the fact that the overall mud content in the basin is higher in this scenario. Panel B. shows the distribution of seagrass fractions over flow velocities. The highest seagrass fractions are concentrated below a flow velocity of $0.2m/sec$ for both scenarios. Panel C. visualises the distribution of seagrass densities over inundation period in the tidal basin. For both scenarios, the same distribution of seagrass densities is found. Panel D. shows the colonised area by seagrass in the tidal basin for the two scenarios and the mean species fraction. Both values are slightly larger for scenario 3a, but no significant differences are found

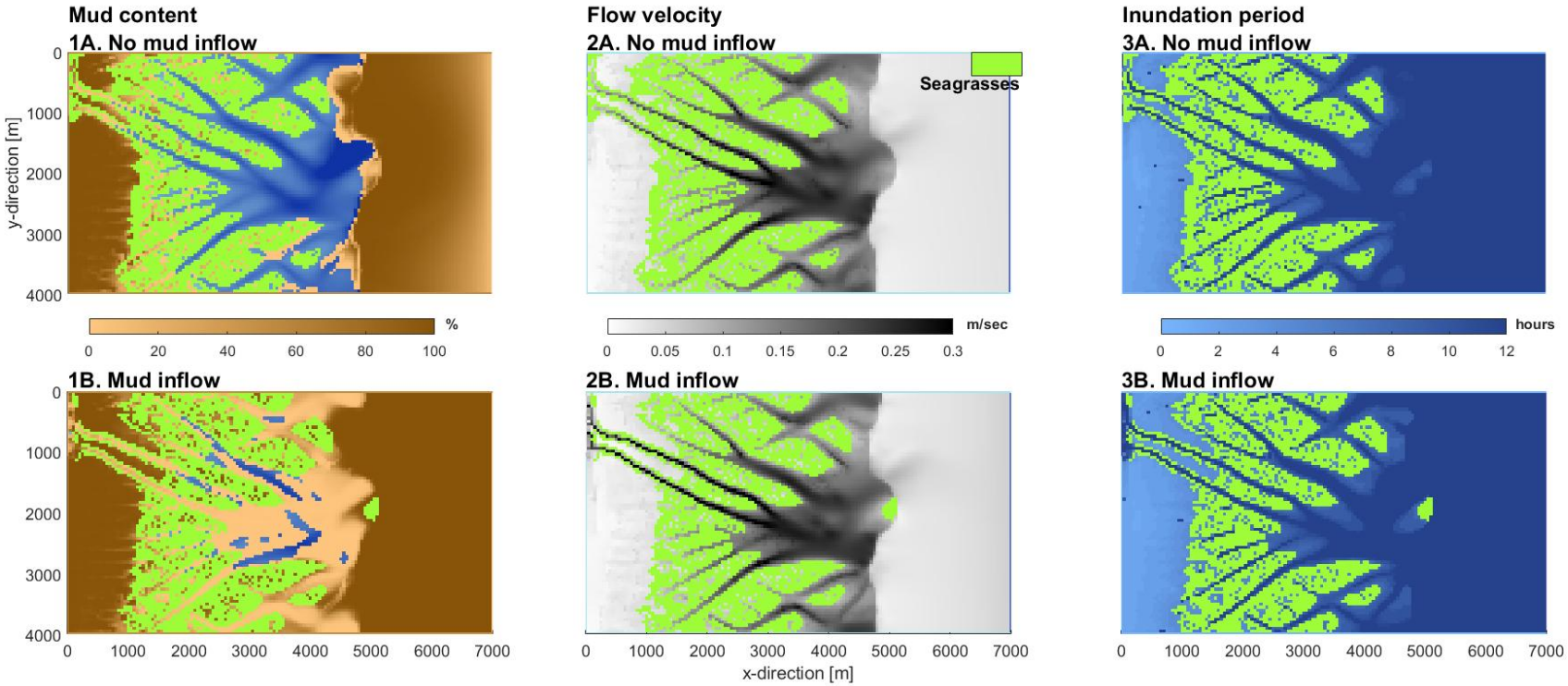

Figure 12: The maps show seagrass distribution (green) over the model domain overlain on base layers showing different physical parameters: mud content, flow velocity (as an average over a tidal cycle) and inundation period. The upper row shows the model results for the scenario where the mud inflow was cut-off (scenario 3a). The lower row of panels shows the scenario where mud is still flowing into the basin (0.1 kg/m^3 with an inflow velocity of 0.5 m^3/sec) (scenario 3b). The area colonised by the seagrass seems not to differ much between the two scenarios. However, its settlement seems to overlap with specific inundation periods. Furthermore, the species is settling on the locations where conditions are relatively calm (low flow velocities) in the intertidal zone.

5.2 Effects of ecosystem engineers on sediment dynamics

The bioturbating lugworm and stabilising seagrass both have a different effect on local sediment dynamics and morphodynamics. The activities of the lugworm are modelled in terms of a lower critical bed shear stress and a higher erosion parameter, whereas the effects of the stabilising seagrasses are computed as a local increase in the drag coefficient. These locally changing parameters as a result of species settlement will have an impact on the morphology of the tidal basin.

5.2.1 Bioturbating activities by the lugworm

To identify the effects of bioturbating activities by the lugworm, the scenario with lugworms (scenario 2b) is compared to the control run without species activities (scenario 1b). In terms of mud content in the tidal basin, it is clear that on the locations where the lugworm settles, the mud content decreases significantly as compared to the control run as opposed to the mud volume in the system, which shows a slight increase as compared to the control scenario (Fig. 13 A&B). Figure 14 A,EF show that at bed elevations between -1 to 1.5 metres, where lugworm concentrations are highest, mud fractions are significantly lower compared to the control run without eco-engineering effects. The mud volume on these locations does change much over the different scenarios. However, an increase in mud volume is found at the higher intertidal. The maps show the same trends. In the locations lugworm densities are high, it can be observed that mud contents are around 30% lower than in the control run. Along the higher intertidal (Fig. 15 A&B), the mud content is significantly higher than for the control run, where no lugworms are present. Similar trends are found in locations near the shallow ends of the tidal channels where mud is being deposited on the bed of these channels.

The same patterns can be found when looking at changes in bed elevation as compared to the control run (Figure 15C). In the location where the species settle, mudflat elevations tend to decrease and sediment is eroded. The sediment is transported towards the inlet of the tidal basin where it will settle at larger water depths where flow velocities are lower. Furthermore, the sediments eroded from the tidal flats are deposited on the bed of tidal channels where bed shear stresses low and at higher elevations of the tidal flats where small flow velocities cause the sediment to settle.

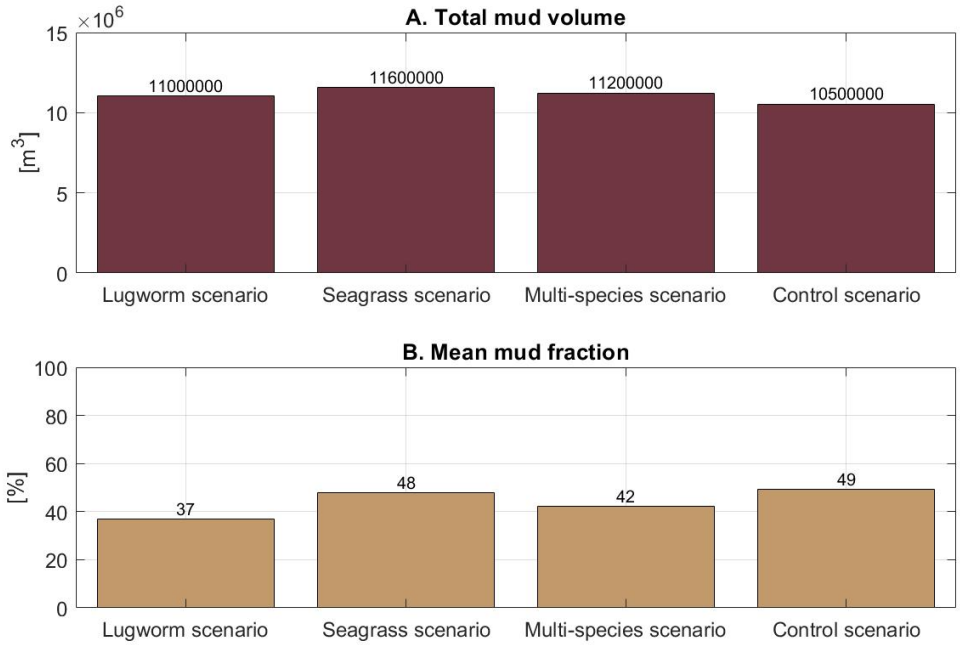

Figure 13: Visualisation of the total mud volume and the mean mud faction in the tidal basin for 4 different scenarios. For the calculations the scenarios with an active mud inflow are considered. The ocean basin is excluded from the calculation of these values. Highest total mud volume can be found for the seagrass scenario (scenario 3b). However, mud fractions are higher for the control scenario (scenario 1b). Lowest values are found for the lugworm scenario (scenario 2b).

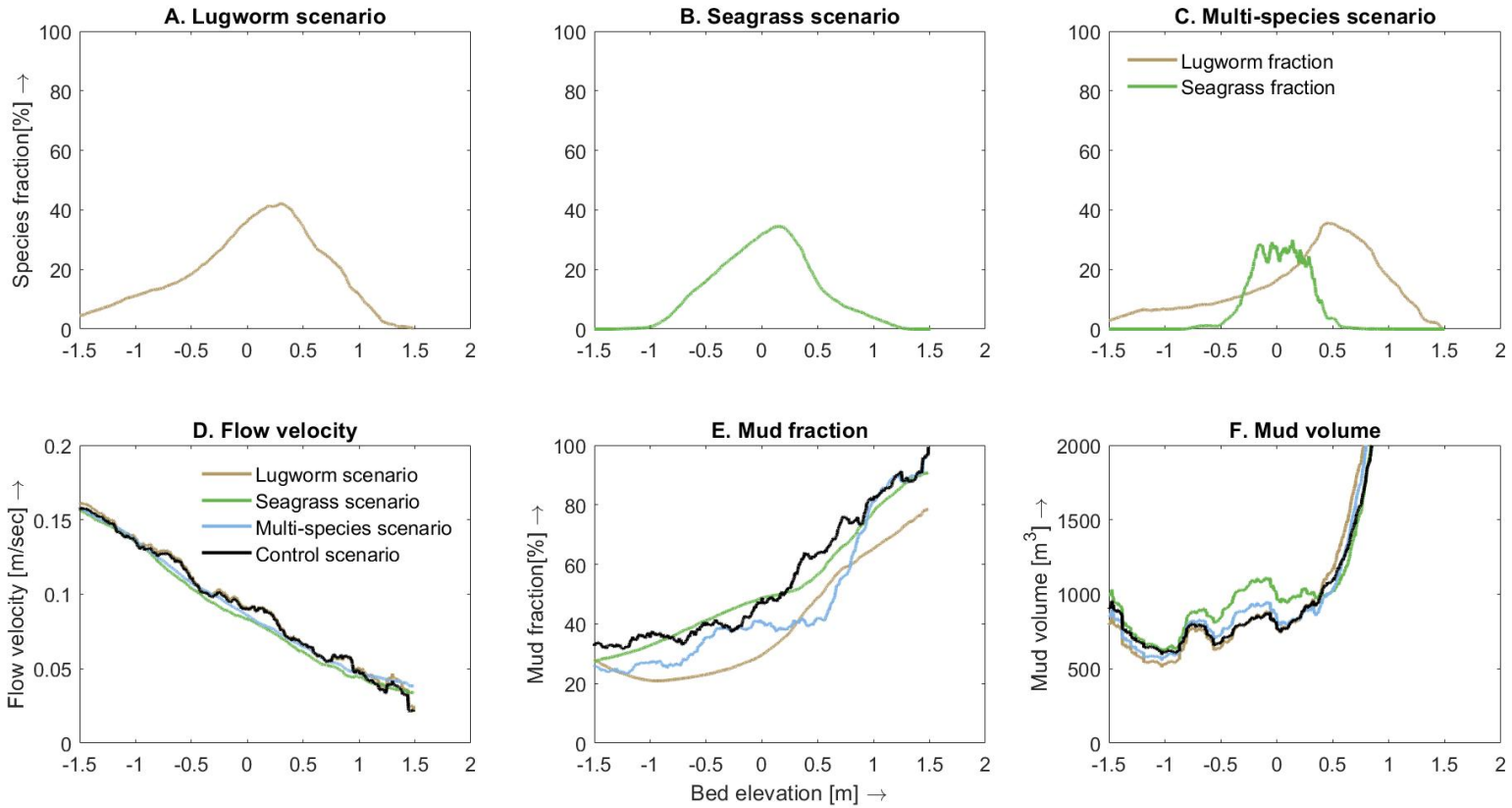

Figure 14: This figure shows species fractions for different scenarios and different physical parameters (flow velocity, mud fraction and mud volume) over the bed elevation of the tidal basin. Panel A. shows the distribution of lugworm fractions over bed elevation, where the highest lugworm fractions are found between -5 and 1 metres of bed elevation. Panel B. shows the distribution of seagrass fractions over bed elevations. A similar distribution to the lugworms is found here. Panel C. shows the distribution of species fractions over the model domain for the multi-species scenario (scenario 5b). The lugworm colonises the higher elevations,as seagrasses are restricted to the lower elevations. Panel D. shows the flow velocities over bed elevation for 4 different scenarios. A reduction in flow velocities can be observed on the elevations where seagrasses are present in the seagrass and the multi-species scenarios. Panel E. visualises a decrease in mud fraction on the elevations where lugworms are present in the scenarios. On the elevations where seagrasses are present, the mud fraction is similar to the control scenario. Panel F shows an increase in mud volume on the elevations where seagrasses are present in the tidal basin and a decrease in mud volume where lugworms are present or where the soil is bare in the seagrass scenario.

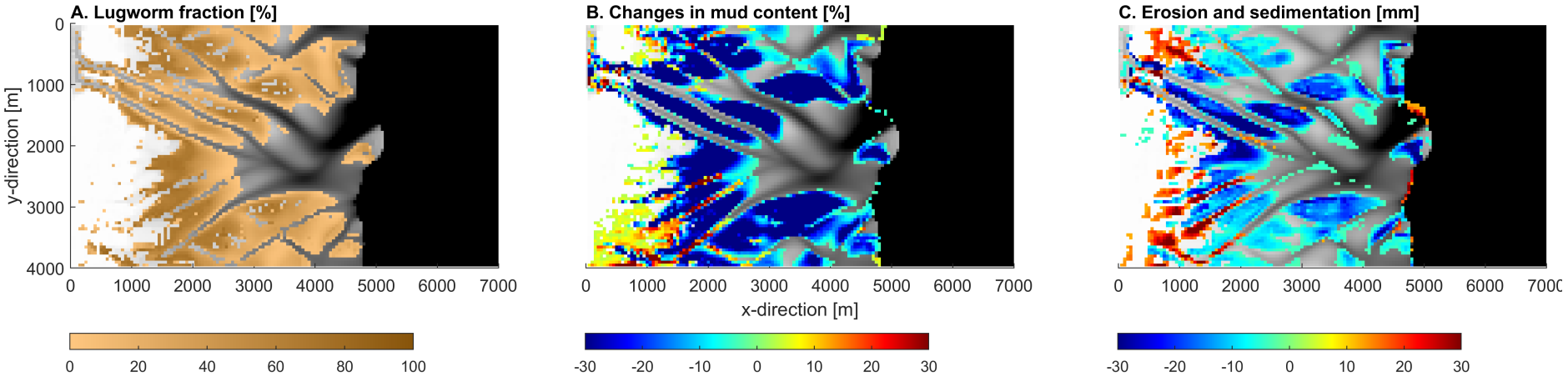

Figure 15: Panel A shows the distribution of the lugworm over the domain. Species fractions are visualised by the colour gradient. Panel B shows the mud concentrations as compared to the control run. Negative values depict locations where mud concentrations are lower than in the control run. Positive values depict locations where mud concentrations are larger than in the control run. Panel C depicts the bed elevation as compared to the control run. Negative values imply a lower bed elevation and positive values higher bed elevations than in the control run. It can be observed that in the locations where the lugworm is present, mud contents and bed elevation are reduced. However, in the tidal channels and further up the tidal flat, mud fractions are higher and an increase in bed elevation is visible for the lugworm scenario.

Figure 16, depicting the cross sections over one tidal channel, clearly shows the decrease in bed elevation as a result of lugworm settling on the tidal flats. Also, an increase in bed elevation of the tidal channels is shown next to a significant decrease in mud content on the tidal flats where the species are present. As the process of elevating channel beds and eroding tidal flats continues over a long timespan, channel patters may shift, as the flow will always search for the lowest location to go to. The lowering of lugworm habitat as a result of bioturbation will have a negative impact on the habitat suitability of the species as flow velocities, bed shear stresses and inundation periods will increase on these locations.

Figure 17 2A&B, shows a comparison with the control run where no ecosystem engineering activities were used for the computations defining morphology and sediment dynamics in the tidal basin. For the control run the habitat suitable for the lugworm was predicted and compared to the colonised area for the run with ecosystem engineering effects (scenario 2b vs a prediction of lugworm abundance on scenario 1b). Since the only difference between the two scenarios are the effects of the species on the morphology, it can be derived whether these activities have a positive or a negative effect on the habitat suitability of the species. As the colonised area by the lugworm is larger for the prediction on the control run than for the run with ecosystem engineering activities, it becomes clear that the bioturbating activities of the lugworm negatively impact the area suitable for the species to settle.

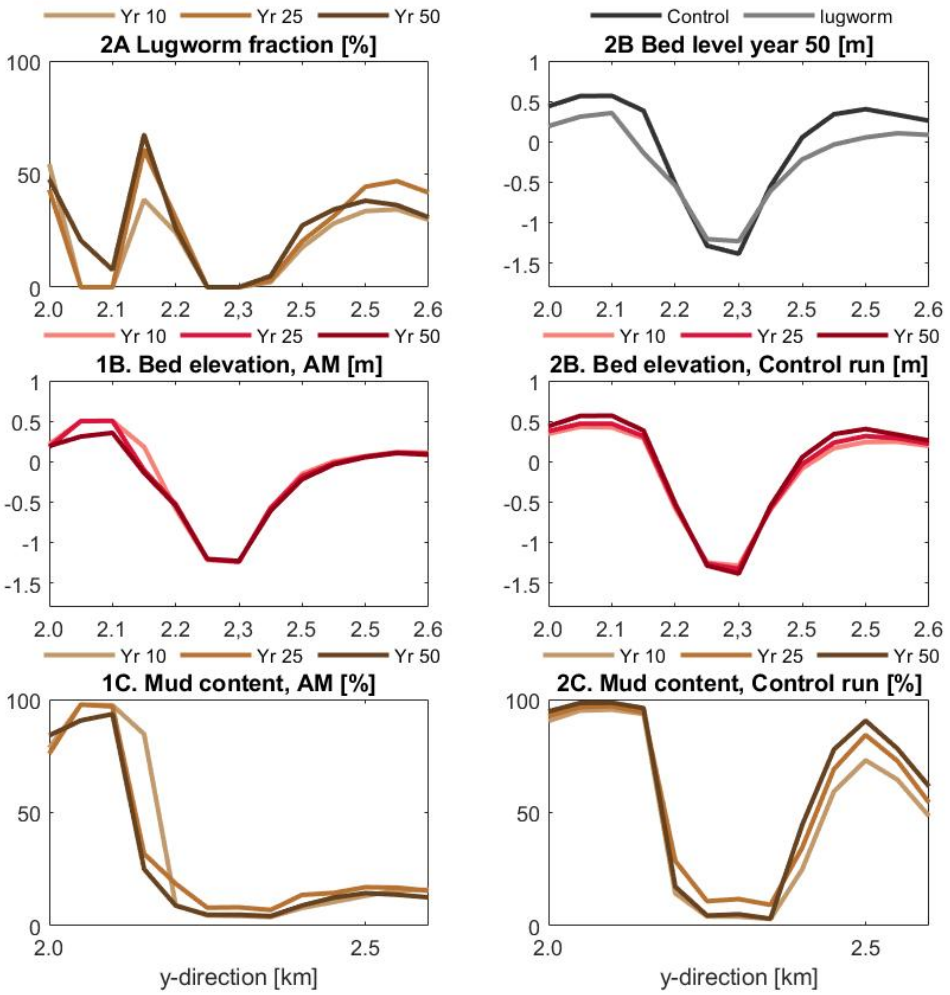

Figure 16: The figure shows data over a cross section of one tidal channel. Panels 1A-1C show species fraction, bed level and mud content for the scenario with the lugworm (AM) over 3 different years. Panel 2B and 2C depict bed elevation and mud concentration over the same cross-section for the control run for 3 different years. Panel 2A shows the bed elevations over the cross section for both the control run and the AM-run over the last year. when comparing the bed elevation profile of the control run to the scenario with ecosystem engineering activities, it can be observed that the activities of the lugworm have a negative effect on bed elevation as they promote erosion. Some of the eroded sediment seems to end up on the channel bed as the bed elevation on this location has increased slightly. Furthermore, the mud content is significantly lower on the locations where the lugworm has settled in the ecosystem engineering scenario.

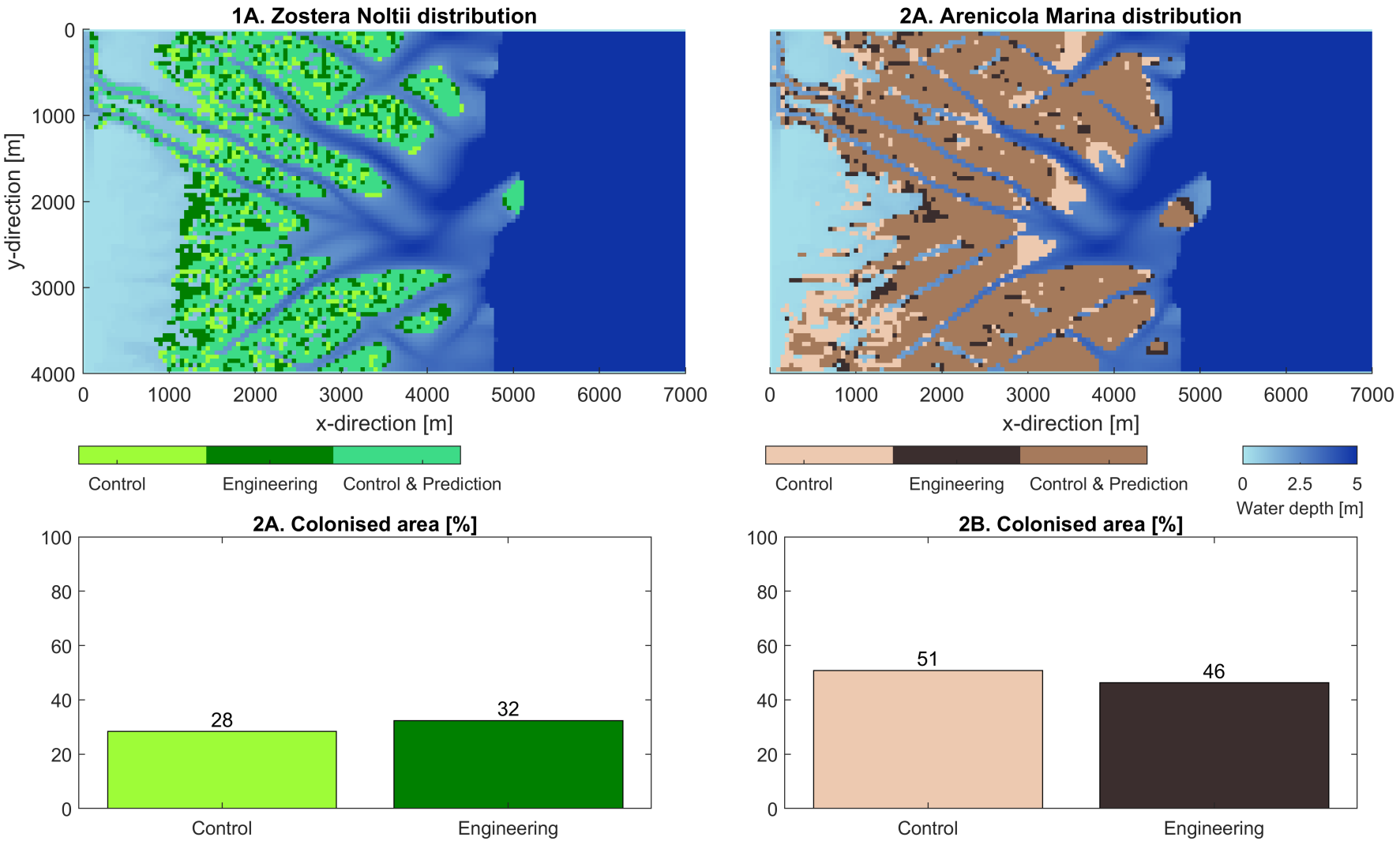

Figure 17: Panels 1A and 2A show habitat suitability of lugworms and seagrasses on the morphology of the control run, where no ecosystem engineering activities were accounted for. The differences in colonised area show the effect of ecosystem engineering activities on habitat suitability. Light green/brown show the colonised area in the control run, dark green/brown the colonised area in the engineering scenario, and intermediate green/brown colonised area in both scenarios. The bar charts below quantify total colonized area, showing that the area colonised by seagrasses in the scenario with ecosystem engineering is larger than the area suitable in the control run. the lugworm area is lower.

5.2.2 Stabilising activities by seagrasses

The scenario with seagrasses (scenario 3b) is compared to the control run (scenario 1b) without eco-engineering effects to identify the effects of the stabilising species on the tidal basin morphodynamics. In locations suitable for seagrasses, the ecosystem engineering effects are modelled through an increase in the drag coefficient within the seagrass patches. As the drag coefficient increases, flow velocities will decrease and sedimentation will be promoted (Table 2).

When looking at the mud content in the domain where ecosystem engineering activities of seagrasses are accounted for compared to the control run, where no ecosystem engineers are present, significant differences can be observed (Fig. 18B). In the locations where species densities are high, mud contents are significantly higher than compared to the control run. However, in the locations where seagrass densities are lower (lighter green colours on the map) and neighbouring cells do not contain any vegetation, mud contents are lower when compared to the control run. This is confirmed by Figure 14 B,D,E&F. At the elevations where seagrasses settle, flow velocities are lower compared to the control scenario. Furthermore, these are the elevations where mud fractions increase, as on lower and higher elevations mud fractions are lower than for the control scenario. Over elevations lower than the window of opportunity of the seagrasses, the mud volume is comparable to the control scenario. Then it shows an increase at the elevations where the vegetation is present and only a small increase on the higher elevations. Similar to the lugworm scenario, mud seems to be deposited at these higher elevations of the tidal flat. The seagrass fields tend to hold on to the mud in the system (Fig. 13A). Tidal flat elevations are for these reasons higher on the locations where seagrass fractions are large, when compared to the control run.

Figure 19 shows cross sectional data over a tidal channel in the tidal basin. Vegetation densities are high on the banks of the channel where they have settled and grown over the years. When comparing the flow velocity profile over the cross section to the control run, the ecosystem engineering activities lower flow velocities on the channel banks and increase flow velocities in the channel (Fig. 191B&2B). Furthermore, mud contents on the channel banks are significantly higher for the species run than for the control run. Due to the active mud inflow boundary, mud content on the tidal flats increases over time in both scenarios. However, the effects of the present seagrasses promote the settlement of mud on these locations significantly (Fig. 191C&2C). Figure 192A shows the bed elevation profile for both the species and the control scenario. It becomes clear how the effects of seagrass settlement on the channel banks promote the sedimentation and elevation of the banks, whereas channel floors are eroded and incision occurs. Over the years, a shift of seagrass settlement towards the inner channel banks is observed. The increasing bed elevation facilitates new habitat possibilities for the species on these locations, which points to a positive feedback between the species and its own habitat. This is also confirmed in Figure 171A&2A. The area colonised by seagrasses in the scenario with ecosystem engineering activities is slightly larger than the area suitable for seagrass settlement in the control run.

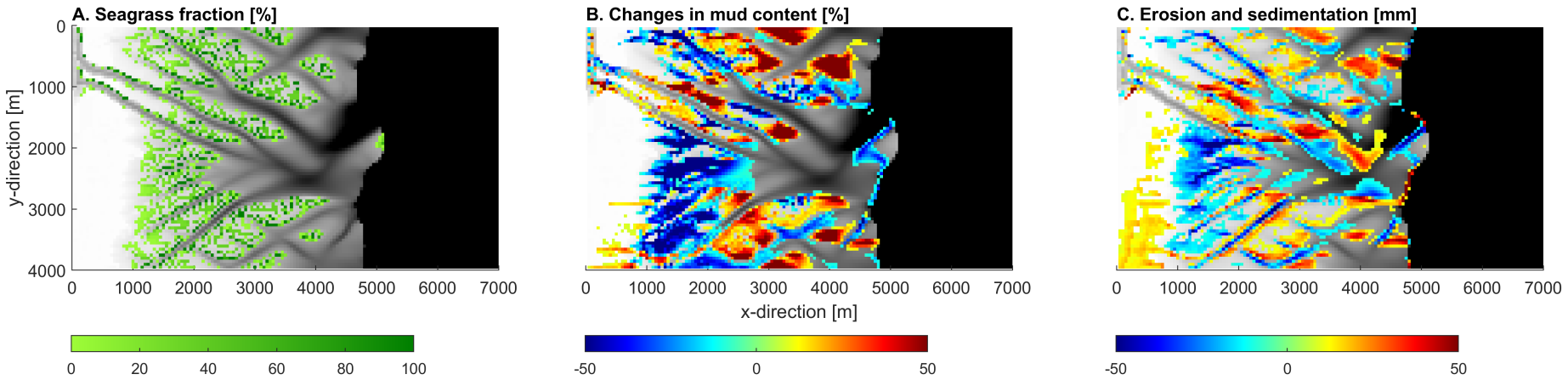

Figure 18: Panel A shows the distribution of seagrasses over the model domain. Species fractions are visualised by the colour gradient. Panel B shows the mud concentrations as compared to the control run. Negative values depict locations where mud concentrations are lower than in the control run. Positive values depict locations where mud concentrations are larger than in the control run. Panel C depicts the bed elevation as compared to the control run. Negative values imply a lower bed elevation than in the control run. Positive values show the locations where bed elevations are higher than in the control run. It can be observed that on the locations where seagrass fractions are high and patches are dense, the bed elevation is increased when compared to the control run. Also, the mud content has increased on these locations. On locations where the vegetation patterns are patchy or species fractions are low, erosion and a decrease in mud fraction can be observed.

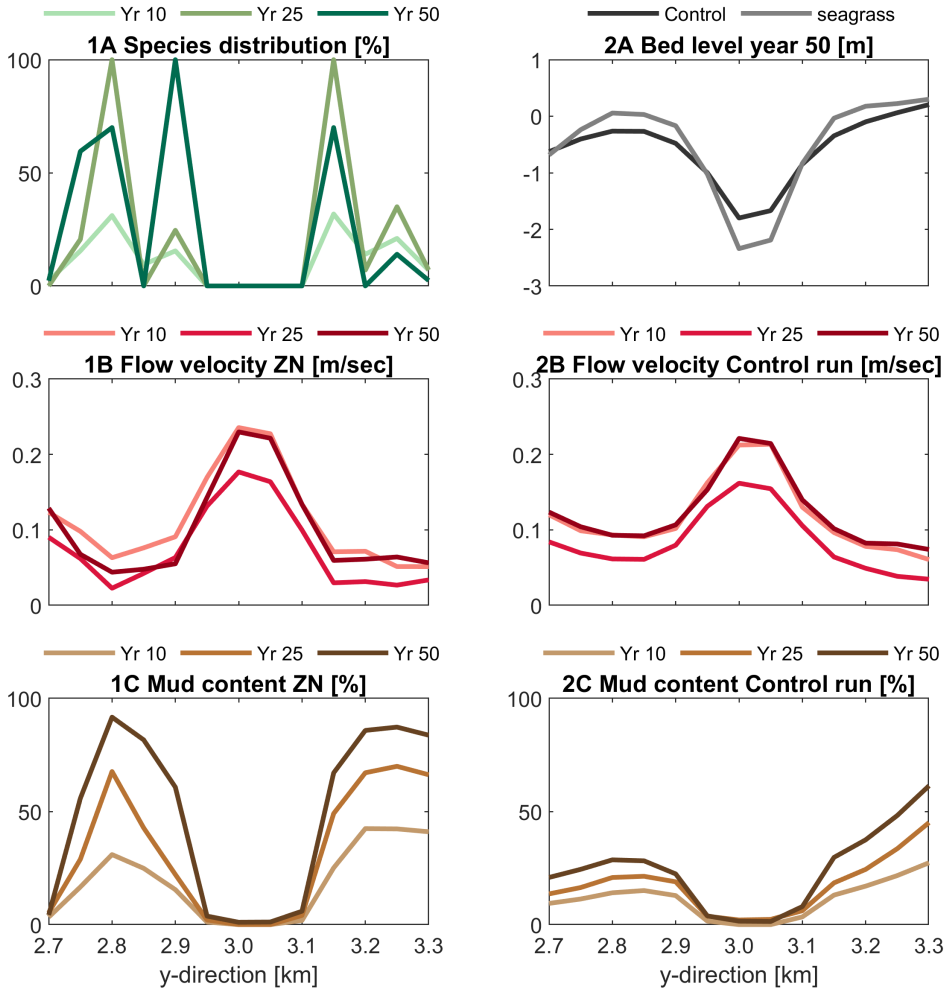

Figure 19: The figure shows the cross section over one tidal channel. Panels 1A-1C show species fraction, bed level and mud content for the scenario with seagrasses (ZN) for 3 different years. Panel 2B and 2C depict bed elevation and mud concentration over the same cross-section for the control run for 3 different years. Panel 2A shows the bed elevations over the cross section for both the control run and the ZN-run over the last year. The activities of ZN have a positive effect on bed elevation and mud content along the channel banks in the scenario with ecosystem engineers. Furthermore, flow velocities in the seagrass fields are lower than on bare channel banks, whereas the flow velocities in the channels increase.

5.2.3 Effects of multiple species on species pattern and sediment dynamics

To be able to identify the combined effects of both seagrasses and lugworms on the morphodynamics within the tidal basin, a multi-species scenario (scenario 5b) is run which accounts for competition between the two ecosystem engineers. As the lugworm is modelled to be dominant over the seagrass (Paragraph 4.2.4), the area colonised by the bioturbating species in the modelled tidal basin is larger than the area colonised by the stabilising seagrass (Fig. 21C). the lugworm is colonising most of the upper tidal flat, whereas the seagrass is more abundant on the tidal flats in the centre of the domain and at lower elevations (Fig. 20 & Fig. 21D). The stabilising seagrasses tend to locally increase the mud content as opposed to the lugworm, which decreases the mud content through its bioturbating activities (explained more in Paragraphs 5.2.1 & 5.2.2).

Sedimentation will occur in the central areas of the tidal basin where seagrass densities on the tidal flats are highest (Fig. 20A & C). Erosion is happening at higher elevations of the tidal flat where the lugworm is the most abundant species. At even higher elevations, where inundation periods are too short for both species to settle, both the mud content and bed elevations show an increase as compared to the control run (Fig. 20). The sediment eroded as a result of lugworm activities will be deposited on these locations on the tidal flat. An increase in mud volume can be found at these elevations (Fig. 14C,E&F). Furthermore, the figure shows a decrease in mud fraction at the elevations where the lugworm is the most abundant species. An increase in mud fraction and mud volume are found on the elevations where seagrasses are present. In the locations where seagrasses occur close to the tidal channels, these species will stabilise the channel banks and promote erosion of the channels (Paragraph 5.2.2). Once the lugworm is dominant on the channel banks, channels will receive more sedimentation (Paragraph 5.2.1). Over the whole tidal basin, it can be observed that channels are more prone to erosion than to deposition of sediments. When compared to the control run, most tidal channels have a slightly lower elevation when ecosystem engineering activities are considered. As seagrasses settle on lower elevations of the tidal flats and closer to the channel banks, it is able to capture the sediment brought into suspension by the lugworms further up the flat. As a result, the suspended sediments will be trapped by the vegetation before reaching the channel (Fig. 22).

Figure 21A,B&C compare the species distribution in the multi-species scenario to the predictions of the species distribution on the control run without ecosystem engineering effects. In the single species runs, stabilising activities by seagrasses had a positive feedback on the settlement and growth of the species whereas bioturbating activities of the lugworm had a negative impact on its abundance (Paragraphs 5.2.1 & 5.2.2). When both species are present, for both the prediction on the control run and for the multi-species scenario, the lugworm is the most abundant and dominant species in the tidal basin, although, the area colonised by lugworms is smaller in the scenario with ecosystem engineering effects (47% predicted on the control scenario vs 35% in the multi-species scenario) (Fig. 21C). For seagrasses the opposite is true, with the colonised area being larger in the multi-species scenario (5% predicted on the control scenario vs 15% in the multi-species scenario). The differences between the control run and the ecosystem engineering run seem to be larger compared to the single-species scenarios where the differences in colonised area between the species scenario and the prediction on the control scenario for both species did not exceed 10%. As such, the ecosystem engineering effects of the two species can amplify the positive and negative feedback mechanisms revealed in Fig. 17.

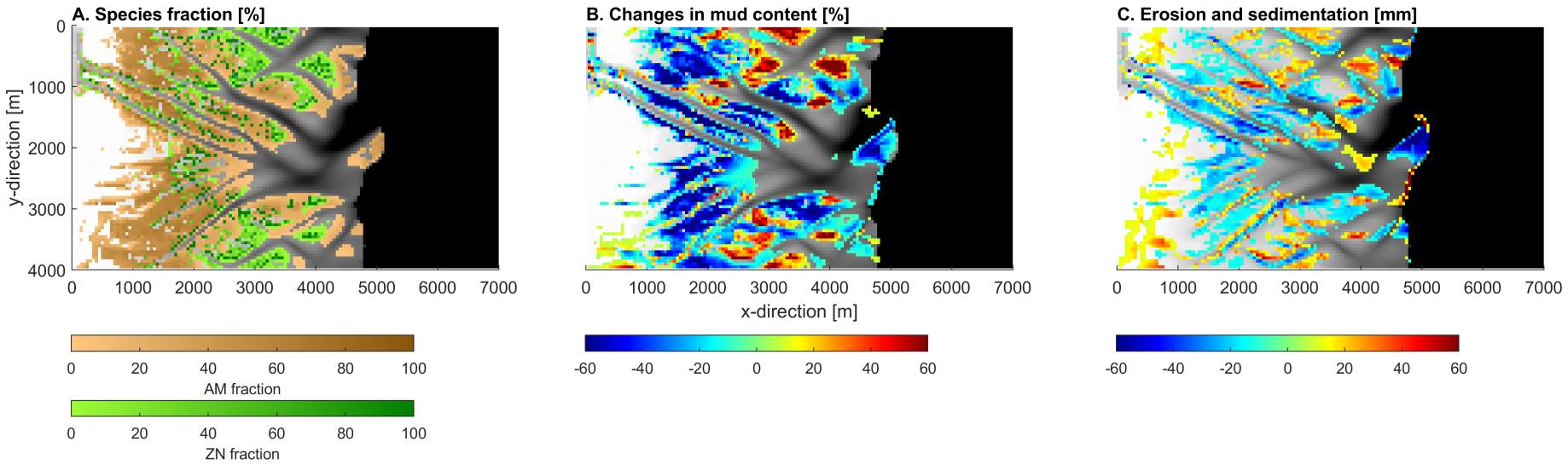

Figure 20: The figure shows species fraction (A), difference in mud content with control run (B), and bed level changes (C) for the scenario with both species on the bed elevation map. Negative values depict locations where mud concentrations and bed elevations are lower than in the control run. Seagrass settles in the lower intertidal zones where it enhances mud fraction and sedimentation of the tidal flats. Further up on the tidal flat, where the lugworm settles, the bed is eroding and mud contents are decreasing.

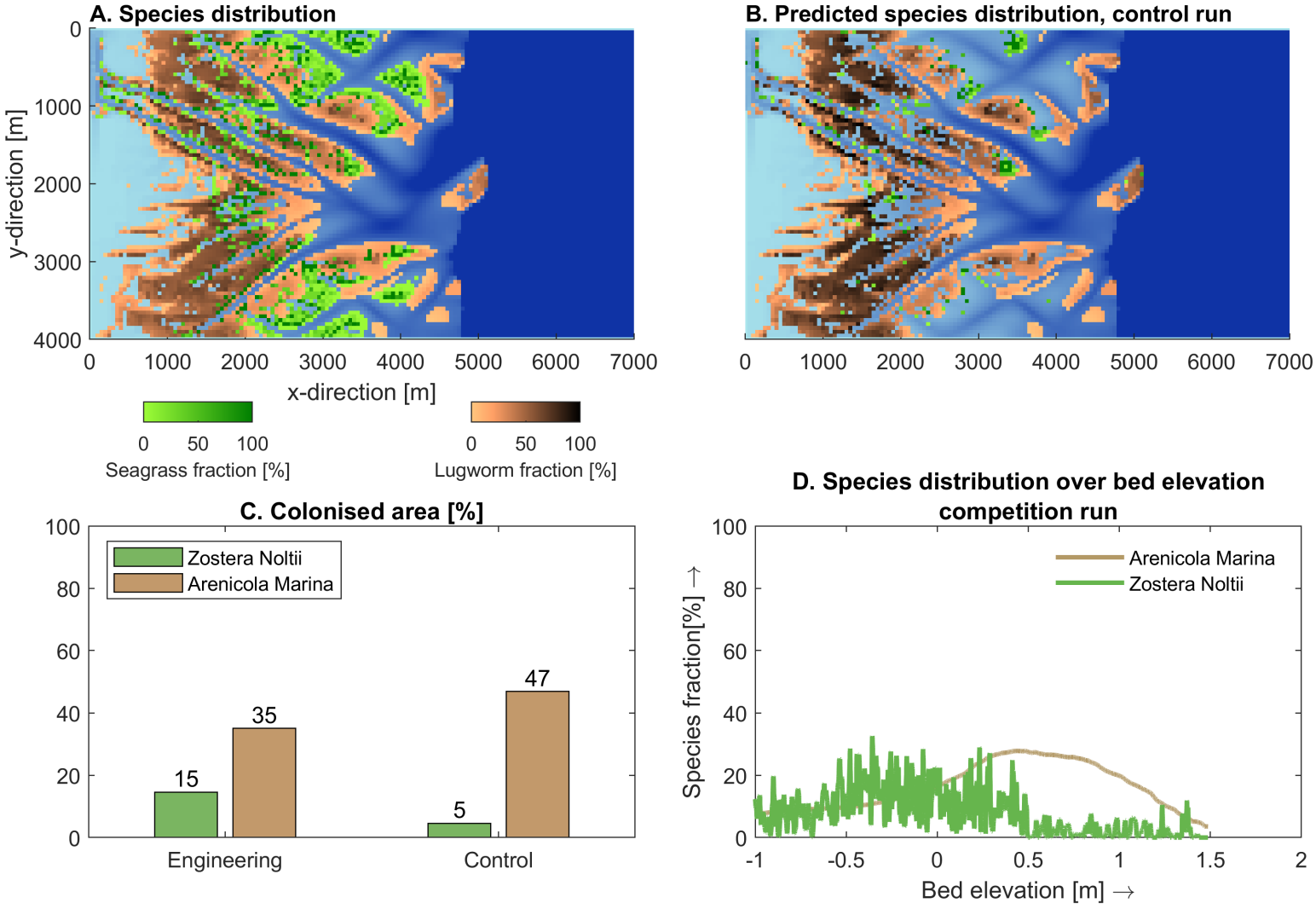

Figure 21: Panel A and B show the distribution of lugworms and seagrasses over the model domain for the multi-species scenario (scenario 5b) (A) and the prediction of both species when competition is accounted for on the morphology of the control run which was obtained without any ecosystem engineering activities (B). The bar chart (C) shows the colonised area by the species for both scenarios. Panel D shows the distribution of lugworms and seagrasses over the bed elevations in the model domain for the competition run with ecosystem engineering activities accounted for (A). The lugworm inhibits the upper intertidal zone, whereas seagrass is most abundant in the lower intertidal. Furthermore, the colonised area by seagrass is significantly larger in the scenario with ecosystem engineering activities accounted for, whereas the area colonised by The lugworm is on the contrary lower for the scenario with ecosystem engineering activities.

5.2.4 Ecosystem engineering feedbacks on morphology and tidal asymmetry

To identify the possible effects of the ecosystem engineers on ebb and flood dominance in the tidal basin, ebb and flood dominance were analysed over different species scenarios and different bed elevations. For the scenario without ecosystem engineering activities, the control run, the tidal basin experiences both ebb and flood dominance (Figure 23). At the higher elevations (intertidal zones) ebb dominance prevails, whereas the lower elevations (subtidal zones) are flood dominant. The lower the bed elevations, the larger the flood dominance.

For the single species scenario where lugworms are present (scenario 2), ebb and flood dominance only slightly change. The lugworm increases the ebb dominance at the higher elevations when compared to the control scenario. However, the species do not have a significant effect on flood dominance in the tidal basin. Changes in ebb or flood dominance are regulated by the lugworm on a local scale, as the species only thrives at the higher elevations in the tidal basin.

For the single species scenario where seagrasses are present (scenario 3), both ebb and flood dominance differ from the control scenario. At the higher elevations in the intertidal, the ebb dominance is slightly more powerful when compared to the control run. The same can be stated for the flood dominance in the lower subtidal areas. However, as bed elevation decreases more, the effect of the seagrasses dampens out.

For the multi-species scenario where both species and competition between the two species is considered (scenario 5), both ebb and flood dominance differ from the control scenario, though not as much as for the seagrass scenario. In general it must be noted that the differences in flow velocities and tidal asymmetry are rather small ($<0.05\ m/sec$).

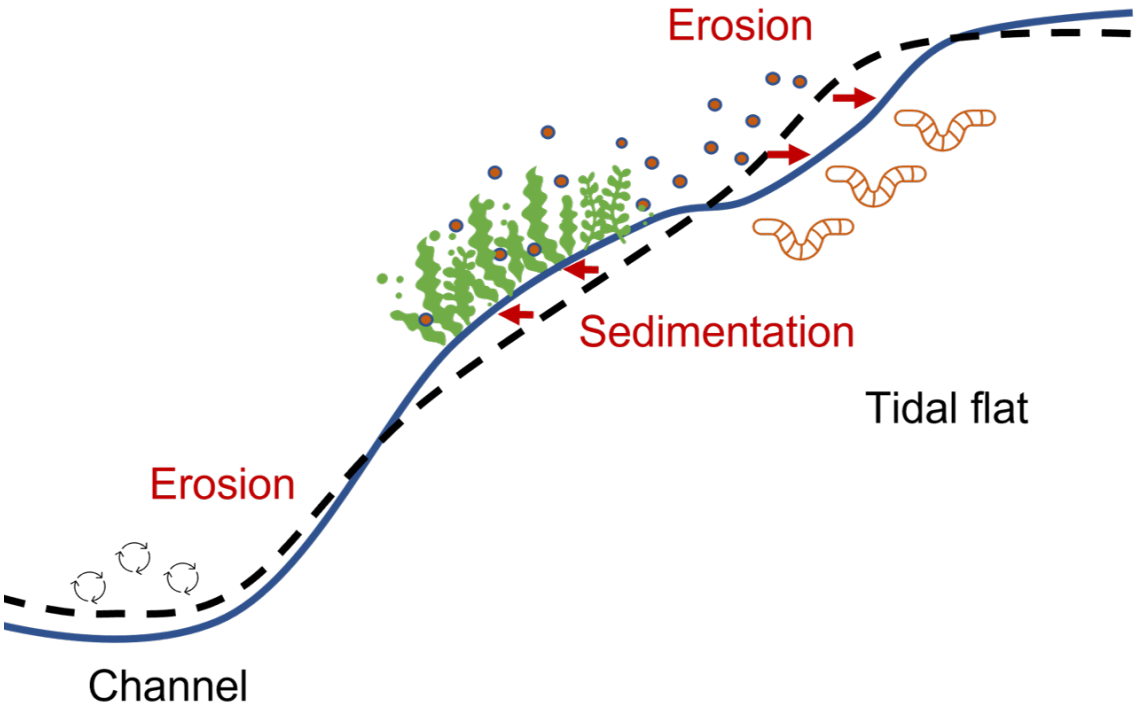

Figure 22: As seagrass settles on overall lower elevations of the tidal flat than the lugworm, it will be able to capture the sediments eroded by the bioturbating activities of the lugworm. As a result sedimentation of the channel bed by these sediments is prevented by the stabilising seagrasses.furthermore, the seagrasses will increase flow velocities in the channels as explained in the text. This will amplify the erosion of the tidal channel. The dotted line depicts the tidal flat profile for the control scenario.

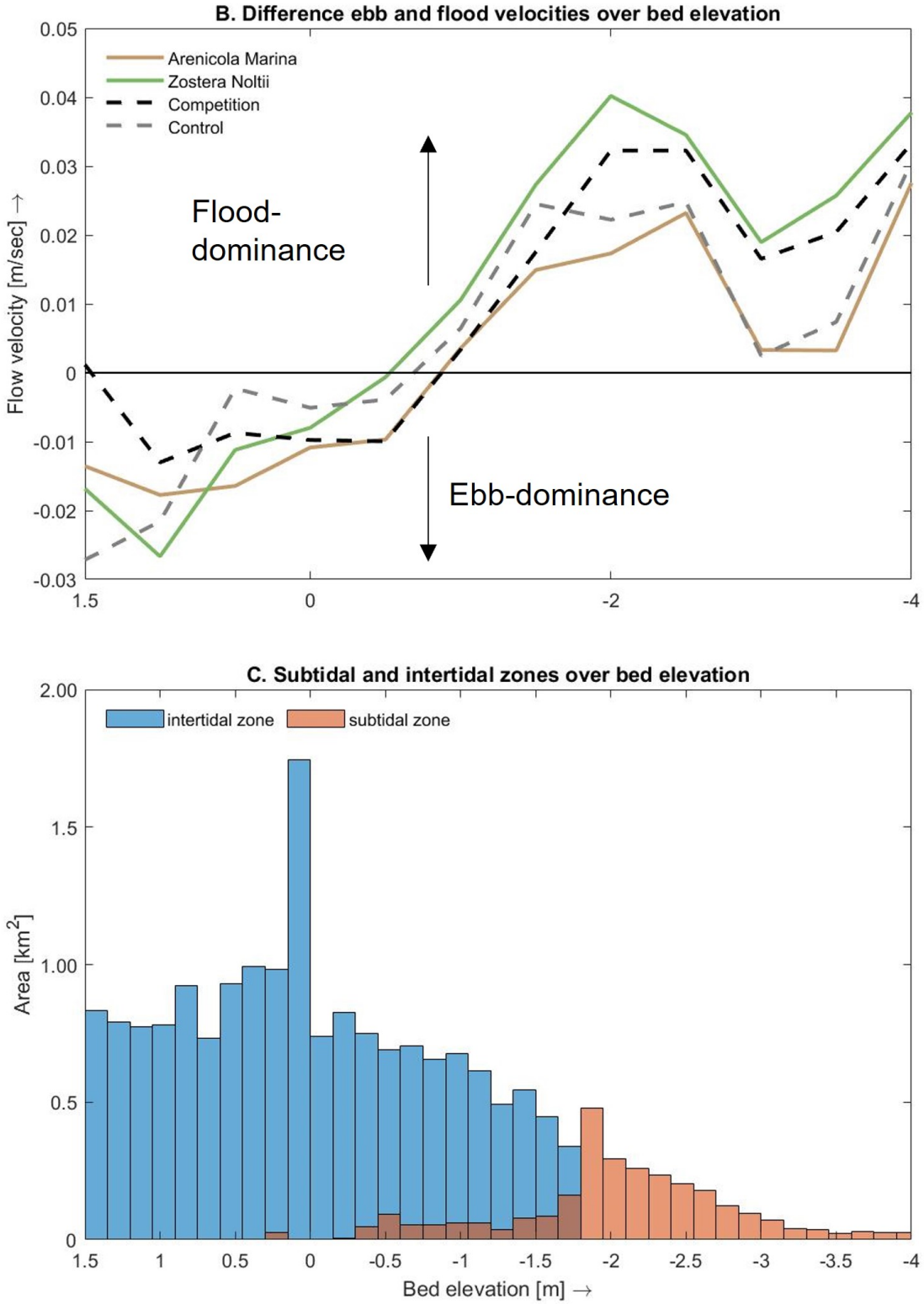

Figure 23: This figure shows the distribution of ebb and flood flow velocities over the intertidal and subtidal areas in the tidal embayment. Panel A shows the ebb and flood dominance over bed elevation calculated as ebb flow velocities subtracted from flood flow velocities. As deeper channels tend to be flood dominated, the upper intertidal is mostly ebb-dominated. Seagrass slightly increase tidal asymmetry in both the intertidal and subtidal zones. The lugworm only slightly increases ebb dominance in the intertidal. For the multi-species scenario, the ebb dominance in the intertidal decreases, whereas the flood dominance in the subtidal area increases. Panel B shows the distribution of the intertidal and subtidal areas over bed elevations in the tidal for the control run, as both species settle in the intertidal zone.

5.3 Interactions between ecosystem engineers

To establish how competition between the two ecosystem engineers determines species distribution within the tidal basin, the scenario with competition mechanisms is compared to the scenario without competition accounted for (scenarios 5 4 respectively) (Fig. 24). The scenario without competition allows for seagrasses and lugworms to colonise all suitable habitat in the domain, independent of the abundance of the other species in a certain location (Fig. 24A). In some areas, this results in both seagrasses and lugworms to be present (gray colour). 22% of the model domain is colonised by both species, as the lugworm covers an area of 36% of the tidal embayment and seagrasses 31% (Fig. 24C). Overall, these values point out a very even distribution of both species over the model domain. 71% of the area colonised by the stabilising seagrasses is also suitable for lugworm settlement, where only 61% of the area colonised by the lugworm is also suitable for seagrasses to occur as well. In these overlapping areas competition mechanisms will determine which of the species will settle in these locations.

As the lugworm is modelled to be dominant over seagrasses,it is as expected that the bioturbating species will colonise a larger area of the tidal embayment when competition is accounted for in the model computations (Fig. 24B). With competition, the lugworm colonises 35% of the model domain, which is almost similar to the area without competition mechanisms. Seagrasses merely colonise 15% of the tidal basin when competition is accounted for. The area which is suitable for both species to settle, is completely colonised by the lugworm (Fig. 24C).

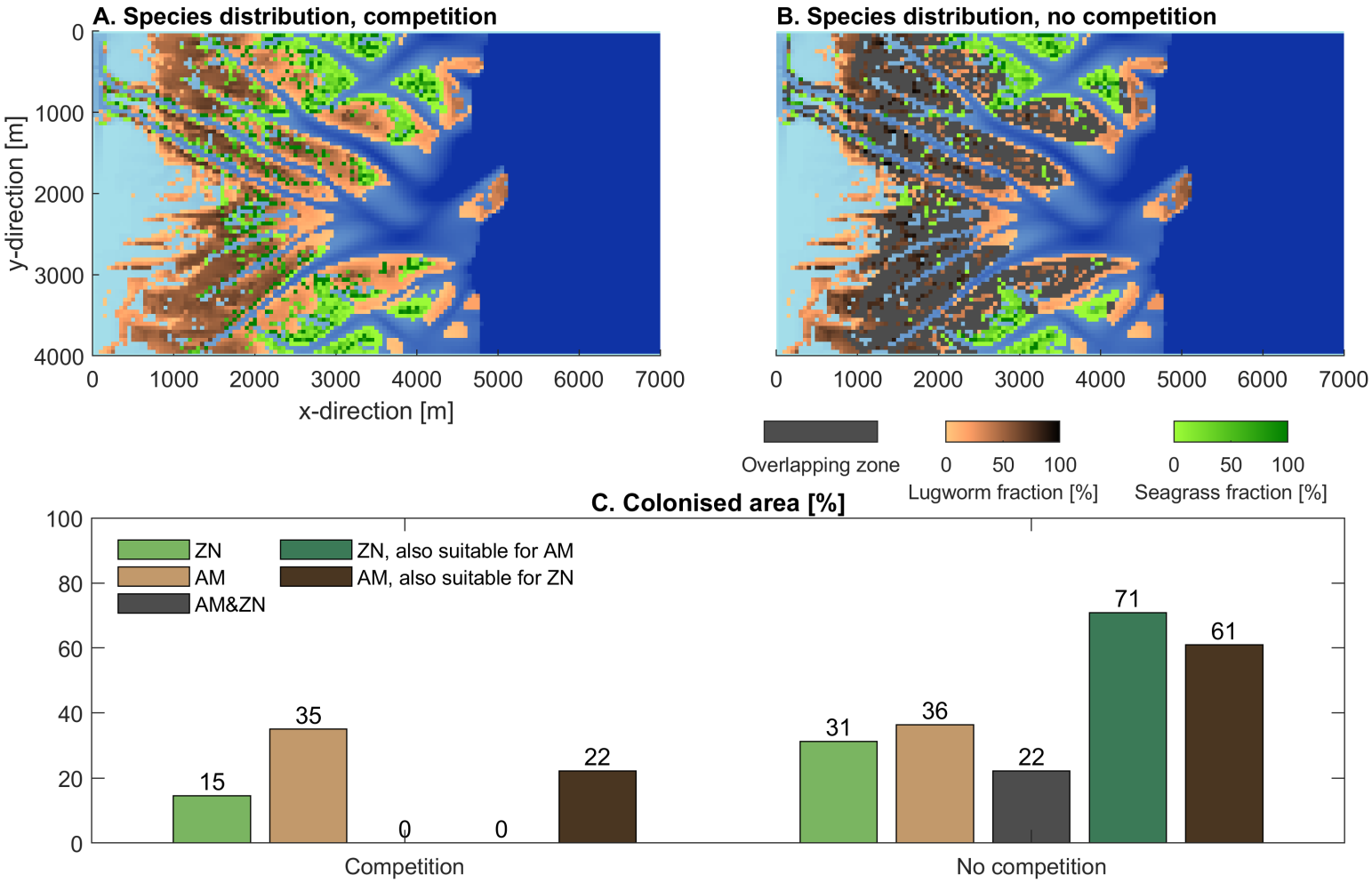

Figure 24: This figure depicts the distribution of the lugworm and seagrasses over the model domain for two different scenarios. In panel A, competition between the two species is accounted for and only one species is allowed to be present in one cell of the model domain. The scenario shown in panel B does not account for competition and allows multiple species to be present in one single cell. Species abundance is only dependant on physical factors, which the species may affect through ecosystem engineering activities. The gray area in panel B shows the area suitable for both species to settle. It becomes clear that for the multi-species scenario with competition, the lugworm colonises all area suitable for the lugworm. Also, the area which would also be suitable for the seagrass to settle on. At the lower elevations in the centre of the domain where mud contents are not suitable for the lugworm, seagrasses are able to settle. The bar chart (C) shows the colonised area as percentages of the model domain. The light green color (only seagrasses (ZN)) shows the area only suitable for seagrasses in both scenarios. The light brown colour (only suitable for the lugworm (AM)) shows the area only suitable for the lugworm. AM&ZN indicates the area where both species have settled in the scenario where this is allowed for (Panel B.). The dark green colour indicates the area suitable for seagrasses, but also suitable for lugworms. The dark brown area indicates the area suitable for lugworms, but also suitable for seagrasses to settle. A significant decrease in the area suitable for seagrass can be observed between the scenario with and without competition, as the lugworm is dominant.

6 Discussion

6.1 Lugworm distribution over the tidal basin

The lugworm is modelled to tolerate certain ranges of flow velocities, mud content and inundation periods based on literature studies (Paragraph 4.2.4). The model results show a distribution of the lugworm in the model domain where the species settle in the intertidal zone in intermediate mud-conditions. Sandy and extremely muddy locations (mud content $> 99\%$) are avoided and the mud content is mainly determining species settlement as the worm tolerates wide ranges of flow velocities and inundation periods (Beukema & De Vlas, 1979). The study by Longbottom (Longbottom, 1970), confirms the fact that nutrient availability strongly determines lugworm presence. Organic matter concentrations were found to be high in muddy sediments and lower in coarser sandy sediments. The lugworms studied, would prefer areas with intermediate nutrient availability over areas with very high or very low nutrient availability. However, nutrient composition and grain size (sand or mud) are two different things, which are interrelated but not similar. In this modelling study, species settlement merely depends on mud content, rather than nutrient availability, assuming a strong relation between the two. Since organic matter content is likely to differ over space, this would affect the species distribution over the domain (Longbottom, 1970). Areas where conditions are calm are likely to contain very high concentrations of organic matter and very fine sediments, unsuitable for the lugworm to dig burrows. On the other hand, in the locations which know intermediate active energy conditions, organic matter is likely lower and will be unsuitable for the lugworm to settle as for the lack of nutrients. Although, these differences are not expected to change the model outcomes significantly.

Furthermore, the bioturbating species knows a life cycle where it migrates up and down the tidal flat in its juvenile state and stays on a fixed location once it reaches adulthood (Farke et al., 1979; Farke & Berghuis, 1979). Where the adults live on the lower reaches of the intertidal, juveniles live more closely to the shoreline. On the shores of the barrier islands of the Wadden Sea, which are overall low-energy environments, juvenile and adult lugworms are able to live on separate heights of the shores (Beukema & De Vlas, 1979; Flach & Beukema, 1995). This results in the juveniles not to be hampered by the turbating activities of the adult species and to reach the adult state successfully. The effects of the lugworm life cycle are not accounted for in the model computations. The distribution of the species over the domain is not determined much by this process. However, juvenile and adult lugworms will affect the morphology in a different way, since turbating activities by the adult lugworms have a larger effect on sediment dynamics than the activities of the smaller juveniles.

The model computations in the Delft 3D environment only account for tidal currents and ignore the presence of waves in the tidal basin. Considering the fact that the modelled tidal basin is relatively small as compared to other tidal basins in the Wadden Sea, the fetch (the force to create wind waves) is rather small in such an area. Former studies have indeed shown that tidal currents are the main drivers for sediment transport in the Wadden Sea, where waves only become important during extreme weather conditions like storms (Janssen-Stelder, 2000; Lettmann, Wolff and Badewien, 2009). During calm conditions waves will promote the deposition of fine sediments on the tidal flats, which would have caused for the mud content on the tidal flats in the modelled domain to be slightly higher (Andersen and Pejrup, 2001).

6.2 Seagrass distribution over the tidal basin

Seagrasses are only able to settle and grow on locations where the inundation periods are between 3 and 8 hours of a tidal cycle, which makes the inundation period the most limiting factor as compared to mud content of the bed. It restricts the growth of the species to the intertidal, which complies with findings in field studies (Schanz & Asmus, 2003; Dolch et al., 2018). Figure 11 implies the growth of seagrasses on locations where inundation periods are longer or shorter than the defined window of opportunity for the species. However, since the maps of Figure 12 3A&B show a clear restriction of the species by inundation period, the results shown in the graph can be clarified through the fact that bed elevations change over the run of 50 years. Species fractions are considerably lower in areas where the inundation periods are longer than 8 hours or shorter than 4 hours, which implies the decay of the species as these locations are no longer a suitable habitat for the species. Due to a decrease in bed elevation and an increase in inundation period in these locations. The seagrasses settle both on muddy and sandy sediments. However, not near the channel beds where flow velocities are too high for the seeds to be able to settle successfully (Peralta et al., 2006).

Overall, the modelled area colonised by the species is considerably larger than the area truly inhabited by seagrasses in the eastern Wadden Sea. Seagrass species are under pressure as a main result of eutrophication of the waters of the sea (Dolch et al., 2018). For this reason, seagrass fields have declined severely over the past decades. Furthermore, seagrasses are not only vulnerable to physical conditions like flow velocity and inundation period as accounted for in our model. They also are prone to the activities of other species thriving in the Wadden Sea and are fed upon by gees and other seabirds (Jacobs, Den Hartog, Braster, & Carriere, 1981; Philippart, 1995a). These are factors which are not taken into account in the modelling computations and will result in a decrease in the overall density of the fields and the total area of the tidal basin colonised by the species.

6.3 Turbating activities by the lugworm

The model results showed how bioturbating activities by the lugworm decrease mud fractions and tidal flat elevations on the scale of a tidal basin. In the intertidal zones where these species settle bed elevation and mud content are directly impacted by the activities of the worm. The mud disappearing from the species grounds settles at higher elevations of the tidal flat, on shallow channel beds where bed shear stresses are low and near the inlet of the basin where large water depths make for low energy conditions, which overall results in an increase of total mud volume in the domain. Furthermore the species locally increases tidal asymmetry in the ebb direction on the tidal flats, which is a novel finding. The effects of ecosystem engineers on tidal asymmetry could be elaborated on further in future research.

The reduction of mud fractions as a result of bioturbating activities, is a process discussed also by (Soissons et al., 2019; Volkenborn et al., 2007; M. Z. Brückner et al., 2021). The study of Soissons et al. (2019) pointed out how bioturbators will increase or decrease the mud content, dependant on the local sediment conditions and suspended particle matter. As bioturbators feed upon the organic matter in suspended muddy sediments, these sediments are filtered out of the water column and end up in the sandy bed. As a result, the mud content of the bed will increase. On the other hand, bioturbating activities will decrease the critical shear stress for the erosion of mud, which will lead to a decrease in mud fraction, which is also what Volkenborn et al (2007) pointed out in their study. However, the mud captured by the lugworms is often stored in greater depths in the bed. Since the model used only accounts for the uppermost surface layers of the bed, neglecting

the capturing abilities of the lugworm is not expected to affect the outcomes significantly. In the study of Brückner (2021), the lugworm was modelled on estuary scale. The study showed a decrease in mud fraction on the locations inhibited by the species and erosion of the tidal flats on these locations. Mud and sand eroded from the bed were transported to locations where bioturbating species were absent and towards the mouth of the estuary, which is similar to the processes found in this modelling work.

Furthermore, the work of M. Brückner et al (2021) showed the negative impact a bioturbator can have on its habitat suitability. These findings comply with the results found in this tidal basin modelling study. The lowering in bed elevation as a result of bioturbation can result in the environment changing from a low energy to a high energy environment as water depths and bed shear stresses will increase. As a result of these energetic conditions, less mud will be settling down on these locations and burrows are more easily destroyed which will make these locations no longer suitable for species settlement. However, these negative feedback loops are still understudied and require more research to be able to explain the specific processes and mechanisms.

Retraubun et al (1996), studied the turbation by the lugworm as means of a field study (Retraubun, Dawson, & Evans, 1996). They discuss the fact that bioturbating activities are highly variable over space and time. Where the larger, adult lugworms settle at the intermediate elevaitons of the tidal flat, impacts on soil erosion will be more significant in these areas compared to the higher elevations where the smaller juvenile species have settled. When juveniles move from their juvenile ground to join the adult species during springtime, the activities on the higher elevations of the tidal flat lower. Furthermore, there are differences over one single tidal cycle and on the scope of a whole year considering summer and winter periods. During low tide, when the tidal flat is exposed, no activity is observed (Retraubun et al., 1996). Furthermore, a higher water temperature seems to increase turbating activities. As for this reason, lugworm activity is more intense during summer months as compared to the winter months. Cadée (1976) also observes these variations dependant on season, moment in the tidal cycle and individual size in a field study on the tidal flats in the Wadden Sea (Cadée, 1976). These variations in time and space are expected to have caused differences in the mud content over the tidal flat gradients. At the higher elevations, modelled mud contents are lower than one would observe in the field. Since juvenile lugworms are settling in these locations.

6.4 Stabilising activities by seagrasses

The presence of seagrass in the model domain enhanced the deposition of mud and sediments on the tidal flats of the basin. Furthermore, flow velocities in the seagrass fields decreased whereas flow velocities in the channels and surroundings of the vegetation patches increased. Former literature explains these scale-dependent feedbacks where hydrodynamic conditions within the seagrass fields are affected differently when compared to the surrounding environment (Temmerman et al., 2007; Vandenbruwaene, Meire, & Temmerman, 2012; Vandenbruwaene, Bouma, Meire, & Temmerman, 2013). The Flow is directed around the vegetated areas rather than over the whole of the flat in the case of a bare tidal flat. The concentration of the flow on certain locations promotes the formation of channels or results in incision and erosion of the already existing channels. These processes are also observed in the model scenarios, as the species settle on the channel banks and the flow concentrates in the tidal channels, the channels erode and the tidal flat increases in elevation. The fact that the presence of seagrasses in the model domain resulted in changes in tidal asymmetry in both the higher and lower elevations (intertidal and subtidal), can be explained through the fact that these species also affect the environment beyond the location of settlement. However, changes in tidal asymmetry as a result of ecosystem

engineers still require more research to express these mechanisms into more detail. Various literature studies describe the positive feedbacks within seagrass fields through which the species enhance habitat suitability (de Boer, 2007; Carr, D'Odorico, McGlathery, & Wiberg, 2016). The results of this study also show an increase in suitable habitat for the species when eco-engineering activities are considered in the model computations.

The model results show a process of fixation and incision of the intertidal channels for the scenarios which account for the ecosystem engineering activities of seagrasses. Schwarz et.al. (2018) discuss how fast (homogeneous vegetation patterns) and slow (patchy vegetation patterns) colonisers can have a different effect on channel formation in intertidal areas. The homogeneous vegetation patterns created by fast colonisers showed the tendency to stabilise and fixate channel patterns, whereas the patchy vegetation patterns of slow colonisers promoted the creation of new channels facilitating further self-organisation of the landscape (Schwarz et al., 2018). By using grid cells of 50x50 metres in this modelling study, seagrasses will be considered as fast colonisers creating homogeneous vegetation patterns and as such stabilising existing channel patterns. Once seagrasses are modelled on a smaller scale, a natural patchy vegetation will induce the creation of new channels in the intertidal landscape (Kendrick, Marbà, & Duarte, 2005).

Differences were found between the locations where seagrass densities were high as compared to the locations with low densities. Seagrasses tend to increase the mud fraction of the bed on the locations where densities are high. A decrease in mud content is observed in the areas with a low species fraction. In both experimental flume set-ups and field studies it is also found that seagrass fields do not necessarily tend to promote deposition and an increase in mud fraction as is expected from their capability of decreasing flow velocities (Harlin, Thorne-Miller, & Boothroyd, 1982; Mellors, Marsh, Carruthers, & Waycott, 2002; Heide et al., 2010; van Katwijk, Bos, Hermus, & Suykerbuyk, 2010). Van Katwijk (2010) explains how turbulence in the upper parts of the vegetation is enhanced when compared to locations where the seabed is bare. However, near the bed the vegetation attenuates the flow and reduces bed shear stresses which enhances sedimentation of fine sediment particles like mud. When vegetation densities are low, the balance between turbulence and attenuation may shift towards a more active environment as compared to a bare mudflat. On these locations, erosion and a decrease in mud content will occur when fine particles are more easily eroded from the seabed. In this study these same trends are observed when comparing areas with a low vegetation density to areas where seagrass fractions are high.

Even though a decrease in flow velocity is observed in the model outcomes, studies have shown that these intertidal vegetative species are less effective when it comes to attenuating tidal currents as compared to the reduction of flow velocities of waves (Hansen & Reidenbach, 2012). Hansen and Reidenbach (2012) explain how seagrass beds are less effective in attenuating waves with longer periods, indicating tidal currents. For this reason, consideration of waves in the model computations might have resulted in higher deposition rates. Since the species are more effective in reducing wave flow velocities.

6.5 Effects of multiple species on species pattern and sediment dynamics

The model outcomes for the scenarios where competition between seagrasses and lugworms is considered show a typical distribution of the species over the tidal flat gradient. The seagrass is restricted to the lower elevations of the tidal flat, since at higher elevations lugworm activities prevent successful settlement and germination of the seeds (Philippart, 1995b; Goerlitz, Berkenbusch, & Probert, 2015). However, former studies are often limited to the negative impact of the lugworm on seagrasses and little is known about the combined

effects of both species on sediment dynamics and morphology. Although the effects of individual species heron are extensively studied (Cadée, 1976; Flach, 1992; Bos et al., 2007; de Boer, 2007). The results of this study show a novel mechanism of how the lugworm erodes the upper elevations of the tidal flat and how the seagrasses will trap the sediments and mud coming from these higher elevations. Mud fractions and mud volumes are significantly higher in the multi-species scenario as compared to the lugworm scenario. Although, only 15% of the basin is colonised by seagrasses, the mud fraction and mud volume values lie close to the seagrass scenario whereas almost 40% of the basin is occupied by the vegetative species. The sediment eroded from the bed by lugworms, can for this reason be considered as an important source of the sediments deposited in the seagrass fields in the multi-species scenario. This process will result in erosion and incision of the tidal channels in the tidal basin.

Furthermore, an amplification in positive and negative feedbacks on the species is found in the multi-species scenario. The positive feedback of seagrass on its habitat had a larger effect in this scenario, as did the negative feedback of the lugworm. Literature emphasises the negative effects of the lugworm on seagrasses (Philippart, 1995a; Valdemarsen et al., 2010, 2011). However, resuspension of sediments by the lugworm which is captured in the canopy of the vegetation may create more elevated areas of tidal flat towards which the vegetation species can expand. The dense rooting systems of the vegetation will prevent the lugworm of taking over in these locations (Philippart, 1994; Goerlitz et al., 2015). However, more research needs to be done into the details of these processes.

7 Conclusions

This study shows that the bioturbating lugworm and the stabilising seagrass affect morphology on the scale of a tidal basin. Lugworms locally erode the bed and reduce the mean mud concentration in the basin (schematised visualisation in Fig. 25A). Although, the effects of this species vary over space and time when seasonal and life cycle variations are considered. Further research is required to understand how these variations affect the impact of the species on tidal basin morphology.
Stabilising seagrasses on the other hand locally elevate the bed and increase the total mud volume in the basin. Furthermore, scale dependant feedbacks result in erosion and fixations of channel beds and bare areas or locations with low seagrass fractions (schematised visualisation in Fig. 25B). Next to bed elevation and mud content, the species both affect tidal asymmetry. Where the lugworm locally increases the tidal asymmetry on higher elevations (ebb direction), seagrasses also increase tidal asymmetry in the flood direction at lower elevations outside of their habitat. However, to understand the mechanisms behind these effects, further research is required.

Furthermore, this study showed mud content being the main limiting factor for lugworm settlement and inundation period being the main limiting factor for seagrass growth over the scale of a tidal basin. As already showed by former studies, seagrasses have a positive feedback on their habitat, whereas the bioturbating lugworm showed to have a negative feedback on its habitat.

Competition mechanisms between the two species were studied. Once lugworms were also present, seagrasses were restricted to the lower elevations of the intertidal zone, whereas the lugworm dominated a larger area at higher elevations. The sediment brought into suspension by the lugworm is captured by the lower lying vegetated areas (schematised visualisation in Fig. 25C). The positive and negative feedbacks of the species seem to be amplified in the multi-species scenario. For this reason, more in depth knowledge is required on the possibilities of the eroding activities by the lugworm to have a positive effect on the habitat suitability of seagrasses. Overall, the presence of both species shows fixation and incision of tidal channels as a result of stabilising seagrasses capturing the sediment eroded at higher elevations of the tidal flat where lugworms are present.

Since this study shows the importance of a combined effect of stabilising and bioturbating ecosystem engineers on the morphology of a tidal basin, more knowledge will need to be gained on the details of these processes. Already quite some investigation is done into the effects of individual species on landscape morphology, though the consideration of species interactions will lead to different results and a better understanding of the way biotics are shaping the abiotic environment.

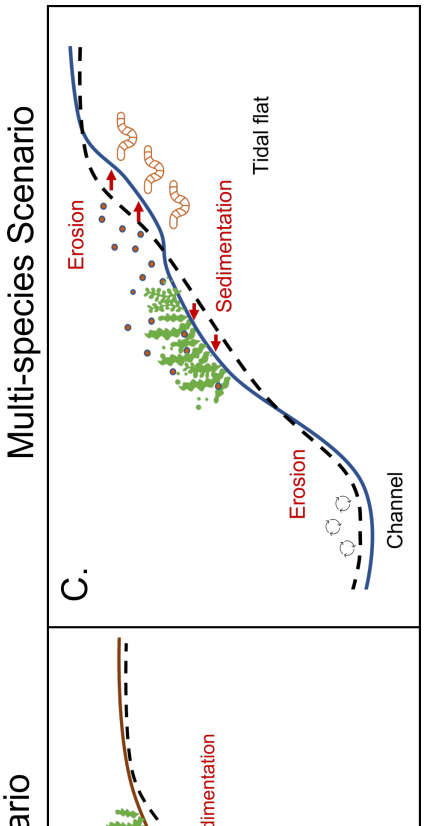

Figure 25: This figure shows schematised visualisations of the effects of the bioturbating lugworm and the stabilising seagrasses on tidal flat and channel morphology. Panel A. shows the erosion of the tidal flat by the bioturbating activities of the lugworm. The sediments end up in the tidal channel where sedimentation occurs. Panel B. shows the local stabilisation of the tidal flat, it also shows the increase in flow velocity next to the seagrass fields in the channels, which result in incision and erosion of the channel bed. Panel C. shows the combined effects of both ecosystem engineers on the tidal flat morphology. Lugworms thrive at the higher elevations of the tidal flat where they will erode the bed. Seagrasses on the lower elevations will capture the sediments brought into suspension by the lugworms and promote erosion and incision of the channels.

8 Appendices

8.1 Appendix I: Critical thinking on computer modelling

As discussed in the work of Oreskes (Oreskes, Shrader-Frechette, & Belitz, 1994), the validation of numerical models in natural studies is impossible. A natural system knows many open boundaries and often knows such a complexity which is impossible to capture in a model environment. During the creation of a model environment, many assumptions are made and boundary conditions are added to the system. These simplifications make sure that the model environment will not be able to depict the scenario as is in reality. Though, it must be considered that this is also not what models should be used for. Models are not made for depicting reality. However, they can be used to play with reality and to be able to isolate certain processes happening in the field. In the case of this study, the interactions between two ecosystem engineering species and their environment is analysed in a model environment. Boundary conditions are determining the abiotic environment and species effects are modelled through an effect on certain abiotic parameters. The model is merely a simplification of a true Wadden Sea basin as it does not account for waves, the tidal boundary is modelled as a change in water level, wind is not considered, human influences are excluded and also no other species are living in the model domain which is far from the realistic situation. However, this modelling study is still able to provide us with a better understanding of how The lugworm and seagrasses will interact with the abiotic environment. By modelling these species, we have isolated the species and the environment to take a closer look at what is happening there. In the field all the above-mentioned external factors also have an effect on morphology which makes it difficult to determine which changes are caused by which forcing. Though, by isolating these species and the environment in a model domain it becomes possible to determine the effects of the ecosystem engineers on one another and on the morphology.

8.2 Appendix II: The model domain - A T-shaped basin

The model domain could also be shaped as a T-shaped basin, which enables the possibility of adding the tidal boundary in the domain as a phase difference. Two separate harmonic boundaries are added to both opposite sides of the ocean basin within the domain. The changes in water level at the one side of the basin will be initiated a little bit sooner than the water levels at the other end of the basin, to mimic the movement of a tidal wave through the basin. To be able to use this function, the shape of the model domain is slightly changed to a T-shaped domain (Fig. 26). The tidal basin is lengthened by two kilometres on each side (total length of the tidal basin is 8000 metres) where the shape of the tidal flat remained. At both ends of the T, a harmonic boundary is added with the same tidal constituents used for the rectangular basin. The phase difference is calculated using a prediction of flow velocity and shear stress. A phase difference of 4 minutes is computed and implemented in the harmonic boundaries of Delft 3D. Since only water level is specified within Delft 3D and not a certain discharge flowing in and out of the basin, the phase difference caused some numerical issues in the centre of the ocean basin where sediment piled up which is transported of the tidal flat. Where the centre of the ocean became very shallow, other parts deepened out. Due to limited time for the model computations the decision is made to move on with the squared basin where only one harmonic boundary is used for the implementation of tides in the model.

8.3 Appendix III: The mud inflow boundary

The mud concentrations in the tidal basin situated in the eastern Wadden Sea varied between 2-20%. As a first try a mud inflow of 0.1 km/m^3 with a water inflow of 0.5 m^3/sec

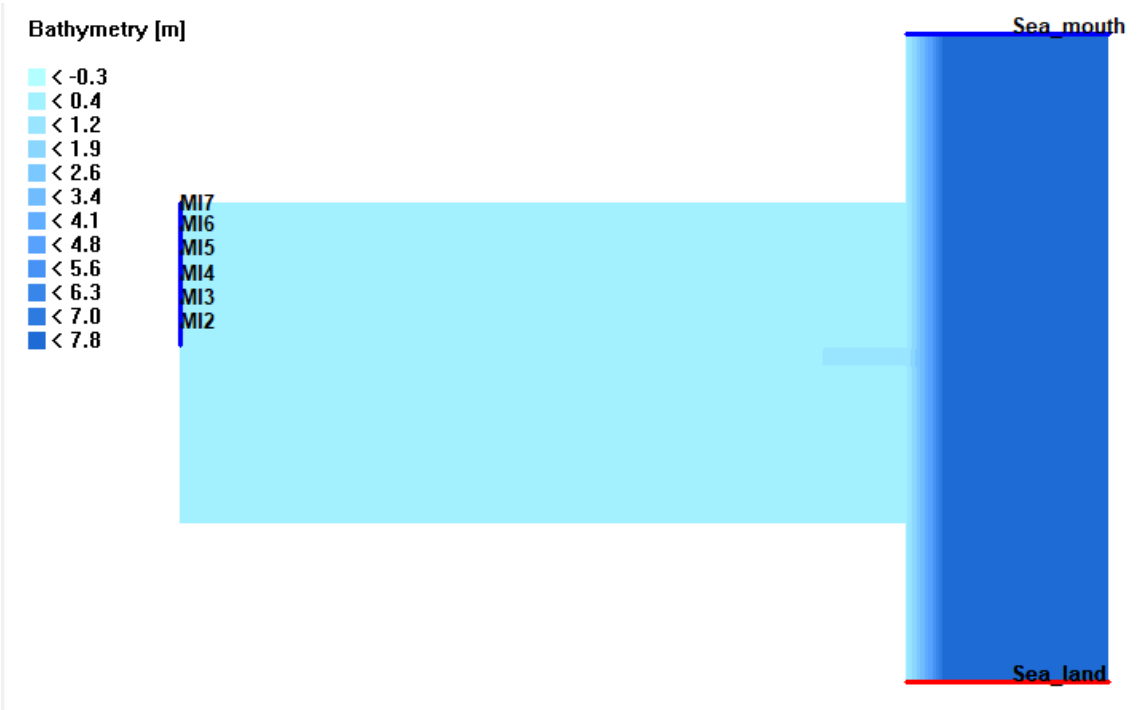

Figure 26: Bathymetry of the basin as computed from a MATLAB code. This T-shaped boundary has two open boundaries on each side of the ocean basin each implementing a harmonic signal on the ocean basin with only 4 minutes difference. The mud-inflow boundary is the open boundary up onto the tidal flat. Through this boundary, the mud is added to the system.

is fed into the domain. The mud is settling in the entire model domain and channels are being filled up with sediments. The evolution of channels is becoming impossible as a result of the high mud inflow concentrations (Fig. 27). The inflow concentration of the sediment is decreased by small steps until the inflow concentration is only $0.01kg/^m3$. For this scenario, the mud still concentrates on the upper parts of the tidal flats but overall, the mud concentrations in the domain is lower and more valid when compared to what is found for the Wadden Sea basin (Fig. 27). Since waves are not considered in the hydrodynamic computations of the Delft 3D FLOW environment and tides are added as a means of one single open boundary determining maximum and minimum water levels at the location of the boundary, the basin represents a low-energy environment when compared to the natural situation in the field. This is the main clarification for the mud not to spread out over the domain easily. To tackle this problem and facilitate the distribution of mud over the domain, the critical erosion parameter for mud is lowered. However, the lowering of the mud inflow into the basin seemed more effective.

8.4 Appendix IV: Cohesive sediments

The sediment transport computations in the Delft 3D environment do not account for cohesion and interactions between sediments. A threshold for cohesive behaviour of the bed ($P_{m,crit}$) can be added where the erosion of the sand will follow the erosion of mud. When the mud fraction exceeds this threshold (the critical mud content for cohesive behaviour), both sand and mud will be eroded from a certain location once the critical bed shear stress for mud is reached. In this study, the effects of this value on the morphology and mud distribution of the tidal basin were tested. Results compared to scenarios without sediment cohesion accounted for, did not show any significant differences (Fig. 28), as a result of a low-energy environment where flow velocities and bed shear stresses did not lead to significant bed level changes.

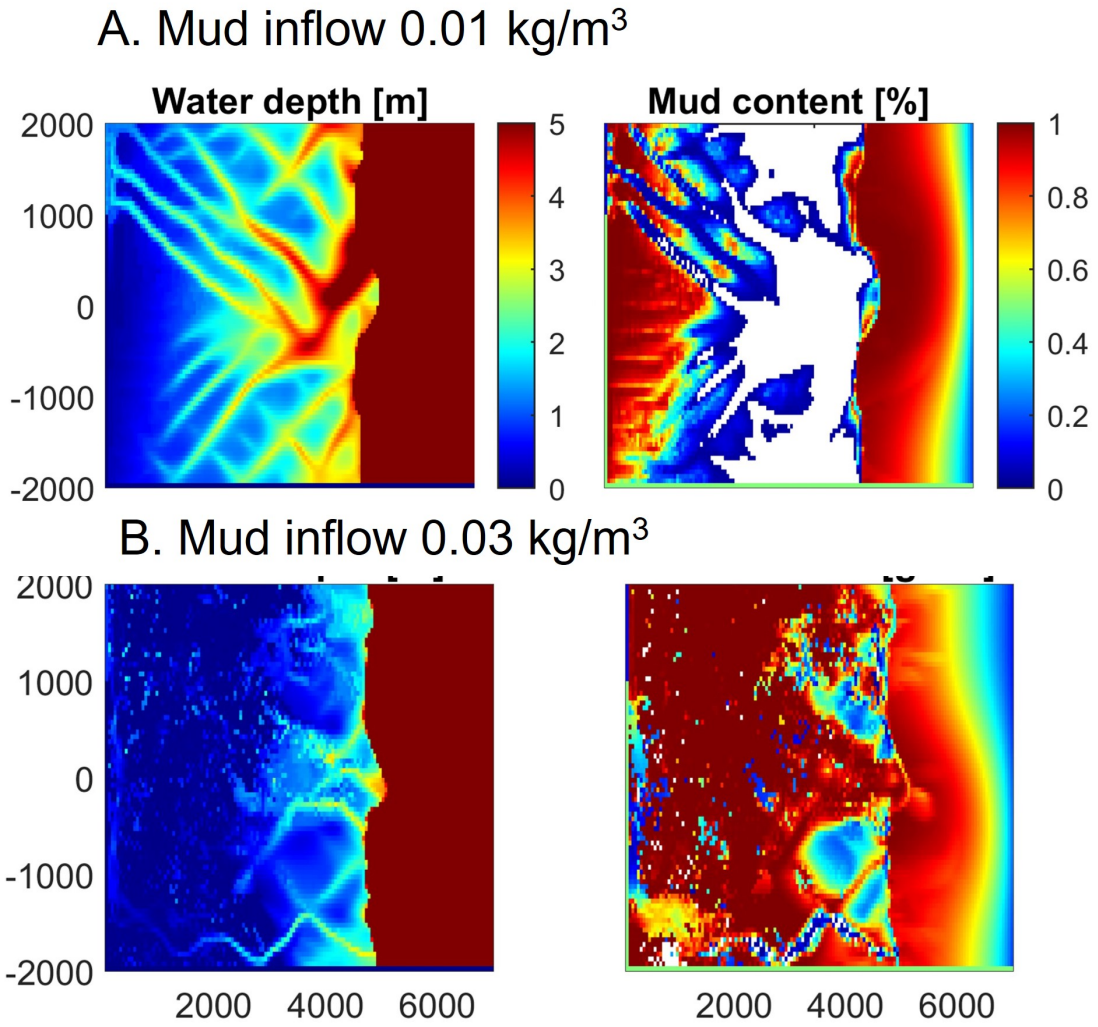

Figure 27: A. The initial basin after 130 morphological years of development with a mud inflow of 0.01 kg/m^3. The mud is only concentrated on the higher elevations of the tidal flat and in the ocean basin. Channels patterns have evolved. This model domain has been used for the research scenarios. B. A scenario where the mud inflow boundary let in a mud inflow concentration of 0.03 kg/m^3 after 30 morphological years. Mud concentrations in the domain are extremely high and all tidal channels have been filled with muddy sediments.

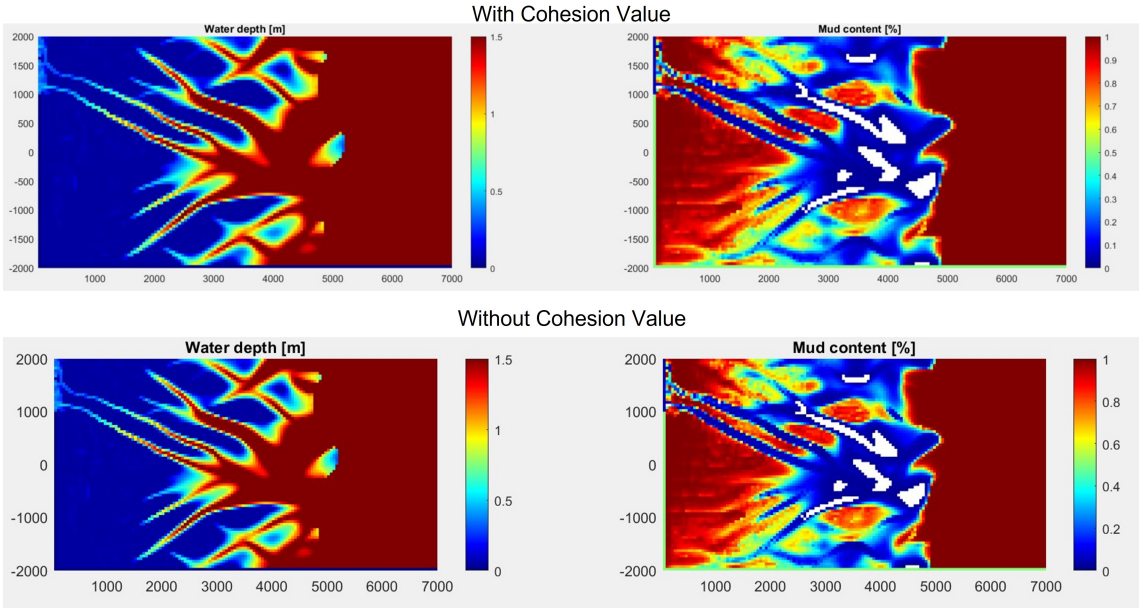

Figure 28: Mud content and bed elevations for the scenario with and without a cohesion value of 0.35 (critical mud content for cohesive behaviour). No differences are observed between both scenarios.

8.5 Appendix V: The morphological scale factor (MORFAC)

Moreover, the effects of the morphological acceleration factor (MORFAC) are tested by looking at the effects of a MORFAC of 30, 60, and 120 on the outcomes of the Delft 3D model runs. For a value of 30, the domain needed more time to reach an equilibrium where channel branches are formed and are relatively stable. This makes sense, since the morphological scale factor simply multiplies morphological change by a certain factor which results in a shorter computation time for an equilibrium to be reached. The value of the MORFAC can be set to any value by the user, although previous studies identified values up to 400 as feasible (Braat, van Kessel, Leuven, & Kleinhans, 2017). When morphological changes are amplified by a large value, more sediment may be eroded from a certain location than is available in the first place. The model will simply add more sediment to the domain to be able to erode the amount of sediment asked for by the morphological change times the MORFAC. To be able to maximise the MORFAC and to keep the computation time of the runs as short as possible, the factor is increased stepwise up to a value of 120. With the adjustments of the MORFAC also the runtime for reaching an equilibrium state is determined. We found that 500 morphological years are needed for the domain to reach a stable state where tidal channels and flats are formed, and mud has settled in the domain.

For the model scenarios where the Delft 3D model is coupled to the species models, the MORFAC is again lowered to a value of 60 since the model only runs for 50 morphological years and a higher morphological scale factor is not required. Since a lower value allows for more precision in the model computations, a value of 60 is preferred.

References

Andersen, T., Lanuru, M., van Bernem, C., Pejrup, M., & Riethmueller, R. (2010, April). Erodibility of a mixed mudflat dominated by microphytobenthos and Cerastoderma edule, East Frisian Wadden Sea, Germany. *Estuarine, Coastal and Shelf Science*, *87*(2), 197–206. Retrieved 2021-10-10, from https://linkinghub.elsevier.com/retrieve/pii/S0272771409004818 doi: 10.1016/j.ecss.2009.10.014

Austen, I., Andersen, T. J., & Edelvang, K. (1999, July). The Influence of Benthic Diatoms and Invertebrates on the Erodibility of an Intertidal Mudflat, the Danish Wadden Sea. *Estuarine, Coastal and Shelf Science*, *49*(1), 99–111. Retrieved 2021-10-10, from https://www.sciencedirect.com/science/article/pii/S0272771498904917 doi: 10.1006/ecss.1998.0491

Baden, S., Emanuelsson, A., Pihl, L., Svensson, C.-J., & Åberg, P. (2012, April). Shift in seagrass food web structure over decades is linked to overfishing. *Marine Ecology Progress Series*, *451*, 61–73. Retrieved 2021-09-11, from https://www.int-res.com/abstracts/meps/v451/p61-73/ doi: 10.3354/meps09585

Bagnold, R. A. (1966). *An Approach to the Sediment Transport Problem from General Physics*. U.S. Government Printing Office. (Google-Books-ID: G096igXqR74C)

Beukema, J. J., & De Vlas, J. (1979, December). Population parameters of the lugworm, arenicola marina, living on tidal flats in the Dutch Wadden Sea. *Netherlands Journal of Sea Research*, *13*(3), 331–353. Retrieved 2021-11-13, from https://www.sciencedirect.com/science/article/pii/0077757979900103 doi: 10.1016/0077-7579(79)90010-3

Blew, J., Günther, K., Laursen, K., Roomen, M., Südbeck, P., Eskildsen, K., ... Rösner, H.-U. (2005). *Overview of Numbers and Trends of Migratory Waterbirds in the Wadden Sea 1980 – 2000.*

Borsje, B. (2006, January). Biological influence on sediment transport and bed composition for the Western Wadden Sea.

Borsje, B., Hulscher, S., de Vries, M., & de Boer, G. (2007, September). Modeling large scale cohesive sediment transport by including biological activity. doi: 10.1201/NOE0415453639-c32

Bos, A. R., Bouma, T. J., de Kort, G. L. J., & van Katwijk, M. M. (2007, August). Ecosystem engineering by annual intertidal seagrass beds: Sediment accretion and modification. *Estuarine, Coastal and Shelf Science*, *74*(1), 344–348. Retrieved 2021-09-11, from https://www.sciencedirect.com/science/article/pii/S0272771407001096 doi: 10.1016/j.ecss.2007.04.006

Braat, L., van Kessel, T., Leuven, J. R. F. W., & Kleinhans, M. G. (2017, October). Effects of mud supply on large-scale estuary morphology and development over centuries to millennia. *Earth Surface Dynamics*, *5*(4), 617–652. Retrieved 2022-02-28, from https://esurf.copernicus.org/articles/5/617/2017/ (Publisher: Copernicus GmbH) doi: 10.5194/esurf-5-617-2017

Brückner, M. Z., Schwarz, C., Coco, G., Baar, A., Boechat Albernaz, M., & Kleinhans, M. G. (2021). Benthic species as mud patrol - modelled effects of bioturbators and biofilms on large-scale estuarine mud and morphology. *Earth Surface Processes and Landforms*, *46*(6), 1128–1144. Retrieved 2021-09-24, from https://onlinelibrary.wiley.com/doi/abs/10.1002/esp.5080 (_eprint: https://onlinelibrary.wiley.com/doi/pdf/10.1002/esp.5080) doi: 10.1002/esp.5080

Brückner, M. Z. M., Schwarz, C., van Dijk, W. M., van Oorschot, M., Douma, H., & Kleinhans, M. G. (2019). Salt Marsh Establishment and Eco-Engineering Effects in Dynamic Estuaries Determined by Species Growth and Mortality. *Journal of Geophysical Research: Earth Surface*, *124*(12), 2962–2986. Retrieved 2021-09-24, from

https://onlinelibrary.wiley.com/doi/abs/10.1029/2019JF005092 (_eprint: https://onlinelibrary.wiley.com/doi/pdf/10.1029/2019JF005092) doi: 10.1029/2019JF005092

Buijsman, M. C., & Ridderinkhof, H. (2007, May). Long-term ferry-ADCP observations of tidal currents in the Marsdiep inlet. *Journal of Sea Research*, *57*(4), 237–256. Retrieved 2021-10-10, from https://www.sciencedirect.com/science/article/pii/S1385110106001596 doi: 10.1016/j.seares.2006.11.004

Burchard, H., Flöser, G., Staneva, J. V., Badewien, T. H., & Riethmüller, R. (2008, March). Impact of Density Gradients on Net Sediment Transport into the Wadden Sea. *Journal of Physical Oceanography*, *38*(3), 566–587. Retrieved 2021-10-10, from https://journals.ametsoc.org/view/journals/phoc/38/3/2007jpo3796.1.xml (Publisher: American Meteorological Society Section: Journal of Physical Oceanography) doi: 10.1175/2007JPO3796.1

Burchard, H., & Hetland, R. D. (2010, June). Quantifying the Contributions of Tidal Straining and Gravitational Circulation to Residual Circulation in Periodically Stratified Tidal Estuaries. *Journal of Physical Oceanography*, *40*(6), 1243–1262. Retrieved 2021-10-10, from https://journals.ametsoc.org/view/journals/phoc/40/6/2010jpo4270.1.xml (Publisher: American Meteorological Society Section: Journal of Physical Oceanography) doi: 10.1175/2010JPO4270.1

Cadée, G. C. (1976, December). Sediment reworking by arenicola marina on tidal flats in the Dutch Wadden Sea. *Netherlands Journal of Sea Research*, *10*(4), 440–460. Retrieved 2022-01-18, from https://www.sciencedirect.com/science/article/pii/007775797690020X doi: 10.1016/0077-7579(76)90020-X

Carr, J. A., D'Odorico, P., McGlathery, K. J., & Wiberg, P. L. (2016, July). Spatially explicit feedbacks between seagrass meadow structure, sediment and light: Habitat suitability for seagrass growth. *Advances in Water Resources*, *93*, 315–325. Retrieved 2022-02-26, from https://www.sciencedirect.com/science/article/pii/S030917081500202X doi: 10.1016/j.advwatres.2015.09.001

Christianen, M. J. A., Belzen, J. v., Herman, P. M. J., Katwijk, M. M. v., Lamers, L. P. M., Leent, P. J. M. v., & Bouma, T. J. (2013). Low-Canopy Seagrass Beds Still Provide Important Coastal Protection Services. *PLOS ONE*, *8*(5), e62413. Retrieved 2022-01-26, from https://journals.plos.org/plosone/article?id=10.1371/journal.pone.0062413 (Publisher: Public Library of Science) doi: 10.1371/journal.pone.0062413

Dataregister Rijkswaterstaat. (n.d.). Retrieved 2022-02-23, from https://maps.rijkswaterstaat.nl/dataregister/srv/dut/catalog.search;jsessionid=7D93D8BC900A3FCDF4E108E5FD3E9AAC#/metadata/8458fdf9-cf21-40e0-a65c-f05fee8b5631

Davis, R. A., & Hayes, M. O. (1984, January). What is a Wave-Dominated Coast? In B. Greenwood & R. A. Davis (Eds.), *Developments in Sedimentology* (Vol. 39, pp. 313–329). Elsevier. Retrieved 2021-10-10, from https://www.sciencedirect.com/science/article/pii/S0070457108701523 doi: 10.1016/S0070-4571(08)70152-3

de Boer, W. F. (2007, October). Seagrass–sediment interactions, positive feedbacks and critical thresholds for occurrence: a review. *Hydrobiologia*, *591*(1), 5–24. Retrieved 2022-02-26, from https://doi.org/10.1007/s10750-007-0780-9 doi: 10.1007/s10750-007-0780-9

De Cubber, L., Lefebvre, S., Lancelot, T., Duong, G., & Gaudron, S. M. (2020, November). Investigating down-shore migration effects on individual growth and reproduction of the ecosystem engineer Arenicola marina. *Journal of Marine Systems*, *211*, 103420. Retrieved 2022-02-23, from https://www.sciencedirect.com/science/article/pii/S0924796320301160 doi: 10.1016/j.jmarsys.2020.103420

de Jong, D. J., van Katwijk, M. M., & Brinkman, A. G. (2005, August). Potentiële groeimogelijkheden voor zeegras in de Waddenzee. , 51.

Delft3D-FLOW User Manual. (n.d.). , 710.

Dolch, T., Folmer, E. O., Frederiksen, M. S., Herlyn, M., van Katwijk, M. M., Kolbe, K., ... Westerbeek, E. P. (2018, January). Wadden Sea Quality Status Report Seagrass. , 24.

Dronkers, J. (1986, August). Tidal asymmetry and estuarine morphology. *Netherlands Journal of Sea Research*, *20*(2), 117–131. Retrieved 2021-10-10, from https://www.sciencedirect.com/science/article/pii/0077757986900360 doi: 10.1016/0077-7579(86)90036-0

Elias, E. (2006). *Morphodynamics of Texel Inlet*. IOS Press.

Elias, E. P. L., Spek, A. J. F. v. d., Wang, Z. B., & Ronde, J. d. (2012, November). Morphodynamic development and sediment budget of the Dutch Wadden Sea over the last century. *Netherlands Journal of Geosciences*, *91*(3), 293–310. Retrieved 2021-10-10, from https://www.cambridge.org/core/journals/netherlands-journal-of-geosciences/article/morphodynamic-development-and-sediment-budget-of-the-dutch-wadden-sea-over-the-last-century/36EDB6D1E1041663AD92F139BF4E4BCE# (Publisher: Cambridge University Press) doi: 10.1017/S0016774600000457

Engelund, F., & Hansen, E. (1967). A monograph on sediment transport in alluvial streams. *Technical University of Denmark 0stervoldgade 10, Copenhagen K.*. Retrieved 2021-11-02, from https://repository.tudelft.nl/islandora/object/uuid%3A81101b08-04b5-4082-9121-861949c336c9 (Publisher: TEKNISKFORLAG Skelbrekgade 4 Copenhagen V, Denmark.)

Farke, H., & Berghuis, E. M. (1979, December). Spawning, larval development and migration of Arenicola marina under field conditions in the western Wadden Sea. *Netherlands Journal of Sea Research*, *13*(3), 529–535. Retrieved 2021-11-23, from https://www.sciencedirect.com/science/article/pii/0077757979900231 doi: 10.1016/0077-7579(79)90023-1

Farke, H., de Wilde, P. A. W. J., & Berghuis, E. M. (1979, December). Distribution of juvenile and adult arenicola marina on a tidal mud flat and the importance of nearshore areas for recruitment. *Netherlands Journal of Sea Research*, *13*(3), 354–361. Retrieved 2021-11-23, from https://www.sciencedirect.com/science/article/pii/0077757979900115 doi: 10.1016/0077-7579(79)90011-5

Flach, E. C. (1992, December). Disturbance of benthic infauna by sediment-reworking activities of the lugworm Arenicola marina. *Netherlands Journal of Sea Research*, *30*, 81–89. Retrieved 2021-11-23, from https://www.sciencedirect.com/science/article/pii/007775799290048J doi: 10.1016/0077-7579(92)90048-J

Flach, E. C., & Beukema, J. J. (1995). Density-governing mechanisms in populations of the lugworm Arenicola marina on tidal flats. *Oceanographic Literature Review*, *6*(42), 483. Retrieved 2021-11-23, from https://www.infona.pl//resource/bwmeta1.element.elsevier-85b2a3c8-8598-334a-8cc8-005071939ef1

Flemming, B., Davis, & Jr, R. (1994, October). Holocene evolution, morphodynamics and sedimentology of the Spiekeroog barrier island system (southern North Sea). *Senckenbergiana maritima*, *24*, 117–155.

Flöser, G., Burchard, H., & Riethmüller, R. (2011, October). Observational evidence for estuarine circulation in the German Wadden Sea. *Continental Shelf Research*, *31*(16), 1633–1639. Retrieved 2021-10-10, from https://www.sciencedirect.com/science/article/pii/S0278434311001257 doi: 10.1016/j.csr.2011.03.014

Folmer, E. O., Beusekom, J. E. E. v., Dolch, T., Gräwe, U., Katwijk, M. M. v., Kolbe, K., & Philippart, C. J. M. (2016). Consensus forecasting of in-

tertidal seagrass habitat in the Wadden Sea. *Journal of Applied Ecology*, *53*(6), 1800–1813. Retrieved 2021-09-11, from https://besjournals.onlinelibrary.wiley.com/doi/abs/10.1111/1365-2664.12681 (_eprint: https://besjournals.onlinelibrary.wiley.com/doi/pdf/10.1111/1365-2664.12681) doi: 10.1111/1365-2664.12681

Folmer, E. O., van der Geest, M., Jansen, E., Olff, H., Michael Anderson, T., Piersma, T., & van Gils, J. A. (2012, December). Seagrass–Sediment Feedback: An Exploration Using a Non-recursive Structural Equation Model. *Ecosystems*, *15*(8), 1380–1393. Retrieved 2022-02-23, from https://doi.org/10.1007/s10021-012-9591-6 doi: 10.1007/s10021-012-9591-6

Friedrichs, C. T., & Aubrey, D. G. (1988, November). Non-linear tidal distortion in shallow well-mixed estuaries: a synthesis. *Estuarine, Coastal and Shelf Science*, *27*(5), 521–545. Retrieved 2021-10-10, from https://www.sciencedirect.com/science/article/pii/0272771488900820 doi: 10.1016/0272-7714(88)90082-0

Goerlitz, S., Berkenbusch, K., & Probert, P. K. (2015, June). Lugworm (Abarenicola affinis) in seagrass and unvegetated habitats. *Helgoland Marine Research*, *69*(2), 159–168. Retrieved 2022-01-22, from https://doi.org/10.1007/s10152-014-0424-1 doi: 10.1007/s10152-014-0424-1

Govers, L. L., Pieck, T., Bouma, T. J., Suykerbuyk, W., Smolders, A. J. P., & van Katwijk, M. M. (2014, June). Seagrasses are negatively affected by organic matter loading and Arenicola marina activity in a laboratory experiment. *Oecologia*, *175*(2), 677–685. Retrieved 2021-11-24, from http://link.springer.com/10.1007/s00442-014-2916-8 doi: 10.1007/s00442-014-2916-8

Hansen, J. C. R., & Reidenbach, M. A. (2012, February). Wave and tidally driven flows in eelgrass beds and their effect on sediment suspension. *Marine Ecology Progress Series*, *448*, 271–287. Retrieved 2022-01-21, from https://www.int-res.com/abstracts/meps/v448/p271-287/ doi: 10.3354/meps09225

Harlin, M. M., Thorne-Miller, B., & Boothroyd, J. C. (1982, January). Seagrass-sediment dynamics of a flood-tidal delta in Rhode Island (U.S.A.). *Aquatic Botany*, *14*, 127–138. Retrieved 2022-01-20, from https://www.sciencedirect.com/science/article/pii/0304377082900924 doi: 10.1016/0304-3770(82)90092-4

Heide, T. v. d., Bouma, T. J., Nes, E. H. v., Koppel, J. v. d., Scheffer, M., Roelofs, J. G. M., ... Smolders, A. J. P. (2010). Spatial self-organized patterning in seagrasses along a depth gradient of an intertidal ecosystem. *Ecology*, *91*(2), 362–369. Retrieved 2021-09-15, from https://onlinelibrary.wiley.com/doi/abs/10.1890/08-1567.1 (_eprint: https://esajournals.onlinelibrary.wiley.com/doi/pdf/10.1890/08-1567.1) doi: 10.1890/08-1567.1

Heide, T. v. d., Eklöf, J. S., Nes, E. H. v., Zee, E. M. v. d., Donadi, S., Weerman, E. J., ... Eriksson, B. K. (2012, August). Ecosystem Engineering by Seagrasses Interacts with Grazing to Shape an Intertidal Landscape. *PLOS ONE*, *7*(8), e42060. Retrieved 2021-09-15, from https://journals.plos.org/plosone/article?id=10.1371/journal.pone.0042060 (Publisher: Public Library of Science) doi: 10.1371/journal.pone.0042060

Ikeda, S. (1982, November). Lateral Bed Load Transport on Side Slopes. *Journal of the Hydraulics Division*, *108*(11), 1369–1373. Retrieved 2021-11-02, from https://ascelibrary.org/doi/abs/10.1061/JYCEAJ.0005937 (Publisher: American Society of Civil Engineers) doi: 10.1061/JYCEAJ.0005937

Jacobs, R. P. W. M., Den Hartog, C., Braster, B. F., & Carriere, F. C. (1981, January). Grazing of the seagrass Zostera noltii by birds at terschelling (Dutch Wadden Sea). *Aquatic Botany*, *10*, 241–259. Retrieved 2022-01-20, from https://www.sciencedirect.com/science/article/pii/0304377081900267 doi: 10.1016/

0304-3770(81)90026-7

James, R. K., Christianen, M. J. A., van Katwijk, M. M., de Smit, J. C., Bakker, E. S., Herman, P. M. J., & Bouma, T. J. (2020). Seagrass coastal protection services reduced by invasive species expansion and megaherbivore grazing. *Journal of Ecology*, *108*(5), 2025–2037. Retrieved 2022-01-26, from https://onlinelibrary.wiley.com/doi/abs/10.1111/1365-2745.13411 (_eprint: https://onlinelibrary.wiley.com/doi/pdf/10.1111/1365-2745.13411) doi: 10.1111/1365-2745.13411

Jones, C. G., Gutiérrez, J. L., Byers, J. E., Crooks, J. A., Lambrinos, J. G., & Talley, T. S. (2010). A framework for understanding physical ecosystem engineering by organisms. *Oikos*, *119*(12), 1862–1869. Retrieved 2021-10-10, from https://onlinelibrary.wiley.com/doi/abs/10.1111/j.1600-0706.2010.18782.x (_eprint: https://onlinelibrary.wiley.com/doi/pdf/10.1111/j.1600-0706.2010.18782.x) doi: 10.1111/j.1600-0706.2010.18782.x

Jones, C. G., Lawton, J. H., & Shachak, M. (1997). Positive and Negative Effects of Organisms as Physical Ecosystem Engineers. *Ecology*, *78*(7), 1946–1957. Retrieved 2021-10-10, from https://onlinelibrary.wiley.com/doi/abs/10.1890/0012-9658%281997%29078%5B1946%3APANEOO%5D2.0.CO%3B2 (_eprint: https://onlinelibrary.wiley.com/doi/pdf/10.1890/0012-9658%281997%29078%5B1946%3APANEOO%5D2.0.CO%3B2) doi: 10.1890/0012-9658(1997)078[1946:PANEOO]2.0.CO;2

Kendrick, G. A., Marbà, N., & Duarte, C. M. (2005, December). Modelling formation of complex topography by the seagrass Posidonia oceanica. *Estuarine, Coastal and Shelf Science*, *65*(4), 717–725. Retrieved 2022-02-26, from https://www.sciencedirect.com/science/article/pii/S0272771405002519 doi: 10.1016/j.ecss.2005.07.007

Lesser, G., Roelvink, J., van Kester, J., & Stelling, G. (2004, October). Development and validation of a three-dimensional morphological model. *Coastal Engineering*, *51*(8-9), 883–915. Retrieved 2021-11-02, from https://linkinghub.elsevier.com/retrieve/pii/S0378383904000870 doi: 10.1016/j.coastaleng.2004.07.014

Leuschner, C., Landwehr, S., & Mehlig, U. (1998, November). Limitation of carbon assimilation of intertidal Zostera noltii and Z. marina by desiccation at low tide. *Aquatic Botany*, *62*(3), 171–176. Retrieved 2021-11-02, from https://www.sciencedirect.com/science/article/pii/S0304377098000916 doi: 10.1016/S0304-3770(98)00091-6

Longbottom, M. R. (1970, September). The distribution of Arenicola marina (L.) with particular reference to the effects of particle size and organic matter of the sediments. *Journal of Experimental Marine Biology and Ecology*, *5*(2), 138–157. Retrieved 2022-01-18, from https://www.sciencedirect.com/science/article/pii/0022098170900134 doi: 10.1016/0022-0981(70)90013-4

Mellors, J., Marsh, H., Carruthers, T. J. B., & Waycott, M. (2002, November). Testing the sediment-trapping paradigm of seagrass: Do seagrasses influence nutrient status and sediment structure in tropical intertidal environments? *Bulletin of Marine Science*, *71*(3), 1215–1226.

Meysman, F. J. R., Galaktionov, O. S., & Middelburg, J. J. (2005, November). Irrigation patterns in permeable sediments induced by burrow ventilation: a case study of Arenicola marina. *Marine Ecology Progress Series*, *303*, 195–212. Retrieved 2022-01-27, from https://www.int-res.com/abstracts/meps/v303/p195-212/ doi: 10.3354/meps303195

Ondiviela, B., Losada, I. J., Lara, J. L., Maza, M., Galván, C., Bouma, T. J., & van Belzen, J. (2014). The role of seagrasses in coastal protection in a changing cli-

mate. *Coastal Engineering*, *87*, 158–168. Retrieved 2022-01-26, from https://www.sciencedirect.com/science/article/pii/S0378383913001889 doi: 10.1016/j.coastaleng.2013.11.005

Oost, A., Colina Alonso, A., Esselinkg, P., Wang, Z. B., van Kessel, T., & van Maren, B. (2021, February). Where Mud Matters; Towards a mud balance for the trilateral Wadden Sea area: mud supply, transport and deposition.

Oreskes, N., Shrader-Frechette, K., & Belitz, K. (1994). Verification, Validation, and Confirmation of Numerical Models in the Earth Science. *Science (New York, N.Y.)*, *263*, 641–6. doi: 10.1126/science.263.5147.641

Partheniades, E. (1965). Erosion and Deposition of Cohesive Soils. *Journal of the Hydraulics Division*, *91*(1), 105–139. Retrieved 2021-11-02, from https://cedb.asce.org/CEDBsearch/record.jsp?dockey=0013640 (Publisher: ASCE)

Paul, M., & Amos, C. L. (2011). Spatial and seasonal variation in wave attenuation over Zostera noltii. *Journal of Geophysical Research: Oceans*, *116*(C8). Retrieved 2021-11-02, from https://onlinelibrary.wiley.com/doi/abs/10.1029/2010JC006797 (_eprint: https://onlinelibrary.wiley.com/doi/pdf/10.1029/2010JC006797) doi: 10.1029/2010JC006797

Peralta, G., Brun, F., Pérez-Lloréns, J., & Bouma, T. (2006, December). Direct effects of current velocity on the growth, morphometry and architecture of seagrasses: a case study on Zostera noltii. *Marine Ecology Progress Series*, *327*, 135–142. Retrieved 2021-11-02, from http://www.int-res.com/abstracts/meps/v327/p135-142/ doi: 10.3354/meps327135

Philippart, C. J. M. (1994). Interactions between Arenicola marina and Zostera noltii on a tidal flat in the Wadden Sea. , 7.

Philippart, C. J. M. (1995a, May). Effect of periphyton grazing by Hydrobia ulvae on the growth of Zostera noltii on a tidal flat in the Dutch Wadden Sea. *Marine Biology*, *122*(3), 431–437. Retrieved 2022-01-20, from https://doi.org/10.1007/BF00350876 doi: 10.1007/BF00350876

Philippart, C. J. M. (1995b, March). Seasonal variation in growth and biomass of an intertidal Zostera noltii stand in the Dutch wadden sea. *Netherlands Journal of Sea Research*, *33*(2), 205–218. Retrieved 2021-11-02, from https://www.sciencedirect.com/science/article/pii/0077757995900071 doi: 10.1016/0077-7579(95)90007-1

Postma, H. (1961, April). Transport and accumulation of suspended matter in the Dutch Wadden Sea. *Netherlands Journal of Sea Research*, *1*(1), 148–190. Retrieved 2021-10-10, from https://www.sciencedirect.com/science/article/pii/0077757961900047 doi: 10.1016/0077-7579(61)90004-7

Prandtl, L. (1945). *Über ein neues Formelsystem für die ausgebildete Turbulenz*. Göttingen: Vandenhoeck & Ruprecht. (OCLC: 315537024)

Reidenbach, M. A., & Thomas, E. L. (2018). Influence of the Seagrass, Zostera marina, on Wave Attenuation and Bed Shear Stress Within a Shallow Coastal Bay. *Frontiers in Marine Science*, *5*, 397. Retrieved 2021-09-11, from https://www.frontiersin.org/article/10.3389/fmars.2018.00397 doi: 10.3389/fmars.2018.00397

Reise, K. (2002, October). Sediment mediated species interactions in coastal waters. *Journal of Sea Research*, *48*, 127–141. doi: 10.1016/S1385-1101(02)00150-8

Reise, K., Baptist, Burbridge, P., Dankers, N., Fischer, Flemming, B., ... Smit, C. (2010, January). The Wadden Sea – A universally outstanding tidal wetland. The Wadden Sea Quality Status Report. The Wadden Sea 2010. *Wadden Sea Ecosystem*, *29*, 7–23.

Reise, K., & Kohlus, J. (2008, March). Seagrass recovery in the Northern Wadden Sea?

Helgoland Marine Research, *62*(1), 77–84. Retrieved 2021-10-10, from http://link.springer.com/10.1007/s10152-007-0088-1 doi: 10.1007/s10152-007-0088-1

Reise, K., Simon, M., & Herre, E. (2001, August). Density-dependent recruitment after winter disturbance on tidal flats by the lugworm Arenicola marina. *Helgoland Marine Research*, *55*, 161–165. doi: 10.1007/s101520100076

Retraubun, A. S. W., Dawson, M., & Evans, S. M. (1996, September). Spatial and temporal factors affecting sediment turnover by the lugworm Arenicola marina (L.). *Journal of Experimental Marine Biology and Ecology*, *201*(1), 23–35. Retrieved 2022-01-18, from https://www.sciencedirect.com/science/article/pii/0022098196000160 doi: 10.1016/0022-0981(96)00016-0

Ridderinkhof, H. (1988, April). Tidal and residual flows in the Western Dutch Wadden Sea I: Numerical model results. *Netherlands Journal of Sea Research*, *22*(1), 1–21. Retrieved 2021-10-10, from https://www.sciencedirect.com/science/article/pii/007775798890049X doi: 10.1016/0077-7579(88)90049-X

Riisgård, H. U., & Banta, G. (1998, December). Irrigation and deposit feeding by the lugworm Arenicola marina, characteristics and secondary effects on the environment. A review of current knowledge. *Vie et Milieu*, *48*, 243–257.

Rijken, M. (1979, December). Food and food uptake in arenicola marina. *Netherlands Journal of Sea Research*, *13*(3), 406–421. Retrieved 2021-11-24, from https://www.sciencedirect.com/science/article/pii/0077757979900140 doi: 10.1016/0077-7579(79)90014-0

Rodi, W. (1980, December). Turbulence models and their application in hydraulics - A state of the art review. *NASA STI/Recon Technical Report A*, *81*, 21395. Retrieved 2021-11-02, from https://ui.adsabs.harvard.edu/abs/1980STIA...8121395R (ADS Bibcode: 1980STIA...8121395R)

Saaltink, R. M. (2018, November). *Wetland eco-engineering with fine sediment* [Dissertation]. Retrieved 2021-12-17, from http://localhost/handle/1874/371815 (Accepted: 2018-10-26T17:58:21Z ISBN: 9789039370254 Publisher: Utrecht University)

Schanz, A., & Asmus, H. (2003, October). Impact of hydrodynamics on development and morphology of intertidal seagrasses in the Wadden Sea. *Marine Ecology Progress Series*, *261*, 123–134. Retrieved 2022-01-20, from https://www.int-res.com/abstracts/meps/v261/p123-134/ doi: 10.3354/meps261123

Schultze, M., & Nehls, G. (2018, November). Wadden Sea Quality Status Report Extraction and dredging. , 11.

Schwarz, C., Gourgue, O., van Belzen, J., Zhu, Z., Bouma, T. J., van de Koppel, J., ... Temmerman, S. (2018, September). Self-organization of a biogeomorphic landscape controlled by plant life-history traits. *Nature Geoscience*, *11*(9), 672–677. Retrieved 2022-02-26, from https://www.nature.com/articles/s41561-018-0180-y (Number: 9 Publisher: Nature Publishing Group) doi: 10.1038/s41561-018-0180-y

Soissons, L. M., Gomes da Conceiçâo, T., Bastiaan, J., van Dalen, J., Ysebaert, T., Herman, P. M. J., ... Bouma, T. J. (2019, November). Sandification vs. muddification of tidal flats by benthic organisms: A flume study. *Estuarine, Coastal and Shelf Science*, *228*, 106355. Retrieved 2022-01-20, from https://www.sciencedirect.com/science/article/pii/S0272771418309909 doi: 10.1016/j.ecss.2019.106355

Strasser, M. (2002, October). Reduced epibenthic predation on intertidal bivalves after a severe winter in the European Wadden Sea. *Marine Ecology Progress Series*, *241*, 113–123. Retrieved 2021-10-10, from https://www.int-res.com/abstracts/meps/v241/p113-123/ doi: 10.3354/meps241113

Temmerman, S., Bouma, T., van de Koppel, J., Wal, D., de Vries, M., & Herman, P. (2007, July). Vegetation Causes Channel Erosion in a Tidal Landscape. *Geology*, *35*, 631–634. doi: 10.1130/G23502a.1

Valdemarsen, T., Canal-Vergés, P., Kristensen, E., Holmer, M., Kristiansen, M. D., & Flindt, M. R. (2010, November). Vulnerability of Zostera marina seedlings to physical stress. *Marine Ecology Progress Series*, *418*, 119–130. Retrieved 2021-11-24, from https://www.int-res.com/abstracts/meps/v418/p119-130/ doi: 10.3354/meps08828

Valdemarsen, T., Wendelboe, K., Egelund, J. T., Kristensen, E., & Flindt, M. R. (2011, December). Burial of seeds and seedlings by the lugworm Arenicola marina hampers eelgrass (Zostera marina) recovery. *Journal of Experimental Marine Biology and Ecology*, *410*, 45–52. Retrieved 2021-11-24, from https://www.sciencedirect.com/science/article/pii/S0022098111004345 doi: 10.1016/j.jembe.2011.10.006

Vandenbruwaene, W., Bouma, T. J., Meire, P., & Temmerman, S. (2013). Bio-geomorphic effects on tidal channel evolution: impact of vegetation establishment and tidal prism change. *Earth Surface Processes and Landforms*, *38*(2), 122–132. Retrieved 2022-01-21, from https://onlinelibrary.wiley.com/doi/abs/10.1002/esp.3265 (_eprint: https://onlinelibrary.wiley.com/doi/pdf/10.1002/esp.3265) doi: 10.1002/esp.3265

Vandenbruwaene, W., Meire, P., & Temmerman, S. (2012). Formation and evolution of a tidal channel network within a constructed tidal marsh. *Geomorphology*, *151-152*, 114–125. Retrieved 2022-01-21, from https://www.sciencedirect.com/science/article/pii/S0169555X12000591 doi: 10.1016/j.geomorph.2012.01.022

van Katwijk, M. M., Bos, A. R., Hermus, D. C. R., & Suykerbuyk, W. (2010, September). Sediment modification by seagrass beds: Muddification and sandification induced by plant cover and environmental conditions. *Estuarine, Coastal and Shelf Science*, *89*(2), 175–181. Retrieved 2022-01-20, from https://www.sciencedirect.com/science/article/pii/S0272771410002283 doi: 10.1016/j.ecss.2010.06.008

van Leeuwen, B., Augustijn, D. C. M., van Wesenbeeck, B. K., Hulscher, S. J. M. H., & de Vries, M. B. (2010, February). Modeling the influence of a young mussel bed on fine sediment dynamics on an intertidal flat in the Wadden Sea. *Ecological Engineering*, *36*(2), 145–153. Retrieved 2021-10-10, from https://www.sciencedirect.com/science/article/pii/S0925857409001116 doi: 10.1016/j.ecoleng.2009.01.002

Viles, H. (2020, October). Biogeomorphology: Past, present and future. *Geomorphology*, *366*, 106809. Retrieved 2021-10-10, from https://www.sciencedirect.com/science/article/pii/S0169555X19302752 doi: 10.1016/j.geomorph.2019.06.022

Volkenborn, N., Hedtkamp, S. I. C., van Beusekom, J. E. E., & Reise, K. (2007, August). Effects of bioturbation and bioirrigation by lugworms (Arenicola marina) on physical and chemical sediment properties and implications for intertidal habitat succession. *Estuarine, Coastal and Shelf Science*, *74*(1), 331–343. Retrieved 2021-10-10, from https://www.sciencedirect.com/science/article/pii/S0272771407001394 doi: 10.1016/j.ecss.2007.05.001

Wang, Z. B., Hoekstra, P., Burchard, H., Ridderinkhof, H., De Swart, H. E., & Stive, M. J. F. (2012, November). Morphodynamics of the Wadden Sea and its barrier island system. *Ocean & Coastal Management*, *68*, 39–57. Retrieved 2021-10-10, from https://www.sciencedirect.com/science/article/pii/S0964569112000026 doi: 10.1016/j.ocecoaman.2011.12.022

Zagwijn, W. H. (1986). *Nederland in het Holoceen /.* (Place: Haarlem : Publisher: Rijks geologische dienst,)

Statement of originality of the MSc thesis

I declare that:

1. this is an original report, which is entirely my own work,

2. where I have made use of the ideas of other writers, I have acknowledged the source in all instances,

3. where I have used any diagram or visuals, I have acknowledged the source in all instances,

4. this report has not and will not be submitted elsewhere for academic assessment in any other academic course.

Student data:

Name: S.M. Vaassen

Registration number: 5318696

Date: 28-02-2022

Signature: